UNIVERSITÀ DEGLI STUDI DI PADOVA

Physics and Astronomy Department "Galileo Galilei"

Master in "Physics"
Curriculum "Physics of Fundamental Interactions"

Master Thesis

Impact of Sommerfeld Correction on the Dark Matter Relic Density

Advisor

Prof. Francesco D'Eramo

Student

Giulio Alvise Dainelli

Academic Year 2024/2025

Contents

Introduction

The existence of Dark Matter is one of the most compelling pieces of evidence for physics beyond the Standard Model. Observations across multiple length scales—from galactic rotation curves to the anisotropies in the Cosmic Microwave Background—support the presence of a non-luminous, non-baryonic form of matter that interacts predominantly through gravity. Yet, the fundamental nature of Dark Matter remains elusive. This enduring mystery continues to drive theoretical and experimental research in particle physics, astrophysics, and cosmology.

The thermal freeze-out mechanism remains one of the most robust and predictive frameworks for explaining the existence and observed abundance of dark matter (DM) in the Universe. In this paradigm, DM particles were once in thermal equilibrium with the Standard Model (SM) plasma, eventually decoupling as the Universe expanded and cooled, leaving behind a relic population. A key feature of this mechanism is that the relic abundance is determined by the DM annihilation cross section at temperatures close to the freeze-out epoch, when the relative velocity of DM particles is low.

However, this standard picture assumes a purely perturbative treatment of DM annihilation processes, neglecting long-range effects that can arise when the DM interacts via a force mediated by light or massless particles. In such scenarios, the quantum mechanical distortion of the initial-state wavefunction leads to a velocity-dependent enhancement of the annihilation cross section a phenomenon known as Sommerfeld effect. First noted in atomic physics (in particular in beta decay) and later recognized as having vital importance in particle physics contexts, the Sommerfeld enhancement can significantly modify freeze-out predictions, especially for heavy DM particles with non-negligible self-interactions.

This thesis is devoted to a rigorous quantum field theoretic treatment of the Sommerfeld effect and its impact on the DM relic density. Starting from the first principles of field theory, we derive the Sommerfeld enhancement by resumming the ladder of Feynman diagrams that contribute to the long-range potential between annihilating DM particles. This approach offers a clear and physically grounded interpretation of the non-perturbative nature of the enhancement, connecting quantum mechanics to diagrammatic methods and shedding light on the limits of conventional perturbative techniques.

Within this context, the Minimal Dark Matter (MDM) scenario offers a particularly elegant and predictive framework. By extending the Standard Model with a single electroweak multiplet and requiring stability through gauge symmetry alone, MDM minimizes the number of free parameters while tightly connecting cosmological viability to electroweak representation theory. The phenomenology of such models is largely determined by the representation chosen and the requirement that the Lightest Neutral Particle (LNP) be electrically neutral and colorless. Nevertheless, these candidates present a rich phenomenology thanks to Sommerfeld corrections providing therefore a controlled setting in which the interplay between electroweak interactions and thermal relic density can be carefully analyzed.

The last part of the thesis is dedicated to extending this analysis beyond the minimal setup. We discuss briefly the relevant approximations we have made in our treatment and the effects of which we have neglected. Next, to show the ubiquitous importance of Sommerfeld correction in the context of thermal

Dark Matter candidates, we study the relevance of the corrections in models in which Dark Matter co-annihilates with colored partners which have strong interactions between them and with the Standard Model. This treatment illustrates the importance of accounting for long-range interactions in a wide class of dark sector theories.

Chapter 1

An Overview on Dark Matter

What is Dark Matter?

Dark Matter is the name we give to the unknown, (almost) pressureless and feebly interacting constituent of our Universe making up for $\sim$ 22% of its total energy. For reference the "normal" matter that is described with striking precision by the Standard Model and with which we interact everyday, makes up for about 5% of the energy of the Universe. The remaining 63% is described from an even more mysterious fluid called Dark Energy. The Standard Cosmological Model or (ΛCDM, Λ stands for Dark Energy and CDM for Cold Dark Matter) employs these two fluids to describe the evolution of our Universe with striking precision.

The term Dark Matter was first introduced to talk about Barionic Matter, specifically planetary matter, that was almost invisible for telescopes. [2] [1]

The term was first used in the modern sense by the astronomer Fritz Zwicky in 1933, observing the Coma cluster [29], but in the past century we have accumulated evidences for the existence of Dark Matter on vast range of scales:

- **Galactic Scales** $\sim 10\,\text{kpc} - 200\,\text{kpc}$.
- **Galaxy Clusters Scales** $\sim 1\,\text{Mpc} - 5\,\text{Mpc}$.
- **Cosmological Scales** $\sim 100\,\text{Mpc}$.

It is important to point out that all these evidences are based on the gravitational interactions of Dark Matter, we could therefore think to explain all of them changing the laws of gravity, but, as we shall see, it is nearly impossible to reproduce all the evidences without introducing new degrees of freedom that effectively mimic Dark Matter.

1.1 Evidences of Dark Matter

1.1.1 Galactic Scales

The first evidences of Dark Matter on Galactic Scales were obtained by Vera Rubin and Kent Ford [5], using the Doppler shift of the 21 cm line of Hydrogen hyperfine transition to measure the speed of gas clouds at various different distances from the centre of the Andromeda galaxy. Their result is reported in figure 1.2.

To understand the significance of these results, we must know that visible matter, in a typical-size galaxy extends to about $\sim 15\,\text{kpc}$ from its centre. Using Newtonian Mechanics and approximating the orbits to

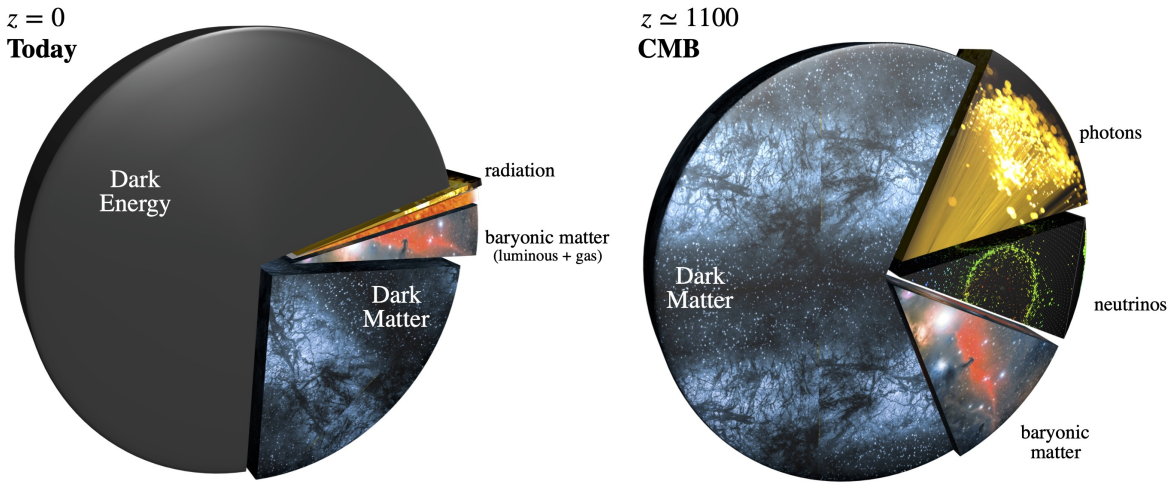

Figure 1.1: Cosmic Pie charts of the Universe today ($z = 0$, $t \simeq 13.8 \cdot 10^9$ years) and at CMB formation ($z = 1100$, $t \simeq 380\,000$ years. Taken from [61].

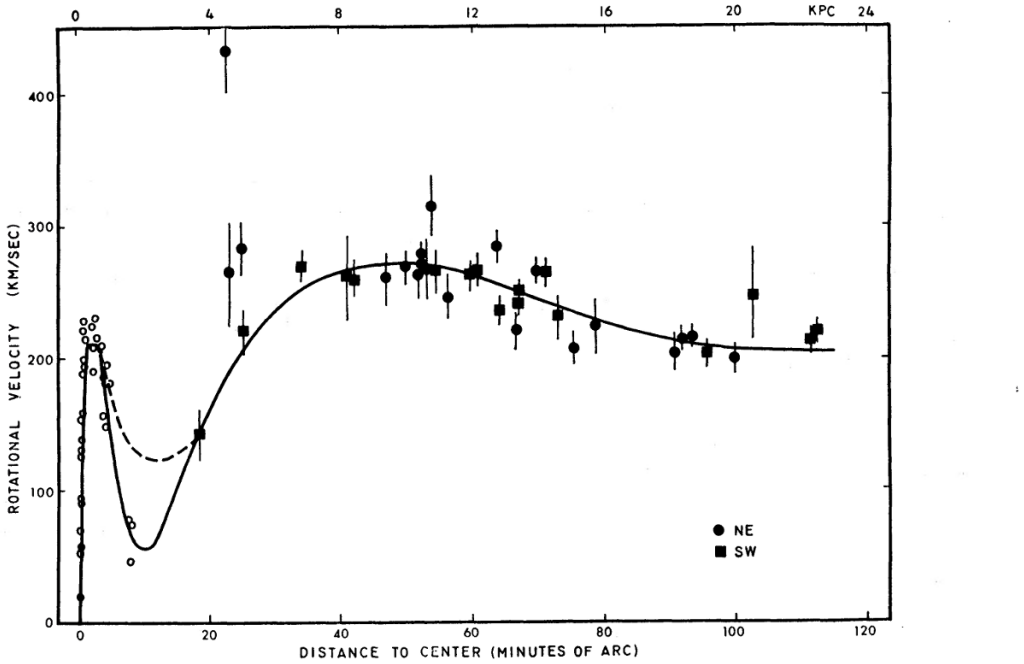

Figure 1.2: Rotational curve of the Andromeda Galaxy (M31) from [5].

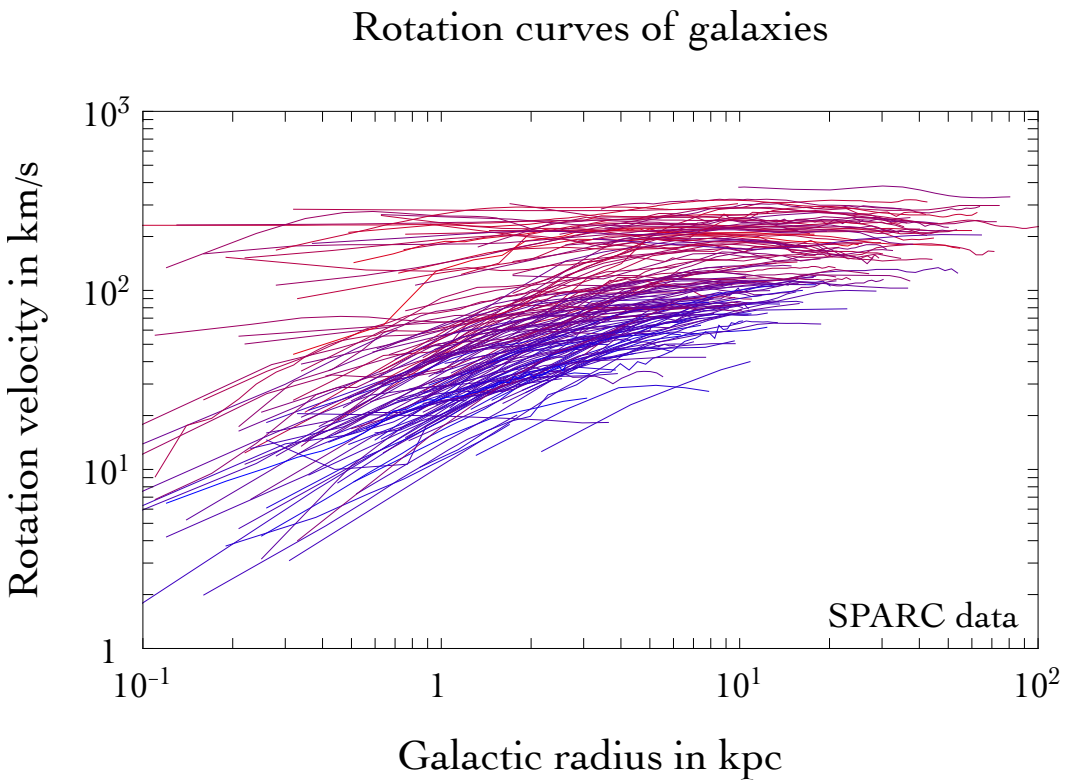

Figure 1.3: SPARC collaboration compilation of 175 galaxies (http://astroweb.cwru.edu/SPARC/).

be circular, we thus expect the typical rotation speeds to be

$$\frac{v_{circ}^2}{r} = \frac{GM(r)}{r^2}$$

$$v_{circ} = \sqrt{\frac{GM(r)}{r}}.$$

The rotation curves should then die off with an approximate $\sim r^{-\frac{1}{2}}$ behaviour once $r \gtrsim 15\,\text{kpc}$ and thus $M(r)$ stops increasing. Instead what Rubin and Ford found was that rotational curves flatten out at large distances from the centre of the galaxy. This can be explained by changing the laws of gravity on galactic scales or assuming there is some matter which is weakly interacting with photons and thus cannot be seen by telescopes in the outskirts of our galaxy. To obtain flat rotational curves we have to assume $M(r) \propto r$ which in turn implies $\rho_{DM}(r) = \frac{1}{r^2}\frac{dM(r)}{dr} \propto r^{-2}$.

Since this first evidence of the existence of DM on galactic scales we have been flooded with more precise data of numerous different galaxies on a much wider range of radii, see for example fig 1.3.

1.1.2 Galaxy Clusters Scales

The Coma Cluster

As said before the first Evidence of Dark Matter was obtained by Zwicky [29] looking at the Coma Cluster, he used the Virial Theorem, which for the Newton potential states

$$\langle T \rangle = -\frac{1}{2}\langle U \rangle$$

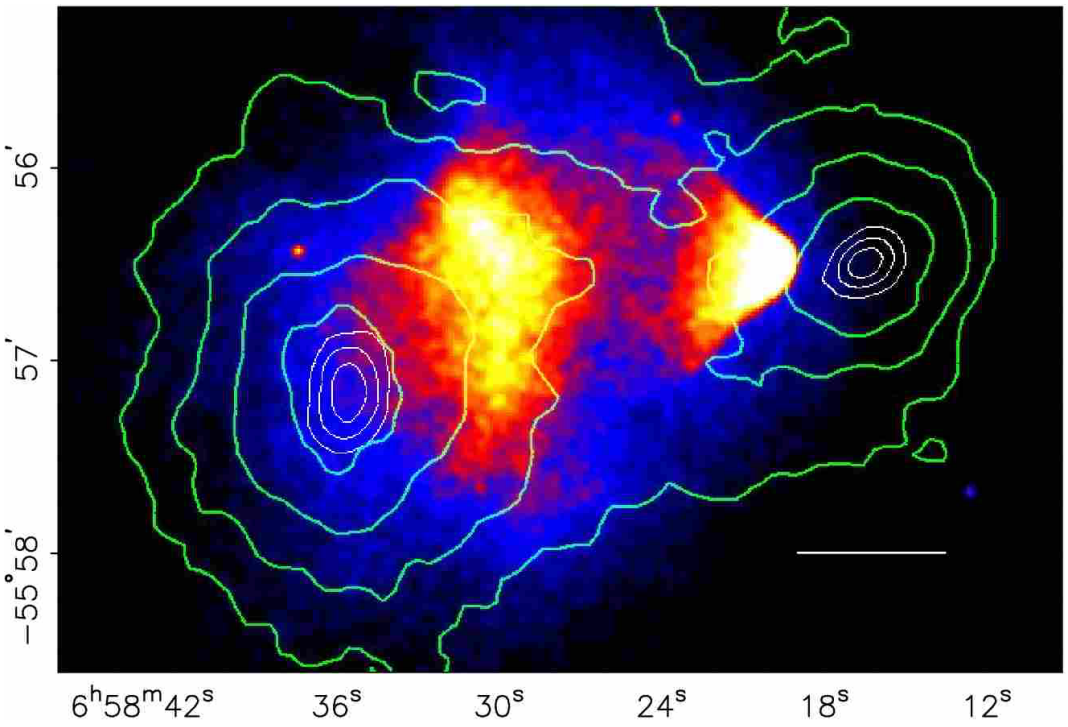

Figure 1.4: Mass (green contours) and gas (red and yellow spots) distribution of the Bullet Cluster inferred from weak gravitational lensing. Taken from [26].

Then for the kinetic energy we have

$$\langle T \rangle = \left\langle \sum_{i \in \text{stars}} \frac{1}{2} m_i v_i^2 \right\rangle \sim \frac{1}{2} M_{\text{coma}} \langle v^2 \rangle$$

instead the gravitational energy

$$\langle U \rangle \sim -\frac{G M_{\text{coma}}^2}{R_{\text{coma}}}$$

the order one proportionality factor depend on the details of the matter distribution in the cluster. We can thus obtain the estimate of the gravitational mass of the cluster

$$M_{\text{coma}}^{(\text{grav})} \sim \frac{R_{\text{coma}} \langle v^2 \rangle}{G} \sim 10^{44}\,\text{kg}$$

When instead he tried to estimate the mass of the cluster, simply counting its stars he obtained

$$M_{\text{coma}}^{(\text{vis})} \sim 10^{42}\,\text{kg}$$

And thus there is a really large fraction of the mass that cannot be seen with telescopes. These data were then reviewed multiple times and this tension was attenuated.

The Bullet Cluster

The presence of mass in some region of the sky can be inferred by weak gravitational lensing. According to general relativity a beam of light directed towards an object of mass M, with impact parameter b is deflected by an angle

$$\alpha \simeq \frac{4GM}{c^2 b}$$

This relation allows us to determine the mass of the object looking at the image of stars or galaxies behind it.

In the figure 1.4 is reported the image of the Bullet cluster after the collision with another cluster. As emphasized by the green contours the system exhibits a separation of the gravitational mass and the visible mass (gas emitting radiation). The explanation in terms of Dark Matter is really simple: the two clusters collide and the visible matter, having a much higher interaction cross-section than DM is slowed down significantly more. This system poses an upper bound to the possible cross section of Dark Matter self-interactions.

$$\sigma < 1.8\,\mathrm{mb}\left(\frac{M}{\mathrm{GeV}}\right) \tag{1.1}$$

This piece of evidence is really hard to explain with a modification of gravity, because it's not just a discrepancy in the magnitude of the observed gravitational mass with respect to the visible mass, the two instead are spatially displaced.

1.1.3 Cosmological Scales

Structure Formation

We start from the linearized Einstein Equations which can be written as

$$\begin{cases} \nabla^2\Phi - 3\mathcal{H}(\Phi' + \mathcal{H}\Psi) = 4\pi G a^2 \delta\rho \\ -(\Phi' + \mathcal{H}\Psi) = 4\pi a^2 G q \\ \partial_{\langle i}\partial_{j\rangle}(\Phi - \Psi) = 8\pi G a^2 \Pi_{ij} \\ \Phi'' + \mathcal{H}\Psi' + 2\mathcal{H}\Phi' + \frac{1}{3}\nabla^2(\Psi - \Phi) + (2\mathcal{H}' + \mathcal{H}^2)\Psi = 4\pi G a^2 \delta P \end{cases} \tag{1.2}$$

For a complete introduction to perturbation theory and to see the careful definition of all the symbols involved see [54], in short Φ and Ψ are the gauge-invariant metric perturbations; $\delta\rho$, δP and Π_{ij} are the perturbations to the Energy-momentum tensor; q is a sort of peculiar velocity; a is the scale factor which appears in FLRW metric; the primed quantities represent derivatives with respect to conformal time ($a(t)\,d\eta = dt$); $\mathcal{H}$ is the Hubble parameter with respect to conformal time (in the sense that $\mathcal{H} = \frac{a'}{a}$); G is the Newton constant.

If we neglect anisotropic stresses ($\Pi_{ij} = 0$), assume adiabatic perturbations ($\frac{\delta\rho}{\delta P} = \frac{\bar{P}}{\bar{\rho}} = w$, the barred quantities are the background values) and assume the Universe is dominated by a single component fluid with constant w we obtain

$$\Phi'' + 3\mathcal{H}(1+w)\Phi' - w\nabla^2\Phi = 0$$

During matter domination $w \simeq 0$ ($a \propto \eta^2$) and the solution of the above equation is

$$\Phi = C_1 + C_2\, a^{\frac{5}{2}}$$

This solution can be substituted in (1.2) to obtain that the comoving density contrast (is the gauge invariant version of the density contrast δ_m and coincides exactly with it in the comoving gauge) has just one growing mode

$$\Delta_m = \frac{\delta\rho}{\bar{\rho_m}} \propto a$$

In radiation domination instead we cannot neglect the Laplacian as $w \simeq \frac{1}{3}$, we thus go to momentum space and obtain

$$\Phi'' + 4\mathcal{H}\Phi' - \frac{k^2}{3}\Phi = 0$$

The solutions to this equation can be found in terms of the variable $\phi = k\eta/\sqrt{3}$:

$$\Phi = 2\mathcal{R}_i \frac{\sin(\phi) - \phi\cos(\phi)}{\phi^3}$$

The Hubble radius is the distance at which we see objects flying away at the speed of light, so it is the horizon of our patch of space-time. In natural units

$$d_H = \frac{1}{H}$$

and the comoving Hubble radius is

$$r_H = \frac{d_H}{a} = \frac{1}{aH} = \frac{1}{\mathcal{H}}$$

The above equation has thus 2 qualitatively different regimes: if $k \ll r_H^{-1}$ or $k \gg r_H^{-1}$, in radiation domination in fact $a \propto \eta$ and $r_H \propto \eta$, the limits $\phi \ll 1$ and $\phi \gg 1$ are therefore indeed the superhorizon and subhorizon limits. In this limits the equation takes the form

$$\Phi = \begin{cases} \frac{2}{3}\mathcal{R}_i & \text{superhorizon} \\ 6\mathcal{R}_i \frac{\cos\left(\frac{k\eta}{\sqrt{3}}\right)}{k^2\eta^2} & \text{subhorizon} \end{cases} \tag{1.3}$$

The solution for the density contrast is now more difficult but (see again [54]) it can be shown that the only growing mode in the deep radiation dominated era is

$$\delta_m \propto \ln(a)$$

We know that matter radiation equality occurs more or less at the same time at which matter decouples from radiation at recombination ($T_{eq} \sim 1\,\text{eV}$). At recombination we can measure matter perturbation from the Cosmic Microwave Background:

$$\left.\frac{\delta\rho}{\rho}\right|_{\text{CMB}} \simeq 10^{-5}$$

Therefore, having $\frac{a_0}{a_{eq}} \simeq \frac{T_{eq}}{T_0} \sim 10^4$ we can easily see that baryonic matter alone is not sufficient to create the density perturbations we see today

$$\left.\frac{\delta\rho}{\rho}\right|_{\text{today}} \sim 10^6 \gg 10^{-1} \sim \left.\frac{\delta\rho}{\rho}\right|_{\text{CMB}} \frac{a_0}{a_{eq}}$$

The only way we can achieve such a growth of density perturbations is for perturbations to go non-linear and thus for example to have a huge fraction of matter (Dark Matter) to decouple from radiation far before recombination and start creating pits for Baryonic matter to fall upon once it decouples from radiation.

Cosmic Microwave Background

The Cosmic Microwave Background or in short CMB is radiation that has last interacted with matter about 380 000 years after the Big Bang. When the temperature of the Universe was greater than $T \sim 1\,\text{eV}$ Hydrogen wasn't able to form because photons were too energetic. The Universe was a plasma of charged particles (protons and electrons) and the mean free path of photons was

$$\lambda = 1.6 \cdot 10^{19}\,\text{m} \qquad \tau = \frac{\lambda}{c} = 1700\,\text{years}$$

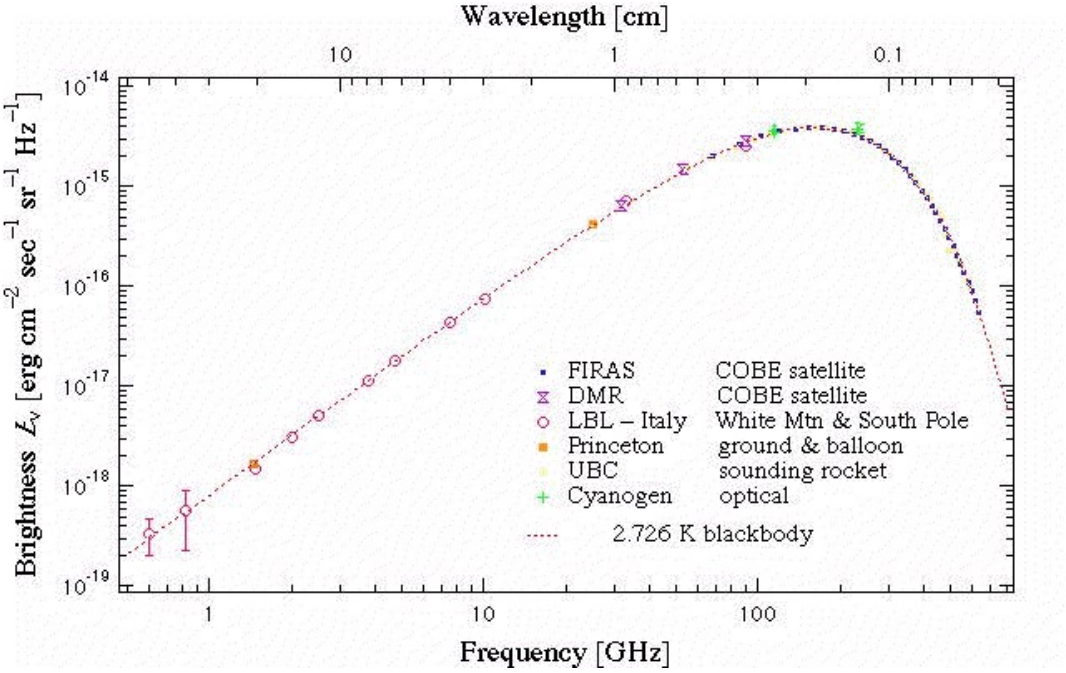

Figure 1.5: Fit of the CMB Spectrum from COBE, showing that CMB has a temperature of 2.726 K. Taken from https://aether.lbl.gov/www/projects/cobe/ .

Thus the mean time between 2 interaction was much shorter than the age of the Universe. Immediately after the Temperature dropped below $\sim 1\,\text{eV}$ Hydrogen formed, the Universe became neutral and radiation stopped interacting with matter. Radiation starts free streaming maintaining an equilibrium distribution and we can measure it today. The main observable from CMB is the power spectrum 1.6. To understand what the quantity plotted on the y-axis is we must expand Temperature fluctuations using spherical harmonics.

$$\delta T = \sum_{l=2}^{\infty} \sum_{m=-l}^{m=l} a_{lm} Y_l^m(\theta, \phi)$$

The power spectrum is then given by the correlator

$$\langle \delta T(\theta, \phi) \delta T(\theta', \phi') \rangle = \sum_l (2l+1) C_l P_l(cos(\theta_{rel}))$$

Where P_l are the Legendre Polynomials and this expression can be interpreted as a definition for C_l. Due to isotropy in fact the correlator is a function only of the relative angle θ_{rel}. The plotted quantity $\mathcal{D}_l$ is defined with a slightly different normalization:

$$\mathcal{D}_l = \frac{l(l+1)}{2\pi} C_l$$

The main evidence of Dark Matter from this measurements is due to the presence of peaks in the power spectrum. From equation (1.3) we can see that the frequency of fluctuations depends on the momentum k and thus when we take, through CMB, a snapshot of fluctuations at decoupling of matter from radiation all the modes are out of phase and we observe a peak structure. Dark Matter plays a central role in determining the size of fluctuations (and thus of the peaks) as can be seen from 1.7.

From the Power Spectrum we have the most precise measure of all the cosmological parameters of the ΛCDM model [51]:

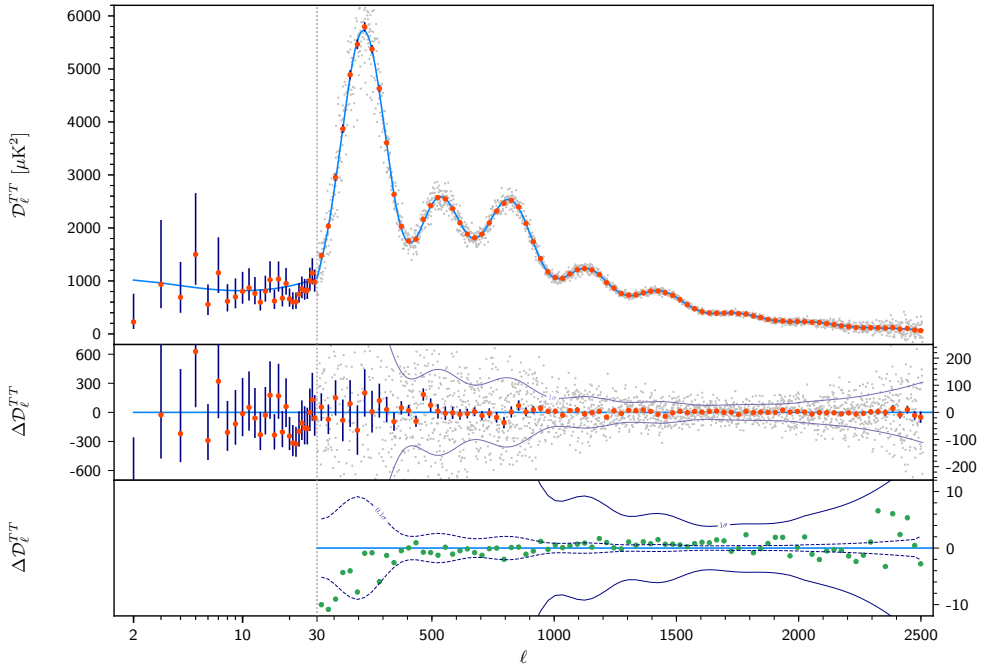

Figure 1.6: CMB temperature power spectrum from [50].

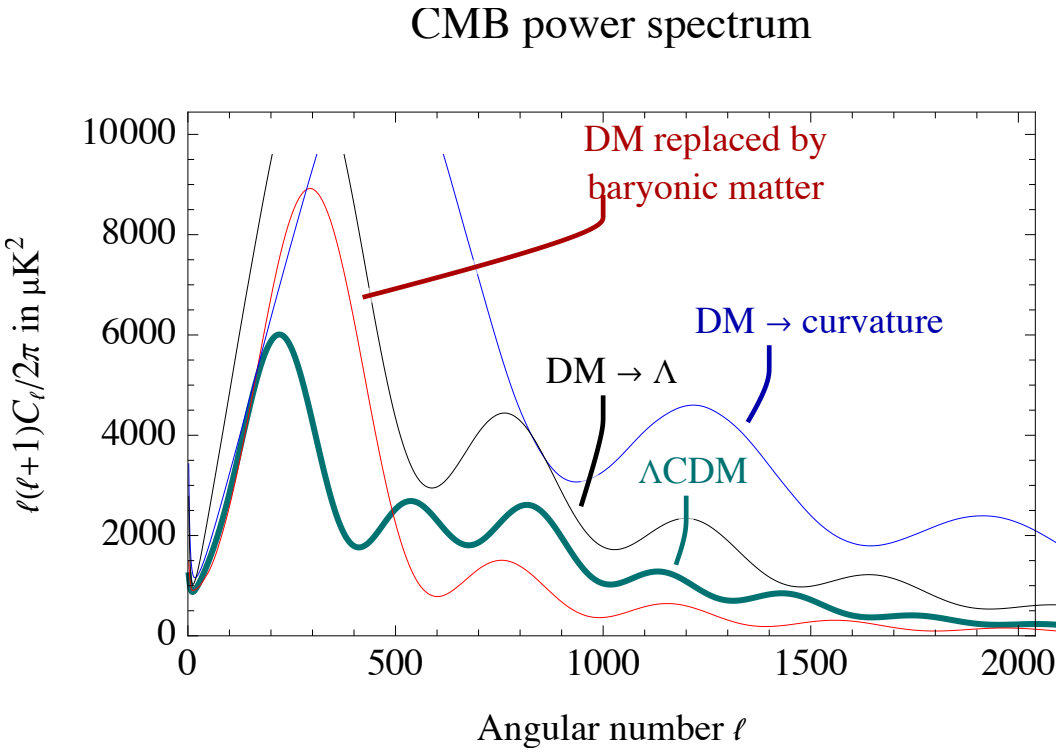

Figure 1.7: Fit of the CMB Power Spectrum from the ΛCDM compared with the power spectrum in which Dark Matter is substituted by other cosmological fluids, taken from [61] and obtained with CAMB interface.

$$H_0 = 100\,\frac{\mathrm{km}}{\mathrm{s}\cdot\mathrm{Mpc}}\cdot h = (67.27 \pm 0.60)\,\frac{\mathrm{km}}{\mathrm{s}\cdot\mathrm{Mpc}}$$

$$\Omega_{matter}h^2 = 0.1430 \pm 0.0011$$

$$\Omega_{DM}h^2 = 0.1200 \pm 0.0012$$

$$\Omega_B = 0.02237 \pm 0 - 00015$$

$$\Omega_\Lambda h^2 = 0.3107 \pm 0.0082$$

The photon density can be estimated from the temperature of the CMB obtaining

$$\Omega_\gamma h^2 \simeq 2.5 \cdot 10^{-5}$$

Instead the total density of radiation can only be estimated because its details depend on the neutrino masses on which we have just some upper and lower bounds.

$$\Omega_{rad}h^2 \sim 10^{-4}$$

Big Bang Nucleosynthesis

Big Bang Nucleosynthesis (BBN) is the process through which we have the formation of light nuclei from proton and neutrons in our Universe. This process is regulated by an important parameter: the photon to baryon ratio.

Deuteron and other nuclei are in fact able to form (exactly like hydrogen at recombination) when it becomes relatively improbable to be hit by a CMB photon with an energy of the order of the nuclear binding energies $\sim 1\,\mathrm{MeV}$. And the time at which this happens is thus regulated from the number of photons that are present for each Baryon. BBN thus permits to estimate

$$\eta_B = \frac{n_\gamma}{n_B} = (6.2 \pm 0.4) \cdot 10^{-10}$$

This is an important consistency check, as the number of photons can be derived by the temperature of the CMB

$$n_\gamma = \frac{2}{\pi^2}\zeta(3)T_{CMB}^3$$

we can thus extract a prediction for Ω_B to compare with the one obtained measuring the CMB Power Spectrum.

$$\Omega_B h^2 = 0.022 \pm 0.002$$

Which is an important self-consistency check of the ΛCDM model.

1.2 Bounds on Dark Matter

Obviously any theory of Dark Matter should reproduce the Dark Matter density inferred by the Power Spectrum of CMB and reported in the previous section. But there are other powerful constraints a theory of DM should satisfy.

1.2.1 Tremaine-Gunn Bound

Dwarf Galaxies are believed to be very rich of Dark Matter compared to bigger galaxies as the Milky Way and can thus offer the most stringent bounds on the DM mass.

We can first derive a bound valid for all particles and also for multi-component Dark Matter and than a much powerful bound valid only for fermionic Dark Matter.

In order for Dwarf Galaxies to form, particles should be delocalized on a scale smaller than the typical radius of these Galaxies $R_{dwarf} \simeq 1\,\text{kpc}$.

$$\lambda_{dB} = \frac{2\pi}{m_{DM} v_0} \simeq \left(\frac{1\,\text{eV}}{m_{DM}}\right) \cdot 2.3 \cdot 10^{-3}\,\text{m}$$

Where we have substituted in the above expression $v \simeq 160\,\text{km/s}$ that can be inferred with the Virial Theorem

$$m_{DM} > 10^{-22}\,\text{eV}$$

For Fermionic Dark Matter a tighter constraint comes from Pauli exclusion principle. In fact the Fermi-Dirac phase space distribution is

$$f_{FD}(E) = \frac{1}{e^{\frac{E-\mu}{T}} + 1} < 1$$

The number of Dark Matter particles in the galaxy can be computed by

$$N_{DM} = g \int_{\text{volume}} \int_{\text{momentum}} f_{FD}(E)\, d^3\mathbf{x}\, d^3\mathbf{p} < g \int_{\text{volume}} \int_{\text{momentum}} d^3\mathbf{x}\, d^3\mathbf{p} = g \left(\frac{4\pi R_{dwarf}^3}{3}\right)\left(\frac{4\pi p_{max}^3}{3}\right)$$

Where g is the internal number of degrees of freedom of the fermion. The maximum Momentum can be computed from the escape velocity

$$p_{max} = p_{esc} \sim \left(\frac{2GM_{dwarf} m_{DM}^2}{R_{dwarf}}\right)^{\frac{1}{2}}$$

if Dark Matter is non-relativistic

$$M_{dwarf} \simeq N_{DM} m_{DM} < \left(\frac{16\pi^2 g R_{dwarf}^3}{9}\right)\left(\frac{2GM_{dwarf} m_{DM}^2}{R_{dwarf}}\right)^{\frac{3}{2}} m_{DM}$$

$$m_{DM} \gtrsim \left(\frac{9}{32\sqrt{2}\pi^2} \frac{1}{g\sqrt{G^3 M_{dwarf} R_{dwarf}^3}}\right)^{\frac{1}{4}}$$

This bound has a mild dependence on the fermion spin and number of fermion species as it goes as $g^{\frac{1}{4}}$ (and increasing the number of fermion species has the only effect of changing g). For DM constituted only by a Dirac spin-$\frac{1}{2}$ fermion the bound is

$$m_{DM}^{(FD)} \gtrsim 10\,\text{eV}$$

1.2.2 Hot Dark Matter

Dark Matter with a relativistic velocity distribution when it decouples from the Standard Model is called hot. We will now show that Hot Dark Matter candidates are excluded.

Free Streaming

After decoupling DM particle thus continue to move (Free Streaming) and travel for a typical distance λ_{FS} before matter radiation equality (as we have already mentioned matter radiation equality is a fundamental moment for structure formation). The result of this motion is to smooth out density fluctuations at such scales and hence severe bounds on Hot Dark Matter can be deduced by Structure Formation.

$$\lambda_{FS} \simeq \frac{t_{NR}}{a(t_{NR})}\left(2\left(1-\left(\frac{t_{dec}}{t_{NR}}\right)^{\frac{1}{2}}\right)+\ln\left(\frac{t_{eq}}{t_{NR}}\right)\right)$$

Where t_{dec} is the time of decoupling, t_{NR} is the time at which the DM particles become non-relativistic ($T_{NR} \simeq m_{DM}$), t_{eq} is the time of matter-radiation equality and we assumed $t_{dec} < t_{NR} < t_{eq}$. Now the details depend on the exact decoupling time from the thermal bath, because when other species decouple they change the temperature of the plasma and thus the Temperature T_{DM} describing the free-streaming velocity distribution of DM is no longer the Temperature T of the thermal bath. To put in some numbers we suppose that $t_{dec} \ll t_{NR}$ (Hot Dark Matter) and that the DM particles we are interested have mass of the order of the keV (we will see that is exactly this mass that gives a free-streaming length of the order of R_{halos}).

$$\lambda_{FS} \sim 100\,\mathrm{kpc}\left(\frac{1\,\mathrm{keV}}{m_{DM}}\right)\left(\frac{T_{DM}}{T}\right)$$

And thus to observe Dark Matter Halos we must have

$$m_{DM}^{(hot)} \gtrsim 1\,\mathrm{keV}$$

Hot Dark Matter relic density

The bound from free-streaming in fact leaves the door open for Hot Dark Matter candidates with masses above the keV. We will now prove that Hot Thermal Relics (particles remaining after the decoupling of a species from the thermal bath) are indeed forbidden as for masses respecting the free-streaming bound they under-produce Dark Matter. If the particle χ is non-relativistic today ($m_\chi \gtrsim 10^{-4}\,\mathrm{eV}$)

$$\rho_\chi = n_\chi m_\chi$$

and n_χ is set by the freeze-out mechanism

$$n_\chi = \frac{45\zeta(3)}{2\pi^4}\frac{g_{eff}}{g*_s(T_{FO})}s_0$$

The freeze-out temperature is set by the details of the decoupling, but all the dependence from T_{FO} is in $g*_s$ which we do not expect it to vary dramatically. If χ is a DM candidate its abundance must be less than the observed Dark matter abundance and thus $\rho_\chi < \rho_{DM}$, from this inequality we obtain a bound for the mass

$$m_\chi < 168\,\mathrm{eV}\frac{1}{g_{eff}}\left(\frac{g*_s(T_{FO})}{106.75}\right) < 168\,\mathrm{eV}$$

The last step has an important caveat, if T_{FO} is really high, our theory in the UV could have more degrees of freedom than the SM, but to open a gap between the Free Streaming bound and this production bound would require the UV theory to have at least 8 times the degrees of freedom of the SM at T_{FO} which seems unlikely.

Neutrino Dark Matter

The previous bounds can be used to rule out neutrino Dark Matter, the SM neutrinos have only weak interactions and thus their interaction rate is

$$\Gamma_\nu \sim G_F^2 T^5$$

Neutrinos decouple when $\Gamma \sim H$ which means $T \sim 1\,\text{MeV}$. We don't know the mass of neutrinos but we know that $\sum m_\nu < 1.35\,\text{eV}$ from direct search in tritium beta decay [60]. Neutrinos therefore definitely constitute Dark Matter, Hot Dark Matter, but the bounds above ensure that they cannot be its main constituent. Indeed the bound on the mass alone is in contrast with the Tremaine-Gunn bound and implies that neutrinos constitute less than 10 % of all DM.

1.2.3 Stability

The presence of Dark Matter in our Universe can be deduced directly from CMB formation to today (through gravitational lensing) and indirectly even to the time of BBN. This suggests that Dark Matter should be stable on cosmological time-scales

$$t_{\text{Universe}} \sim \frac{1}{H_0} \sim 14\,\text{Gyr}$$

We can have even more stringent bounds on Dark Matter decay from structure formation, in fact (unless we fine-tune its decay products) a decay would convert a large fraction of the DM energy into hot particles that, as seen above, would destroy structure formation. We then have [42]

$$f\Gamma_{DM} \gtrsim 15.9 \cdot 10^{-3}\,\text{Gyr}^{-1}$$

where f is the DM fraction that is allowed to decay. For 1 component DM this bound becomes

$$\tau_{DM} \gtrsim 63\,\text{Gyr}$$

The bound is much stronger if the decay products are SM particles with strong or electromagnetic charge [48]

$$\tau_{DM} \gtrsim (1 - -5) \cdot 10^{28}\,\text{s} \sim 10^{12}\,\text{Gyr}$$

1.2.4 Self-interactions

Bounds on Dark Matter self-interactions can be derived from collisions between galaxy clusters as shown in equation (1.1). We just report here the same bound.

$$\sigma < 1.8\,\text{mb}\left(\frac{M}{\text{GeV}}\right)$$

1.2.5 Charge

Dark Matter clearly cannot be charged with charges of order of $\sim e$ otherwise we would see it with telescopes. Dark Matter could in every case have a charge that is a fraction of e (see for example the section on the Dark Photon). Clearly this fraction must be really small or we would have the same problem of Baryonic matter at structure formation, this Dark Matter is thus called millicharged Dark Matter. The bounds on Dark Matter charge as a function of the mass is reported in figure 1.8

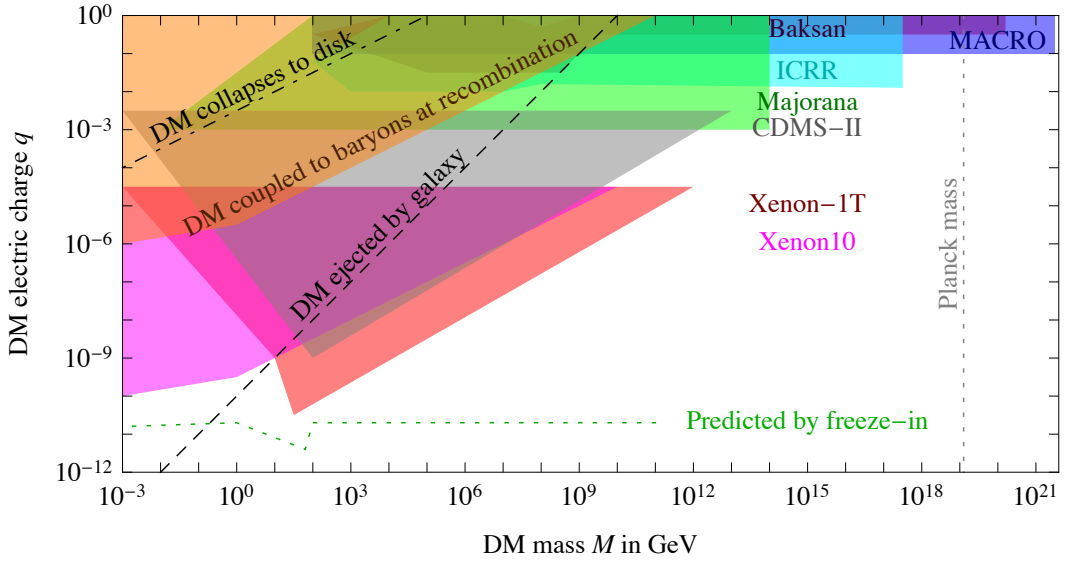

Figure 1.8: Bounds from different experiments on millicharged Dark Matter, taken from [61].

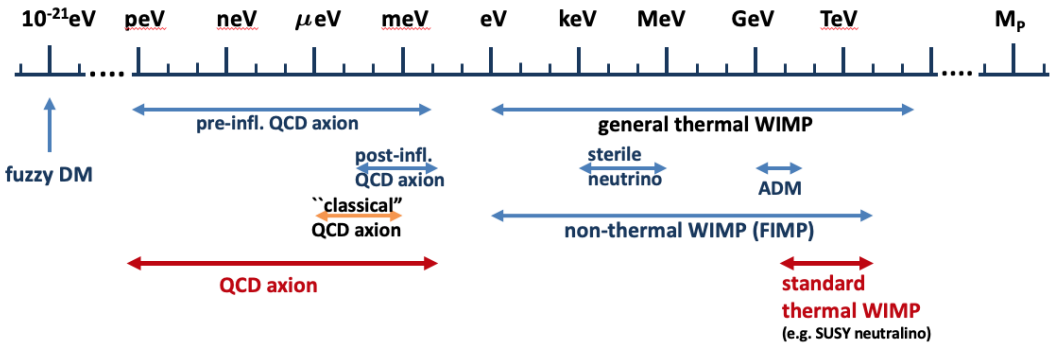

Figure 1.9: Different Dark matter candidates at different mass ranges. Taken from https://cds.cern.ch/record/2764484/plots.

1.3 Popular Candidates

Dark Matter is divided into thermal and non-thermal candidates based on whether or not they were in equilibrium with the thermal bath at some point in their evolution. We will now briefly analyse the most popular and studied Dark Matter candidates 1.9.

1.3.1 Weakly Interacting Massive Particles

Weakly Interacting Massive Particles or WIMPs have a self-explanatory name. They are a cold thermal candidate that was popular for mainly two reasons:

- **The *WIMP miracle***: Particles having a mass at the weak scale and interactions with cross sections of the order of weak forces naturally reproduce the observed Dark Matter abundance.
- **Supersymmetry**: Supersymmetry provided a natural setting to have stable WIMPs.

Today both these reasons have lost strength as we recognized that the WIMP miracle is basically a WIMP coincidence and we haven't had to this day any hint of Supersymmetry from colliders. Furthermore the WIMP paradigm has been extensively tested and its available parameter space (for spin-independent interactions) has almost all been excluded, see figure 1.10.

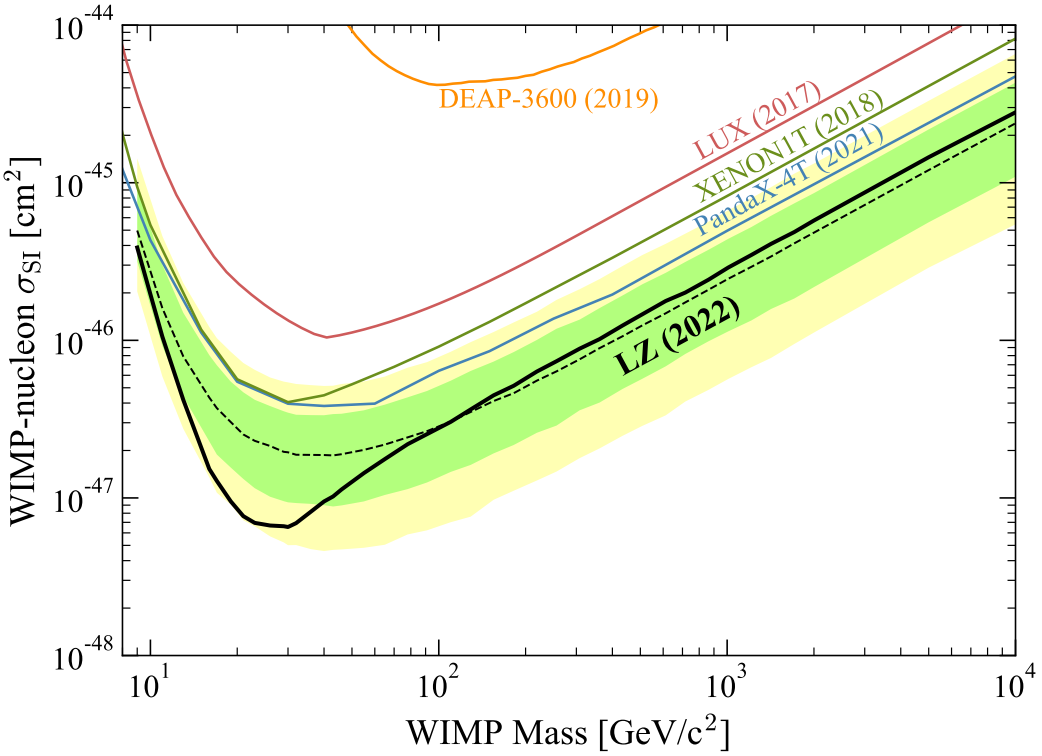

Figure 1.10: WIMP parameter space exclusion plot from direct detection for spin independent scattering [58].

For a cold relic density χ the density today is roughly

$$\Omega_\chi \simeq \frac{m_\chi n_\chi(T_{FO})}{\rho_{crit}} \sim \frac{m_\chi s_0}{T_{FO}\rho_{crit}M_P\langle\sigma v\rangle}$$

If we now use that roughly $m_\chi \sim T_{FO}$ (a more serious calculation would give $m_\chi \simeq 25T_{FO}$) and that

$$\rho \sim T_{eq}T^3 + T^4 \Rightarrow \rho(T_0) \sim T_{eq}T_0^3 \sim T_{eq}s_0$$

where T_{eq} as before is the Temperature of matter-radiation equality. With all these rough approximations, correct up to factors of order 10, the condition for a Cold Dark Matter candidate to reproduce DM abundance becomes

$$\langle\sigma v\rangle \sim \frac{1}{T_{eq}M_P}$$

And therefore the WIMP miracle boils down to the fact that we can express the weak scale as the geometric mean of T_{eq} and M_P

$$\frac{1}{v^2} \sim \frac{m_\chi^2}{v^4} \sim G_F^2 T_{FO}^2 \sim \langle\sigma v\rangle \sim \frac{1}{T_{eq}M_P}$$

1.3.2 Axions

For a complete review on the theoretical framework of axions and their phenomenological consequences see [52].

QCD-Axions

The QCD-Axion is a CP-odd pseudo-Nambu-Goldstone Boson that we introduce in order to solve the Strong CP problem.

The Strong CP Problem is a naturalness problem that arises once we notice that we could add the term

$$\mathcal{L}_\theta = \frac{\theta}{64\pi^2} G^A_{\mu\nu} G^A_{\rho\sigma} \epsilon^{\mu\nu\rho\sigma}$$

to the QCD Lagrangian and that this term, although it is a 4-derivative, contributes to the action because of boundary conditions. Experimental measures then yield

$$\bar{\theta} = \theta + \arg\det M_{quark} \ll 10^{-10}$$

where $\bar{\theta}$ is the $U(1)_A$ invariant version of θ. To solve this problem we introduce a new $U(1)_{PQ}$ global symmetry [9][10][8] [7]which is anomalous under the strong interactions and spontaneously broken at a scale f_{PQ}.

The result is a new particle with a model-independent coupling to gluons and some freedom in the other couplings due to the exact UV completion of the theory.

The most studied UV completions for axions are:

- **KSVZ axion**[11][12]: We add to the Standard Model a complex scalar σ charged under $U(1)_{PQ}$ and a Dirac vector-like (meaning its left and right components transform in the same way under $U(1)_{PQ}$) fermion $\mathcal{Q}$ in the fundamental representation of colour, singlet under weak isospin and neutral under hypercharge.

  $$\mathcal{L}_{KSVZ} = \partial_\mu \sigma^\dagger \, \partial^\mu \sigma - V(\sigma) + \bar{\mathcal{Q}} i \gamma^\mu D_\mu \mathcal{Q} - (y_{\mathcal{Q}} \sigma \bar{\mathcal{Q}} \mathcal{Q} + \text{h.c})$$

  And $V(\sigma)$ is the standard spontaneous symmetry breaking potential. The axion ϕ is again the Goldstone mode of σ. Integrating out the heavy radial mode and doing a chiral rotation of fields, gives the effective Lagrangian

  $$\mathcal{L}_{EFT} = \frac{1}{2} \partial_\mu \phi \, \partial^\mu \phi + \frac{\alpha_s}{16\pi v_{PQ}} \phi \, G^A_{\mu\nu} G^A_{\rho\sigma} \epsilon^{\mu\nu\rho\sigma}$$

  The axion could have also an electromagnetic coupling to $F\tilde{F}$ if the heavy quarks $\mathcal{Q}$ do not reside in the fundamental representation of color. In this model we require the anomaly to be generated by a new fermion $\mathcal{Q}$ which is heavy in the broken phase an can be integrated out. This permits the KSVZ axion to couple to gauge bosons only.

- **DFSZ axion** [13][14]: We add to the Standard Model a new Higgs doublet and a scalar field σ. We thus have two higgs doublets H_u and H_d used to give mass to the SM quarks and leptons (instead of H and $\tilde{H}$). The DFSZ UV Lagrangian is

  $$\mathcal{L}_{DFSZ} \supset -y_u^{(ij)} (Q^\dagger)^{(i)} H_u u^{(j)} - y_d^{(ij)} (Q^\dagger)^{(i)} H_d d^{(j)} - y_e^{(ij)} (L^\dagger)^{(i)} H_d e^{(j)} + h.c + V_{DFSZ}(H_u, h_d, \sigma)$$

  $$V_{DFSZ}(H_u, H_d, \sigma) = V(|H_u|^2, |H_d|^2, |\sigma|^2, |H_u H_d|^2) + \lambda (H_u H_d (\sigma^\dagger)^2 + h.c)$$

  and Peccei-Quinn charges are computed imposing the invariance of this Lagrangian under the PQ symmetry (so for example $2q_\sigma = q_{H_u} + q_{H_d}$). We can have slight modifications to this Lagrangian, for example coupling the lepton sector to $\tilde{H}_u$ as done in the SM, but the idea is basically the same. Both the gauge symmetry of the SM and the PQ symmetry are spontaneously broken and in the low energy EFT the axion couplings become

  $$\mathcal{L}_{EFT} \supset \frac{N\alpha_s}{16\pi f_a} \phi \, G^A_{\mu\nu} G^A_{\rho\sigma} \epsilon^{\mu\nu\rho\sigma} + \frac{\alpha_{em}}{16\pi f_a} \frac{E}{N} \phi F_{\mu\nu} F_{\rho\sigma} \epsilon^{\mu\nu\rho\sigma} + \frac{\partial_\mu}{2 f_a} [c_u \bar{u} \gamma^\mu \gamma^5 u + c_d \bar{d} \gamma^\mu \gamma^5 d + c_e \bar{e} \gamma^\mu \gamma^5 e]$$

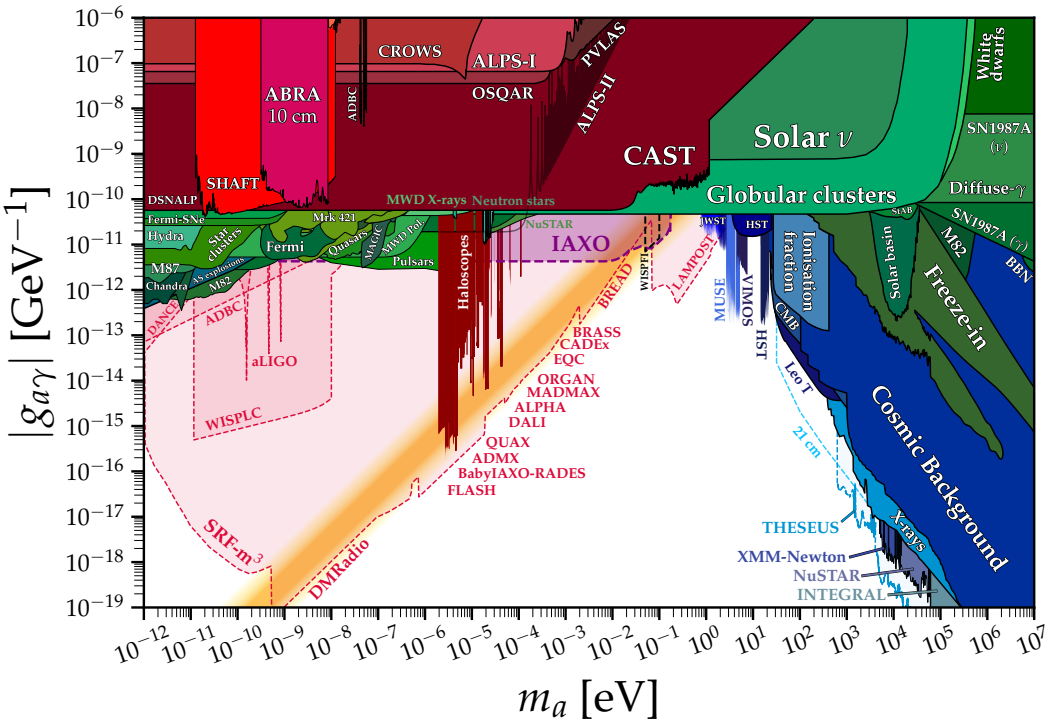

Figure 1.11: Parameter space exclusion plot for QCD axions and Axion-Like Particles. On the x axis we have the axion mass and on the y-axis the coupling of axions to photons. The dashed limits are predicted experimental sensitivities of approved future experiments. It must be noticed that although at the moment almost all axion searches rely on the axion coupling to photons, alternatives have been proposed, for example CASPEr [34] will look directly for the axion coupling to gluons reaching the QCD-line.

with the conventions

$$N = n^\circ\text{domain wall} \qquad \frac{E}{N} = \frac{8}{3} \qquad \tan(\beta) = \frac{v_u}{v_d} \qquad c_u = \frac{1}{3}\cos^2(\beta) \qquad c_d = c_e = \frac{1}{3}\sin^2(\beta) \qquad f_a = \frac{v_{PQ}}{N}$$

Axion-Like Particles

Axion-Like Particles (or ALPs) are particles that have the same derivative-type couplings of the QCD-Axion, and of all Goldstone Bosons in general, but have more freedom (at the price of being theoretically less motivated), because we allow them not to solve the Strong CP problem. Their coupling to gluons is therefore no more fixed by the single parameter f_{PQ} that sets the mass of the ALP. We can therefore have for example really heavy ALPs without implying a strong coupling to gluons, that would make them visible and decaying into Hadrons. It has to be mentioned that String Theory provides a theoretical setting in which ALP would appear naturally.

1.3.3 Dark Photon

Dark Photons [16] are massive $U(1)$ gauge bosons that could constitute ultralight boson Dark Matter. The Lagrangian of the field A' is

$$\mathcal{L}_{DP} = -\frac{1}{4}F_{\mu\nu}F^{\mu\nu} - \frac{1}{4}F'_{\mu\nu}F'^{\mu\nu} - \frac{1}{2}\epsilon F_{\mu\nu}F'^{\mu\nu} - \frac{1}{2}m^2 A'_\mu A'^\mu$$

Where we have included the kinetic term of the SM photon γ and allowed for a mixing parameter ϵ in the kinetic term. Diagonalizing the kinetic part of the Lagrangian we immediately see that the Dark Photon

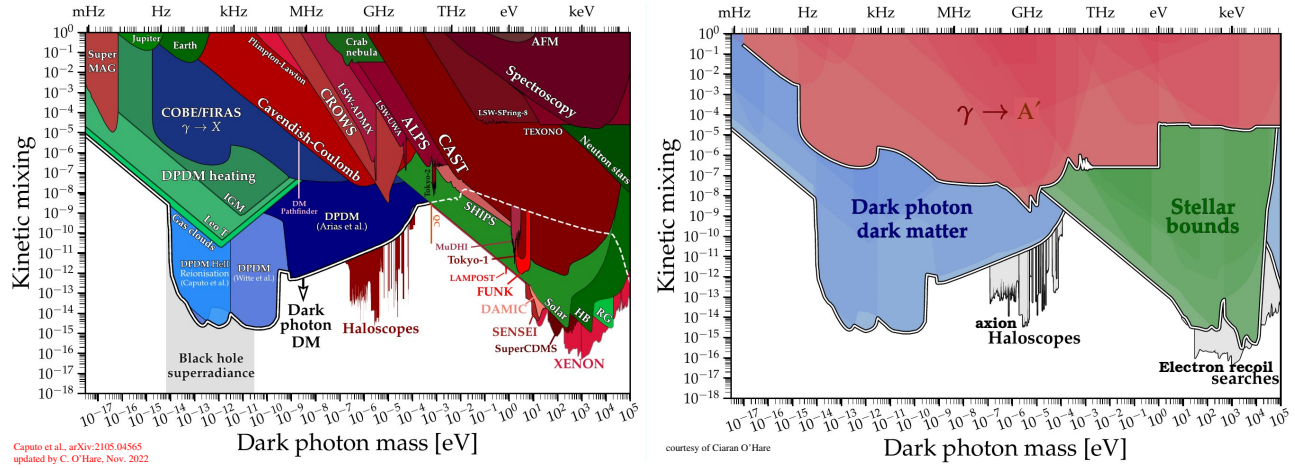

Figure 1.12: Dark photon parameter space exclusion plot taken from [62] and their grouping. The first image comes from [53], the second is a courtesy of C. O'Hare.

would have interactions of order $\sim \epsilon e$ (Using the Dark Photon as a mediator could thus give millicharged Dark Matter). The mass of the Dark Photon can be introduced in a Gauge invariant way by a new Higgs Sector or by the Stuckelberg Mechanism [62].

We report in figure 1.12 the exclusion plot for the Dark photon parameter space (m, ϵ). The Dark photon has to be light (otherwise it would be a sort of WIMP Dark Matter), we thus need Dark photons to be produced by a non-thermal mechanism to evade free-streaming bounds. A Misalignment Mechanism for the Dark Photon is not efficient, but other production mechanisms are possible, for example using inflation [23].

1.3.4 Sterile Neutrinos

Sterile Neutrinos are one of the most straightforward ways to extend the standard model. They permit to give a mass to the SM left-handed neutrinos, at the same time they are a gauge singlets under all the SM gauge groups. They thus interact only through their mixing with SM neutrinos and are therefore a good Dark Matter candidate.

Being uncharged under every SM gauge group their Lagrangian admits the so called Majorana mass term

$$\mathcal{L}_{\nu \text{ masses}} = -y\epsilon^{ij} H_i L_j N^\dagger - \frac{1}{2} N N + \text{h.c.}$$

Where we wrote for semplicity the Lagrangian for only one lepton and sterile neutrino generation but it is easily generalizable to more than one (for the conventions on the Standard Model Lagrangian see the Appendix). Unfortunately the Majorana mass required for them to give a small mass to SM neutrinos in a natural way is at the GUT scale, while the mass required for them to constitute the majority of DM is at keV − MeV scales. The main production mechanism of sterile Neutrinos is through oscillation from standard neutrinos, sterile neutrinos therefore have a non-thermal spectrum [20]. The region of parameter space in which right-handed neutrinos would constitute all Dark Matter is unfortunately excluded by gamma-rays telescope observations.

1.3.5 Primordial Black Holes

Primordial Black Holes (PBH) are the only way in which baryonic matter can constitute a large fraction of Dark Matter. The DM evidences we have from CMB and BBN point towards having a large fraction of the Universe's energy budget not interacting with light at those early epocs. Since no neutral long-lived

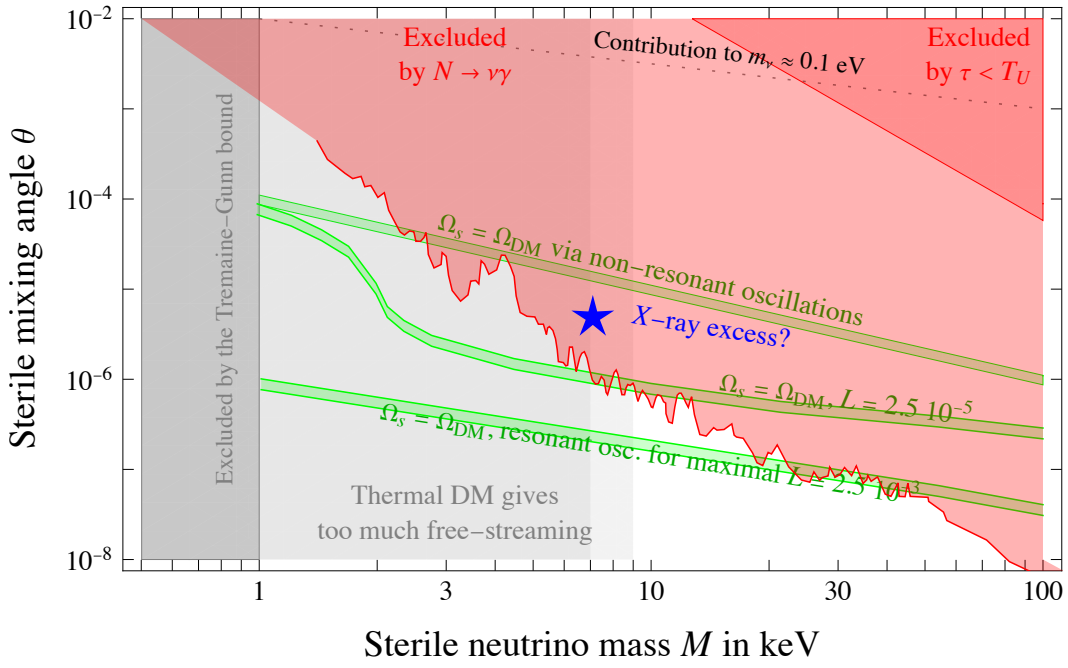

Figure 1.13: Sterile Neutrinos exclusion plot, taken from [61]. The red region is excluded from DM decays into X-rays [31], while in the dark red region DM also has a lifetime that is shorter than the age of the Universe. Production via non-resonant neutrino oscillations reproduces the DM abundance in the upper green band, while resonant oscillations give the lower green bands, which assume the indicated lepton asymmetry [31]. The light gray region below $M < 9$keV is excluded by free-streaming, if DM has thermal velocity; such bound becomes somewhat weaker, if DM has a mildly sub-thermal velocity distribution (mid-dark gray). Below the dotted line the N contribution to the active neutrino masses is below their observed values. The star indicates the possible 3.5keV excess, which has for long time been interpreted as evidence of Sterile Neutrino DM, but is due to background signal of potassium isotopes [38][59].

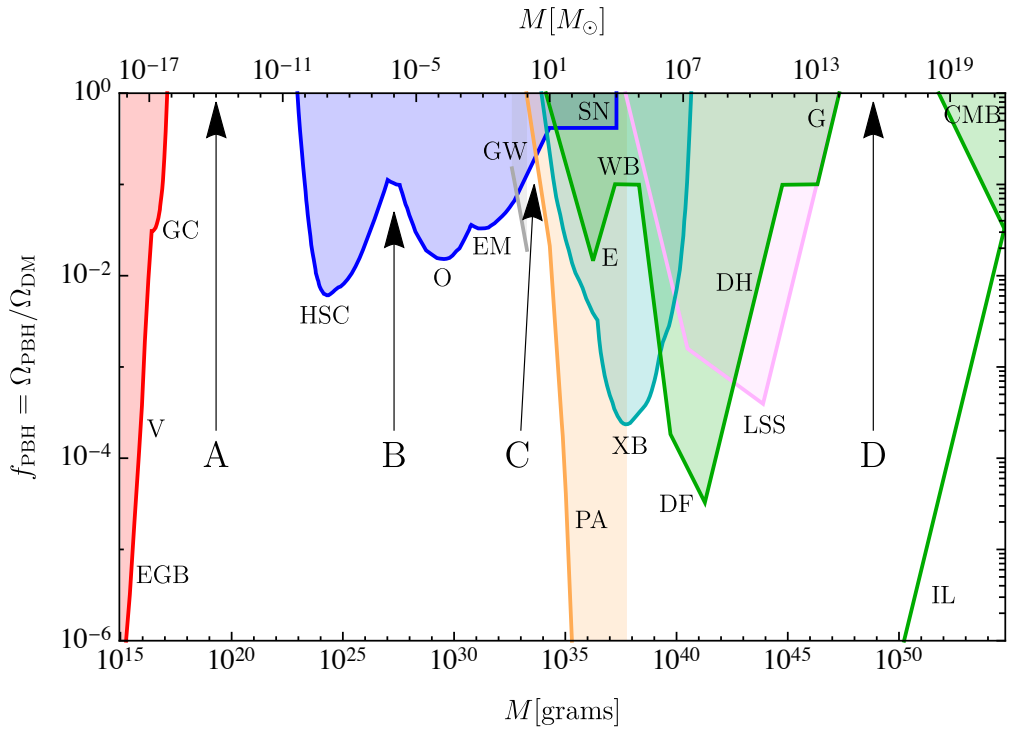

Figure 1.14: Constraints on the primordial black hole dark matter fraction fPBH for a monochromatic mass function. The individual bounds are from evaporation (red), lensing (blue), gravitational waves (GW) (grey), dynamical effects (green), accretion (light blue), CMB distortions (orange) and large-scale structure (purple). The evaporation limits come from the extragalactic γ-ray background (EGB), the Voyager positron flux (V) and annihilation-line radiation from the Galactic centre (GC). The lensing constraints derive from microlensing of supernovæ (SN) and of stars in M31 by Subaru (HSC), the Magellanic Clouds by the Experience pour la Recherche d'Objets Sombres (EROS) and Massive Compact Halo Object (MACHO) collaborations (EM), and the Galactic bulge by the Optical Gravitational Lensing Experiment (OGLE) (O). The dynamical bounds are from wide binaries (WB), star clusters in Eridanus II (E), halo dynamical friction (DF), galaxy tidal distortions (G),heating of stars in the Galactic disk(DH) and the cosmic microwave background dipole (CMB). The large-scale structure (LSS) limits are due to the requirementthat various cosmological structures do not form earlier than observed. The accretion constraints derive from X-ray binaries (XB) and Planck measurements of cosmic microwave background distortions (PA). Finally, the incredulity limits (IL) correspond to one PBH per relevant environment (galaxy, cluster, Universe). Note that these are actually lower bound. The four mass windows (A, B, C, D) indicate regions in which PBHs could have an appreciable density, assuming the validity of the mentioned constraints. The plot and the whole caption is taken from [63].

bound states are known to be possible in the Standard Model at such high temperatures, the only way baryonic matter would have to not interact with light would be to sit inside Black Holes.
PBH are thus the only Dark Matter candidate not requiring explicitly the introduction of a new particle, but they would nonetheless require new physics to explain how the large density fluctuations needed for their formation (see [63] for possible formation mechanisms), could occur in the Early Universe.
The mass of PBH is subjected to strong constraints from CMB formation, gravitational lensing, Hawking radiation and others [63] reported in figure 1.14.

In recent years the mass and spin of Black Holes measured by the LIGO collaboration has further sparked interest around PBH with masses of the order of $M \sim 3M_\odot$

1.3.6 Dark Sectors

Until now we have simply discussed Dark Matter candidates consisting in relatively minimal additions to the Standard Model consisting of adding a particle or one force mediator. We could instead think of Dark

Matter having a rich structure, exactly like normal matter containing different particles and maybe also bound states. In this models DM could be coupled to one or more dark forces, which can have a light or massless mediator. The presence of this Dark Forces changes significantly the phenomenology of Dark Matter enhancing or suppressing also interactions that aren't mediated from those.

The requirement that Dark Matter is not constituted by a single particle relaxes the constraint on the scale of new physics. This Dark Sector can have only gravitational interaction with the Standard Model, or interact with it through some other portal. The lowest dimensional portals available to interact with the SM are:

- $\mathcal{L} = -\frac{1}{2}\,\epsilon\, B^{\mu\nu} F'_{\mu\nu}$ – dark photon A'_μ kinetically mixed with hypercharge,
- $\mathcal{L} = (AS + \lambda S^2) H^\dagger H$ – dark scalar S coupled to the Higgs,
- $\mathcal{L} = y_N L H N$ – dark fermion N coupled via the lepton portal,
- $\mathcal{L} = \frac{\partial_\mu a}{f_a} \overline{\psi} \gamma^\mu \gamma^5 \psi$ – axion-like pseudoscalar a coupled to the axial current.

Gravitational DM

If instead Dark Matter is interacting only gravitationally we have its tree-level interactions of order

$$\sim \frac{T_{\mu\nu} T^{\mu\nu}}{M_P^2 s}$$

Where s is the Mandelstam variable. The production of GDM is thus dominated by production at high energies, in particular right after reheating

$$T_{RH} \sim \sqrt{\Gamma_\phi M_P}$$

Except in the limit of instantaneous inflaton decay $\Gamma_\phi \to \infty$ in which

$$T_{RH} = T_{max} \sim (E_I^2 M_P \Gamma_\phi)^{\frac{1}{4}}$$

and E_I is the energy density scale during inflation ($\rho_\phi = E_I^4$).

$$Y_{DM} \sim e^{-\frac{2M}{T}} \frac{T_{RH}^3}{M_P^3}$$

This implies that the minimal reheating temperature for which gravitational Dark Matter is viable is $T_{RH} \sim 10^{12}\,\text{GeV}$.

QCD-like bound states

Dark Matter can be strongly coupled under some dark color group whose dynamics becomes non-perturbative under some scale Λ_{DC}. These particles are then confined in bound states. Over Λ_{DC} our fundamental particles can be charged also under the SM groups, but are combining into neutral states (exactly as the neutron is composed by charged particles, but is neutral) under these scales.

It is appealing then to think that also the Dark Sector Lagrangian, exactly like the SM one, presents accidental symmetries which result in stable particles.

Chapter 2

Minimal Dark Matter

In this chapter we are going to study a very interesting extension of the standard model known as Minimal Dark Matter (MDM) and its main constraints. The model was first introduced in by Strumia, Cirelli and Fornengo [25].

2.1 The Model

The model is called Minimal for multiple reasons: we are adding only one field χ (a multiplet) to the Standard Model and we are considering it to be coupled to the Standard Model only through covariant derivatives, meaning we do not introduce explicit couplings except those which are necessary to ensure gauge invariance. This in turn means that the only parameter on which all the predictions of the model do depend is the multiplet mass M. Our new Lagrangian is therefore

$$\mathcal{L} = \mathcal{L}_{SM} + \mathcal{L}_{MDM}$$

$$\mathcal{L}_{MDM} = C \begin{cases} (D_\mu \chi)^\dagger (D^\mu \chi) - M^2 \chi^\dagger \chi \\ \bar{\chi}(i\not{D} - M)\chi \end{cases} \qquad C = \begin{cases} 1 \text{ for complex fields} \\ \frac{1}{2} \text{ for real fields} \end{cases}$$

We will also require our field χ to have the following features to provide a credible Dark Matter candidate:

- it has no strong interactions. [17]
- One of the components of the multiplet is neutral, meaning $0 = Q = T_3 + Y$. So, if our particle is in a $2s+1$ dimensional representation of the weak isospin group, we have s possible assignments of hypercharge (if χ is complex).

2.1.1 Mass term for Complex Fields

If our multiplet is a complex scalar field, writing an $SU(2)$ invariant mass term is no challenge. The standard

$$\mathcal{L} = (D_\mu \chi)^\dagger (D^\mu \chi) - M^2 \chi^\dagger \chi$$

is explicitly gauge invariant. We could set up a discussion (as we will do in the following section for Real Fields) regarding whether the mass term we wrote above is the most general $SU(2)$ invariant one. If we take the most general form

$$\chi^\dagger \mathbb{M} \chi$$

where $\mathbb{M}$ is a complex Hermitian matrix, we can immediately conclude, by Schur's Lemma, that M has to be proportional to the identity and so the term we have written is completely general.

For Dirac Fermions instead we have a less straightforward job. The Dirac Lagrangian is

$$\mathcal{L} = \bar{\chi}(i\not{D} - M)\chi = iX_L^\dagger \bar{\sigma^\mu} D_\mu X_L + iX_R^\dagger \sigma^\mu D_\mu X_R - MX_R^\dagger X_L - MX_L^\dagger X_R$$

If we take χ to be charged under the weak isospin group as the Standard Model fermions, it is an easy check that the mass term is not invariant and the Higgs Mechanism is needed. This would force us to introduce a Dark Higgs and a handful of other parameters our model therefore would not have only one parameter. A way out of these issue is to consider also right-handed components of our fermionic field χ in the same representation of $SU(2)_L$ as the left-handed ones. This would make the mass term gauge invariant in the exact same way of complex scalar field one. This means that weak interactions couple to right-handed and left-handed components of χ with the same strength. Such a fermion χ is said to be vector-like.

2.1.2 Mass term for Real Fields

In this section we want to investigate when a Real Field admits an $SU(2)$ invariant mass term. With this term we indicate real scalar fields, Majorana fermions and in general every field whose mass in the Lagrangian is given by the field bilinear

$$\mathcal{L} \supset \chi^T S \chi$$

for some matrix S. In the expression we have omitted all the possible fermionic or tensor structure because we want to focus on the invariance under the gauge groups of the Standard Model. This bilinear has no chance to be $U(1)$ invariant and we must therefore require it to be neutral under hypercharge

$$Y = 0$$

we want now to be completely general and study its transformation under a general unitary representation $D(g)$ of a gauge group G.

$$\chi^T A \chi \to \chi^T D^T(g) S D(g) \chi$$

The invariance under this transformation for every element of the group g would imply

$$\begin{aligned} D^T(g^{-1}) S D(g^{-1}) &= S \\ (D^\dagger(g))^T S D^\dagger(g) &= S \\ D^*(g) &= S D(g) S^{-1} \\ D(g) &= S^{-1} D^*(g) S \end{aligned} \tag{2.1}$$

But this implies that the representation is similar to its conjugate representation and therefore the representation is not genuinely complex. We analyse in detail reality and pseudo-reality of $SU(2)$ representations in the Appendix D.
It turns out that $SU(2)$ has only real and pseudo-real representations. The first ones are the one with integer spin, while the second ones have half-integer spin. As $Y = 0$ we obtain that for a Real Field $Q = T^3$. If we want a component of the multiplet to be a legitimate Dark matter candidate, it has to be neutral. This tells us that we only care about integer spin representations and, for what we have argued above, we care only about real representations.

Mass Spectrum

Thanks to group theory we now know that there exists a basis in which the mass term of our Real Field takes the form

$$\mathcal{L} \supset \frac{C}{2}\chi^T\chi \qquad C = \begin{cases} M^2 & \text{for bosons} \\ M & \text{for fermions} \end{cases}$$

Unfortunately neither of these fields are charge eigenstates. For the real scalar field this is how far we can get, because it only makes sense to consider it in an explicitly real representation of $SU(2)$, but for Majorana fermions we can find S in the charge eigenbasis.
Taking the representation in which $Q = T_3$ is diagonal we have

$$T_3 = \begin{pmatrix} s & 0 & \cdots & & \\ 0 & s-1 & \cdots & & \\ \vdots & \vdots & \ddots & \vdots & \vdots \\ & & \cdots & -s+1 & 0 \\ & & \cdots & 0 & -s \end{pmatrix} \tag{2.2}$$

The rising and lowering operators are usually taken to be real, and so T_1 is real while T_2 is purely imaginary, which is clearly not explicitly real (for the representation to be real the generators of the Lie Algebra have to be purely imaginary), and thus $S \neq \mathbb{I}$. The infinitesimal version of (2.1)

$$-T_i^* = ST_iS^{-1}$$

thus requires to find a matrix which is commuting with T_2 and anti-commuting with T_1 and T_3. The anti-commutation relation with T_3 forces the matrix to be anti-diagonal and the anti-commutation relation with T_1 gives us a recurrence relation between the entries on the anti-diagonal:

$$S_{m,\,-m} = -S_{(m-1),\,(1-m)}$$

Up to a rephasing of the basis we can bring S to the form

$$S = \begin{pmatrix} & & \cdots & 0 & 1 \\ & & \cdots & 1 & 0 \\ \vdots & \vdots & \iddots & \vdots & \vdots \\ 0 & 1 & \cdots & & \\ 1 & 0 & \cdots & & \end{pmatrix}$$

We can now see that, in the charge eigenbase, the mass matrix S mixes the $2s+1$ Majorana fermions we had initially forming s Dirac fermions with charges $\pm e$, $\pm 2e$, $\pm 3e$, ..., $\pm se$ and a neutral Majorana fermion.

2.2 Corrections to the mass

2.2.1 Loop Corrections

At tree-level all the components of the Dark Matter multiplet have the same mass not to break the $SU(2)$ symmetry. When the symmetry is spontaneously broken, under the weak scale, the loop correction can distinguish between charged and uncharged components of the multiplet. Charge thus creates a mass splitting. In our model Dark Matter couples only to gauge bosons, therefore at 1-loop level, these will be the only relevant interactions.

In Appendix B we go through the entire loop computation and all the Feynman diagrams involved. The final result is

$$M_Q - M_{Q'} = \frac{Mg^2}{16\pi^2}\left[s_W^2(Q^2-Q'^2)\tilde{f}\left(\frac{m_Z}{M}\right)+(Q-Q')(Q+Q'-2Y)\left[\tilde{f}\left(\frac{m_W}{M}\right)-\tilde{f}\left(\frac{m_Z}{M}\right)\right]\right] \tag{2.3}$$

$$\tilde{f}(r) = \begin{cases} -\frac{r}{4}\left[2r^3\ln(r) - Kr + (r^2-4)^{\frac{3}{2}}\ln\left(\frac{r^2-2-r\sqrt{r^2-4}}{2}\right)\right] & \text{for bosons} \\ \frac{r}{2}\left[-2r+2r^3\ln(r)+\sqrt{r^2-4}(r^2+2)\ln\left(\frac{r^2-2-r\sqrt{r^2-4}}{2}\right)\right] & \text{for fermions} \end{cases}$$

The only subtleties in this formula are associated with the UV diverging constant K. When $Y=0$, K does not contribute to the mass splitting as it multiplies

$$(Q^2-Q'^2)(m_W^2 - m_Z^2 c_W^2) = 0$$

Otherwise we are forced to introduce a non-minimal coupling of MDM to the Standard Model to reabsorb this divergence and obtain physical predictions, we will see how in the next section.

We ignore for now the K term and take the limit $\tilde{f}(r) \xrightarrow{r\to 0} 2\pi r$, to correctly evaluate it we must properly take into account the branch cuts. If we take the square root and the logarithm to have branch cuts on the real negative axis, the function $\tilde{f}(r)$ has a branch cut on all the imaginary axis and another branch cut between $+2$ and -2. It can be showed that approaching the origin from the half-plane in which $\mathrm{Re}\{r\} > 0$ gives $2\pi r$ and approaching the origin from the half-plane where $\mathrm{Re}\{r\} < 0$ gives $-2\pi r$. For the definition of r we are clearly interested only on the extension to the positive half-plane and thus we get the desired result, both for fermions and bosons.

Taking this limit in the mass-splitting we obtain that the mass splitting when $M \gg m_Z$, m_W is independent on the multiplet mass and spin:

$$M_Q - M_{Q'} = \frac{m_Z g^2}{4\pi}\sin^2\left(\frac{\theta_W}{2}\right)(Q-Q')((Q+Q')c_W + 2Y)$$

This has a physically clear interpretation, as noted in [25].

From this formula we can see that the lightest partner of the multiplet has charge

$$Q_{\text{light}} = \begin{cases} -\left\lfloor \frac{Y}{c_W}\right\rfloor & \text{if } \frac{Y}{c_W} - \left\lfloor \frac{Y}{c_W}\right\rfloor < \frac{1}{2} \\ -\left\lfloor \frac{Y}{c_W}\right\rfloor - 1 & \text{if } \frac{Y}{c_W} - \left\lfloor \frac{Y}{c_W}\right\rfloor > \frac{1}{2} \end{cases}$$

The order of magnitude of our mass splitting is

$$\Delta M = \frac{m_Z g^2}{4\pi}\sin^2\left(\frac{\theta_W}{2}\right) = (166 \pm 1)\,\text{MeV} \tag{2.4}$$

The order of magnitude of this mass splitting tells us immediately that beta decays of the heavier components of our multiplet are be kinematically allowed. This means that the only stable component of the multiplet is the lightest one. If we want it to be a Dark Matter candidate, it should be neutral. Being [64]

$$c_W = 0.87660 \pm 0.00017$$

This value is close to one enough to have

$$Q_{\text{light}} \sim Y$$

at least for low values of Y. This implies that, in order for Minimal Dark Matter to represent a viable Dark Matter candidate, without introducing non-minimal couplings to the Standard Model, the multiplet χ must have

$$Y = 0 \quad \text{or} \quad Y = s$$

where s is with the previous definitions the maximum value allowed for T_3 of a "spin-s" representation.

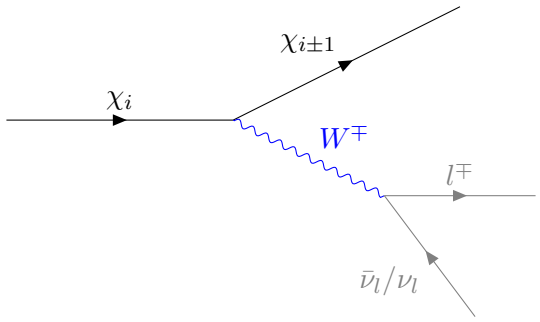

Figure 2.1: Beta decay of heavier components of the multiplet χ

2.2.2 Non-minimal couplings

Scalar Minimal Dark Matter further admits the following renormalizable operators, correcting the mass at tree-level or loop-level:

$$\lambda_H(\chi^\dagger T^a_\chi \chi)(H^\dagger T^a_H H) \qquad \lambda'_H(\chi^\dagger\chi)(H^\dagger H) \qquad \lambda_\chi(\chi^\dagger T^a_\chi\chi)^2 \qquad \lambda'_\chi(\chi^\dagger\chi)^2$$

The only tree-level corrections are given by the first two terms after SSB. The second term just gives an overall correction to the tree-level mass. The second term instead induces also a mass splitting, which is given by

$$\Delta M_H = \frac{\lambda_H v^2}{8M} T^3_\chi \simeq \left(7.6\,\text{GeV}\frac{\text{TeV}}{M}\right)\lambda_H T^3_\chi$$

At 1-loop level all terms give a correction to the mass, but again only the first can give a contribution to the mass splitting. The loop correction gives a diverging contribution proportional to $\lambda_H T_3$ and we can reabsorb it tin the renormalization of λ_H.

Finally for completeness also the diverging constant K in the previous section can be reabsorbed in the renormalization of M and λ_H. In fact both the mass splitting proportional to K in (2.3) and λ_H in this section are proportional to Q, once we realize that Y is a constant for every component of the multiplet. Therefore if we look at a scalar complex field we are forced to introduce this new coupling. Taking

$$|\lambda_H| \gtrsim \frac{1}{50}\frac{M}{\text{TeV}}$$

would change significantly our model and could allow for $Q = 0$ even when $Y \neq 0$. To have a model with the lowest number of important parameters we will take

$$|\lambda_H| \lesssim \frac{1}{100}$$

In such a way that we can neglect the shift induced by this operator in our phenomenology. In this approximation, we are forced to have $Y = 0$ or $Y = s$ in order to have a stable neutral particle.

2.3 Neutral Partner as Dark Matter

2.3.1 Beta Decay

The heavier components of the Dark Matter multiplet can undergo semi-leptonic decay on lighter components. The kinematically allowed decays are onto electrons, muons and pions. For simplicity we will focus only on the decay on electrons, since is the only one in which 2 out of the three particles can be considered massless. Muons and pions have respectively masses of 105 MeV and 140 MeV which is really

near to the mass splitting between the components of the multiplet. In this approximation the rate is easily given by

$$\Gamma = \frac{G_F^2 M_i^5}{192\pi^3} F\left(\frac{M_{i\pm1}}{M_i}\right)$$

$$F(x) = \begin{cases} \frac{1}{2}(1-x^2)^4 & \text{B-E} \\ \frac{1}{6}(1-x)^4(3+4x-2x^2+4x^3+3x^4) & \text{F-D} \end{cases}$$

The life-times of the heavier states, for a tree-level mass of the order of the TeV are below $1\,\mu$s. Therefore there is no chance for heavier components to constitute Dark Matter and we are forced to assume $Y = 0$.

Also the Decay on pions is easily computed, having 2 body phase space. And we find

$$\Gamma = \frac{G_F}{8\sqrt{2}\pi}\frac{f_\pi^2}{m_W^2} M_i \left[(M_i^2 - M_{i\pm1}^2 + m_\pi^2)^2 - 4M_i^2 m_\pi^2\right]^{\frac{1}{2}} \begin{cases} \frac{1}{2}\left(\frac{3M_i^2+M_{i\pm1}^2-m_\pi^2}{M_i^2}\right)^2 & \text{B-E} \\ \frac{M_i^4+2M_{i\pm1}^4+m_\pi^4-5M_i^2M_{i\pm1}^2-3m_\pi^2M_{i\pm1}^2+2M_i^2m_\pi^2+2M_iM_{i\pm1}^3}{M_i^4} & \text{F-D} \end{cases}$$

This decay is very important for direct detection since it generates a soft pion which could result in a missing trace at colliders. For example a pion emitted in the transition from the charge-1 component to the neutral one would have a speed

$$v_\pi = \frac{p_\pi}{E_\pi} \sim 0.26$$

2.3.2 Stability

To be a good Dark Matter candidate the Lightest Neutral partner has to be stable.

We can achieve all of this introducing a $\mathbb{Z}_2$ symmetry associated with the multiplets of particles we have added, but we want to discuss when this can be avoided.

It is fairly easy to see that for low-dimensional multiplets we can always construct with the $SU(2)$ doublets in the Standard Model a structure that allows their one particle decay.

Combining n doublets in a tensor product we can achieve at most a representation with dimension

$$d_{max}^{(n)} = n + 1$$

this can be seen using Clebsch-Gordan decomposition. Thus a scalar n-multiplet can always be combined with $n+1$ Higgses to achieve a decay. This operator has an energy dimension of

$$[\chi HH....HH] = n$$

where in a symbolic notation we are indicating only the involved fields and not the explicit contractions or complex conjugations. The whole discussion can be repeated for a fermion with operators containing to SM doublets (one of which needs to be a fermion) like

$$[\bar{\chi} LH...H] = n + 1$$

Once we start introducing non-renormalizable operators the operator needs to be suppressed from some scale Λ^p. To make an estimate the lifetime of a particle induced by such an operator would be

$$\tau \sim \Lambda^{2p} M_\chi^{-1-2p}$$

For masses $M_\chi \sim$ TeV, the request to have

$$\tau \sim 10^{28}\,\text{s} = 10^{55}\,\text{TeV}^{-1}$$

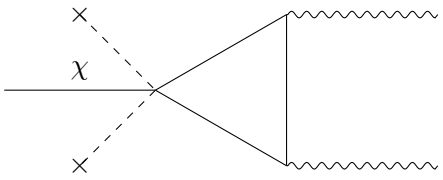

Figure 2.2: Loop-induced decay from the $\chi\chi\chi HH$ operator.

implies

$$\Lambda \gtrsim \begin{cases} 10^{27}\,\text{TeV} & \text{for } p=1 \\ 10^{14}\,\text{TeV} & \text{for } p=2 \\ 10^{9}\,\text{TeV} & \text{for } p=3 \\ .... \end{cases}$$

We therefore list also dimension 5 operators since the suppression scale would need to be greater than the Planck Mass in order to have a sufficient decay timescale.

High dimensional multiplets (from the fermion quintuplet and the scalar eptuplet) should therefore be automatically stable in the same way the proton is stable in the SM! However there is a subtlety for the scalar eptaplet [36]: even if we cannot write a renormalizable operator containing just one power of χ, we can design operators with 3 powers of χ which allow the decay of χ at loop level through a triangle diagram to gauge bosons 2.2. For example we can consider operators like:

$$\chi\chi\chi HH$$

The tensor representation $\mathbf{7}\otimes\mathbf{7}\otimes\mathbf{7}\supset\mathbf{1}\oplus\mathbf{3}^3$, we indicated the multiplicity of the representation at the exponent. The Standard model has no scalar singlet to which we can couple and thus the minimal operator is the one written above. We can construct the SM part both as a singlet or a triplet made up of $H^\dagger H$ and as a triplet HH.

This operator can mediate an annihilation with a Higgs Boson in an unbroken phase and induces and creates a decay operator for the χ particle once the Higgs field acquires a VEV. The loop is clearly dominated by energies of order of M_χ. Thus the timescale of χ induced by this operator turns out being

$$\tau \sim \left(\frac{1}{M_\chi} g^4 \left(\frac{M_\chi^4 M_\chi^2}{M_\chi^6}\right)^2 \frac{v^4}{\Lambda^2}\right)^{-1}$$

$$\Lambda \gtrsim 10^{23}\,\text{TeV}$$

2.3.3 Naive determination of the Relic Density

The relic density of Minimal Dark matter is given by co-annihilations, see Appendix C for more details. Being the mass of MDM much greater than the weak scale, the cross sections $\langle\sigma v\rangle_{ij}$ can be computed in the limit in which the $SU(2)_L\otimes U(1)_Y$ is unbroken. For scalars the 3-particle vertex is proportional to the momentum, all s-channel annihilation to matter content of the Standard model is thus p-wave suppressed [1] or involve an extra power of g and we can neglect them at least in a first approximation. The only relevant annihilations are thus annihilation into gauge bosons

$$\langle\sigma v\rangle_{eff}^{(\text{s-wave})} \simeq \frac{g^4\,(3-4n^2+n^4)+16\,Y^4b^4+8g^2b^2Y^2(n^2-1)}{64\pi\,M^2\,g_\chi} \qquad \text{if } \chi \text{ is a scalar} \tag{2.5}$$

[1] To see it it is sufficient to look at the Feynman rule for the scalar QED vertex in the s-channel:

$$\text{Vertex} \propto ie(p_1^\mu - p_2^\mu)$$

Where $g_\chi = 2n$ for a complex scalar and $g_\chi = n$ for a real scalar. For fermions instead we must consider also decays on the matter content of the Standard Model. Obtaining

$$\langle\sigma v\rangle_{eff}^{(\text{s-wave})} \simeq= \frac{g^4\ (2n^4+17n^2-19)+4Y^2b^4(41+8Y^2)+16g^2b^2Y^2(n^2-1)}{128\pi\ M^2\ g_\chi} \qquad \text{if } \chi \text{ is a fermion.} \tag{2.6}$$

And now $g_\chi = 4n$ for a Dirac fermion and $g_\chi = 2n$ for a Majorana fermion. Obviously non minimal couplings give additional contributions to this annihilation rates, for example the renormalizable operator needed to renormalize the scalar DM mass

$$\lambda_H(\chi^\dagger T^a_\chi \chi)(H^\dagger T^a_H H)$$

gives the only annihilation (intended as pure annihilation and not co-annihilation when $Y = 0$) contribution between the LNPs. And its contribution is easy to compute, but we will disregard all these terms and stick to minimality.

If we now solve the Boltzmann equation for co-annihilations in the standard instantaneous freeze-out approximation, meaning that we consider the relic density to be fixed when

$$H \sim \Gamma = 3\langle\sigma v\rangle_{eff} n_{eq}$$

The relic density is then well-approximated by

$$\frac{n_{DM}(T)}{s(T)} \approx \sqrt{\frac{180}{\pi\ g_{SM}}}\frac{1}{M_P\ T_f\langle\sigma v\rangle_{eff}}, \qquad \frac{M}{T_f} \approx \ln\frac{g_\chi M M_P\langle\sigma v\rangle_{eff}}{240\ g_{SM}^{1/2}} \sim 26$$

$$\rho_{DM}(T_0) = M n_{DM}(T_0) = \sqrt{\frac{180}{\pi\ g_{SM}}}\frac{M s_0}{M_P\ T_f\langle\sigma v\rangle_{eff}} \tag{2.7}$$

In order to match the experimental evidence that

$$\Omega_{DM}h^2 = \frac{\rho_{DM}}{\rho_{crit}}h^2 = 0.1200 \pm 0.0012$$

This determination of the Dark Matter mass has some problems:

- We neglected p-wave suppressed contribution to the cross section.
- We neglected contributions which are more than quartic in the couplings
- We assumed instantaneous freeze-out.

The first and third issue can be taken into account quite easily simply using a numerical simulation of the Boltzmann equation, with the cross section that will acquire a dependence from temperature. The second issue is more serious: a priori we could just say that we can retain just a finite number of higher loop contributions and obtain the desired precision. It turns out, as we will see in the next sections higher loop computations are enhanced like $1/v$ and this implies that for $v \sim \frac{1}{g}$ we have to take into account an infinite number of diagrams! Notice that such a behaviour could mean that higher loop p-wave suppressed processes could behave as s-wave processes, but they would be suppressed by a higher power of the coupling and therefore is not a major concern. This effect is known as Sommerfeld Enhancement and will be the subject of all the following chapters.

If we choose the CM frame where

$$p_1 = (E_p, \vec{p}) \quad p_2 = (E_p, -\vec{p})$$

we immediately have

$$p_1 - p_2 = (0, 2\vec{p})$$

signaling the p-wave suppression. Obviously also decay to gauge bosons in the s-channel is p-wave suppressed, but decays to gauge bosons are possible also in the t and u channels and via the 4-particle vertex.

Quantum numbers $SU(2)_L$	$U(1)_Y$	Spin	DM can decay into	DM mass in TeV	$M_{\mathrm{DM}^\pm} - m_{\mathrm{DM}}$ in MeV	Events at LHC $\int \mathcal{L}\, dt$ =100/fb	σ_{SI} in $10^{-45}\,\mathrm{cm}^2$
2	1/2	0	EL	0.54 ± 0.01	350	320÷510	0.2
2	1/2	1/2	EH	1.1 ± 0.03	341	160÷330	0.2
3	0	0	HH^*	2.0 ± 0.05	166	0.2÷1.0	1.3
3	0	1/2	LH	2.4 ± 0.06	166	0.8÷4.0	1.3
3	1	0	HH,LL	1.6 ± 0.04	540	3.0÷10	1.7
3	1	1/2	LH	1.8 ± 0.05	525	27÷90	1.7
4	3/2	0	HHH	2.9 ± 0.07	729	0.01÷0.10	7.5
4	3/2	1/2	(LHH)	2.6 ± 0.07	712	1.7÷9.5	7.5
5	0	0	(HHH^*H^*)	5.0 ± 0.1	166	$\ll$1	12
5	0	1/2	-	4.4 ± 0.1	166	$\ll$1	12
7	0	0	VB $(\chi\chi\chi HH)$	8.5 ± 0.2	166	$\ll$1	46

Table 2.1: Summary of the main properties of Minimal DM candidates, in particular we show for each multiplet the mass for which it reproduces the entire Dark Matter density seen in the universe. The table is taken from [25], where the rows containing multiplets that would require a non-minimal coupling to the Standard Model to have a Lightest Neutral Particle were removed. The results for the thermal mass and the mass splitting have been reproduced. The 7th column gives the 3σ range for the number of events expected at LHC. The last column gives the spin-independent cross section, assuming a sample vale $f = 1/3$ for the uncertain nuclear matrix elements

2.4 Bounds on Minimal Dark Matter

2.4.1 Direct Detection

Once we have fixed the Minimal Dark Matter mass all its phenomenology is fixed by the charged components splitting we have computed in Appendix B.

Direct detection experiments usually try to observe elastic scattering of Dark Matter with heavy nuclei. MDM models with $Y \neq 0$ have tree-level Z boson exchange with nuclei this results in a scattering cross section which is orders of magnitude above the current limits 1.10 set by the LZ collaboration. Clearly the interaction strength is proportional to Y since the Z-boson is known to couple to

$$c_W^2 J_\mu^{(3)} - s_W^2 J_\mu^{(Y)} = -J_\mu^{(Y)} + c_W^2 J_\mu^{(em)} = -J^{(Y)}$$

The last step follows from EM-charge neutrality of DM.
For complex scalars and fermions (we need them to be complex to have $Y \neq 0$) the scattering cross section of the vector-like spin-independent interaction is given by

$$\sigma = \frac{G_F^2 Y^2}{2\pi E_{CM}^2}(N - (1 - 4s_W^2)Z)^2 \begin{cases} [4M^2M_N^2 + p^2(4E_{DM}E_N + 4M_N^2 + 2M^2) + 4p^4] & \text{for scalars} \\ \left[M^2M_N^2 + p^2\left(E_{DM}E_N + \frac{M^2}{2} + \frac{M_N^2}{2}\right) + \frac{7p^4}{4}\right] & \text{for fermions} \end{cases}$$

Where E_{CM} is the center of mass energy, $M_N \sim 100\,\mathrm{GeV}$ is the mass of the nucleus, E_{DM} and E_N are respectively the DM and nucleus energy in the CM frame, p is the modulus of the three-momentum of one of the 2 particles in the CM frame and finally N and Z are the number of protons and of neutrons in the nuclei.
Notice we are assuming the wavelength of DM is greater than the dimension of the nucleus to have coherent scattering, but in this case this approximation is not optimal since

$$v \ll \frac{1}{R_N M} \sim 10^{-5}$$

but we believe Cold Dark Matter to have typical velocities around $v \simeq 300\mathrm{km/s} \sim 10^{-3}$, since this is the speed at which the sun is moving. This formula simplifies quite neatly in the NR limit (we can assume

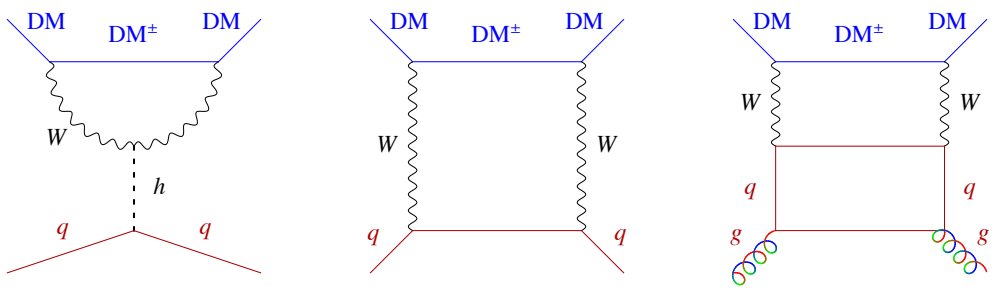

Figure 2.3: Main One and Two-Loops interaction of Fermionic Minimal Dark Matter with nuclei, taken from [61]. Obviously also the crossing symmetries of these diagrams should be considered such as the crossed W-boson exchange in the second diagram.
For scalar MDM there are three additional diagrams in which the upper part of each diagram is substituted by a loop with the 4-particle vertex. Effectively the graphs we would obtain simply require to remove the mediated charged partner and stick together the two vertices.

for WIMPS) and for $M \gg M_N$ (as freeze-out estimates give M$\sim$ 10TeV), and the cross-section becomes independent from the DM mass

$$\sigma = c\frac{G_F^2 Y^2 M_N^2}{2\pi}(N-(1-4s_W^2)Z)^2 \begin{cases} c=4 & \text{for scalars} \\ c=1 & \text{for fermions} \end{cases}$$

This cross section would be of order $\sim 10^{-30}\,\text{cm}^2$ and is forbidden from direct detection, which requires $\sigma \lesssim 10^{-46}\,\text{cm}^2$.

The only way to still allow MDM candidates with $Y \neq 0$ is to give up minimality and allow for a new term in the Lagrangian generating mass splitting between the two Weyl components of the Dirac Spinor. This is what happens in supersymmetry with the Higgsino which is the most difficult candidate to exclude with data from future experiments [56].

In this way the lightest candidate becomes a Majorana fermion and cannot have vector-like interactions mediated by the Z boson. The phenomenology of this model is then determined by the mass shift δm_0 with the next-to lightest neutral particle (the other Weyl component of the Dirac spinor). The mass splitting is bounded from below by DD searches and BBN.

2.4.2 Direct Detection for $Y = 0$

If MDM is Hypercharge neutral, spin-independent vectorial interactions at tree-level are automatically suppressed and the most relevant Direct Detection interactions are at loop level. see figure 2.3.
The two one-loop integrals are clearly dominated by energies of the order of the W-boson mass (it is obvious once we Wick rotate our integrand). After the Wick rotation the second diagram (having an extra propagator) gains a relative minus sign with respect to the first one, this allows to have accidental cancellations which significantly deplete the one-loop amplitude, forcing us to consider even 2-loop effects.

We can create an EFT to describe this interaction [25] on the lines of what [19] does for supersymmetry.

$$\mathcal{L}_{eff}^W = (n^2-(1\pm 2Y)^2)\frac{\pi\alpha_W^2}{16M_W}\sum_q\left[\left(\frac{1}{M_W^2}+\frac{1}{m_h^2}\right)[\bar{\chi}\chi]m_q[\bar{q}q] - \frac{2}{3M}[\bar{\chi}\gamma_\mu\gamma_5\chi][\bar{q}\gamma_\mu\gamma_5 q]\right]$$

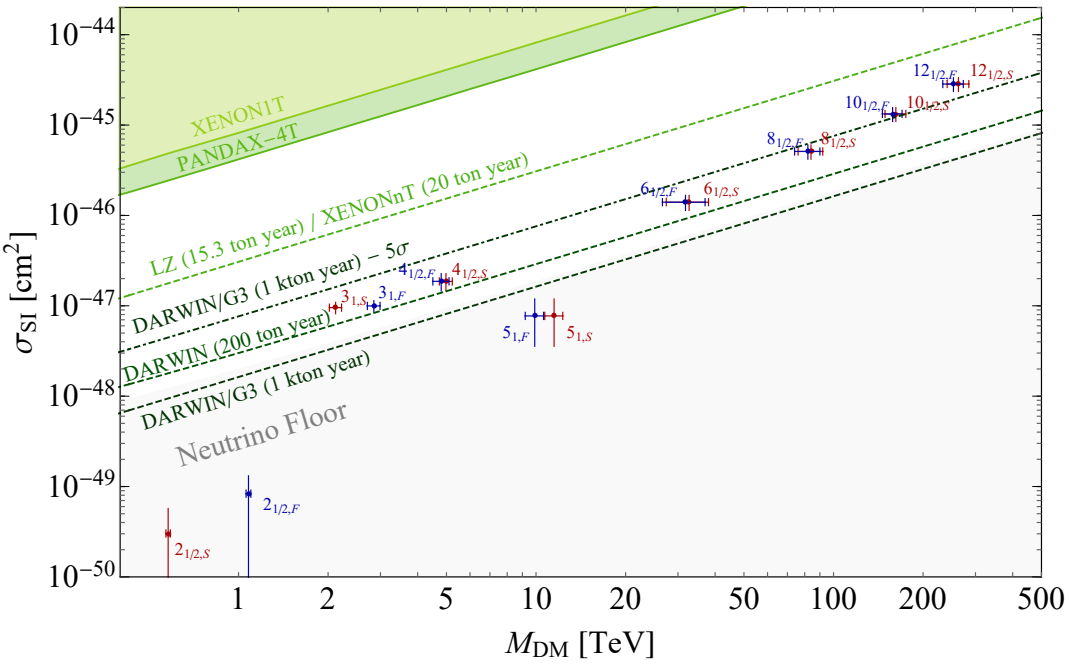

Figure 2.4: Expected SI cross-sections for different complex WIMPs for minimal splitting as defined in Sec. . The **blue dots** correspond to Dirac WIMPs and the **red dots** to complex scalar WIMPs. The vertical error bands correspond to the propagation of LQCD uncertainties on the elastic cross-section (), while the horizontal error band comes from the uncertainty in the theory determination of the WIMP freeze out mass. The **light green** shaded region is excluded by the present experimental contraints from XENON-1T and PandaX-4T , the **green dashed** lines shows the expected 95% CL reach of LZ/Xenon-nT and DARWIN

2.4.3 Indirect Detection

In this section I will follow [55] to review the current bounds and future prospects from indirect detection on MDM.

Minimal Dark Matter has a quite clear annihilation channel to $\gamma\gamma$ and γZ at one-loop, see figure 2.5. The cross sections of these channels are highly increased by the effect of the Sommerfeld Enhancement. After all these are the same cross sections we expect at freeze-out. Being Minimal Dark Matter non-relativistic and much more massive than the Z boson, we can see that the gamma rays energies from annihilation are

$$E_\gamma \simeq M$$

where M is the MDM mass. These energies are in the right energy window for Earth-Based Cherenkov tele-

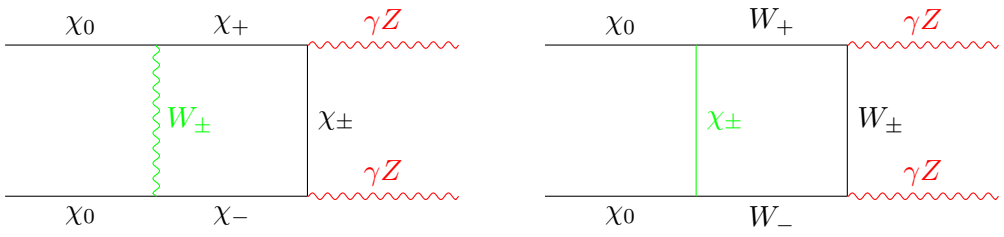

Figure 2.5: These are the 1-loop diagrams relative to the annihilation of two Dark Matter particles in at least one photon. This is the diagram common to both scalars and fermions, involving only the 3-particle vertex. Clearly for scalars we have other 2 diagrams using the 4-particle vertex.

scopes, which look for gamma ray burst with $E_\gamma > 100\,\text{GeV}$. The current Cherenkov Observatories have an energy resolution around $10\% - 20\%$ at $\sim 1\,\text{TeV}$ [39] [44] [47]. The future CTAO will have an even greater accuracy with an energy resolution of about 5% (https://www.ctao.org/for-scientists/performance/) and will push its sensitivity down to thermal cross section of $\langle \sigma v \rangle \lesssim 10^{-27} cm^3 s^{-1}$ possibly definitively excluding every MDM candidate.

All these telescopes have a wide acquisition range and can scan in a single acquisition energies from $100\,\text{GeV} \lesssim E_\gamma \lesssim 100\,\text{TeV}$ and search gamma ray peaks above the gamma continuum. The problem is that, in order to subtract the background from every measurement, a careful astrophysical analysis of the target and of the emission lines of all known physics is needed and this is really difficult to carry-out for a vast range of energies. It is therefore of capital importance to have an accurate theoretical estimate for the Dark Matter mass, and as we will see this implies having to take into account finite-velocity energy corrections besides the standard Sommerfeld Enhancement.

The bounds we can obtain from direct detection depend on the astrophysical target: on one hand we want to point our telescope towards targets with a high J-factor defined as

$$J = \frac{1}{\Delta\Omega} \int d\Omega \int_{\text{l.o.s.}} d\ell \, \rho\big[r(\ell, \psi)\big]^2$$

where ρ is the Dark Matter density. On the other end we want to have the quietest background possible. For these reason the strongest bounds come from the analysis of dwarf Spheroidal galaxies (dSphs) instead of from the Galactic Centre. Figure 2.6 shows the projected bounds of CTAO on the thermal cross section. As we see only really tiny regions of possible masses remain viable. Furthermore the cross section is heavily dependent on the Dark Matter mass because of the Sommerfeld corrections.

2.4.4 Bounds from Colliders

Minimal Dark Matter at colliders would have some unique feature that would allow to tag even a small amounts of events. Its main features are Disappearing Tracks, Missing Invariant Mass, Charged Tracks and Electroweak Precision Observables.

- **Electroweak Precision Observables**: Obviously adding a multiplet to the Standard Model changes the running of the couplings that can be probed with LEP or future collider data. Coupling only to gauge bosons, MDM will mainly impact their self energies and all the corrections to other observables will be through an only-gauge-bosons-point function embedded in other diagrams. Therefore our main observable will be oblique corrections. Unfortunately, for Dark Matter masses of $\sim 1\,\text{TeV}$ or more, these precision corrections are unnoticeable. To experimentally probe these energies we would need a muon collider with a centre of mass energy $\sqrt{s} \sim 30\,\text{TeV}$ [56] [55] which is outside any collider reach in the next future.
- **Charged Tracks:** Charged Tracks are in particular by the Next-to Lightest Neutral Particle which have the lowest relative mass splitting. Due to the small mass splitting, they are relatively long-lived and could leave a trace in the colliders.
- **Disappearing Tracks**: The Next-to Lightest Neutral Particle can decay, as we have seen in the previous section to the LNP and a really soft charged pion. This pion is really difficult to detect because pions with transverse momenta

  $$p_T \lesssim 30\,\text{MeV}$$

  have, in a magnetic field of strength $B = 2\,\text{T}$ a radius of curvature

  $$R = \frac{p_T}{eB} \lesssim 10\,\text{cm}$$

Figure 2.6: Expected CTA sensitivities (dashed black lines) with 68% and 95% CL intervals derived as in Ref. [41] assuming 50 hours observation time towards Draco (green) and Triangulum II (magenta). We show the SE annihilation cross-section into the channels that contribute to the monocromatic gamma line signal (i.e. $\gamma\gamma$ an γZ) for a scalar 7-plet (blue) and a fermionic 7-plet (red). The vertical bands show the predicted thermal masses for the scalar 7-plet (blue) and the fermionic 7-plet (red), where the theory uncertainty is dominated by the neglected NLO contributions. Taken from [55].

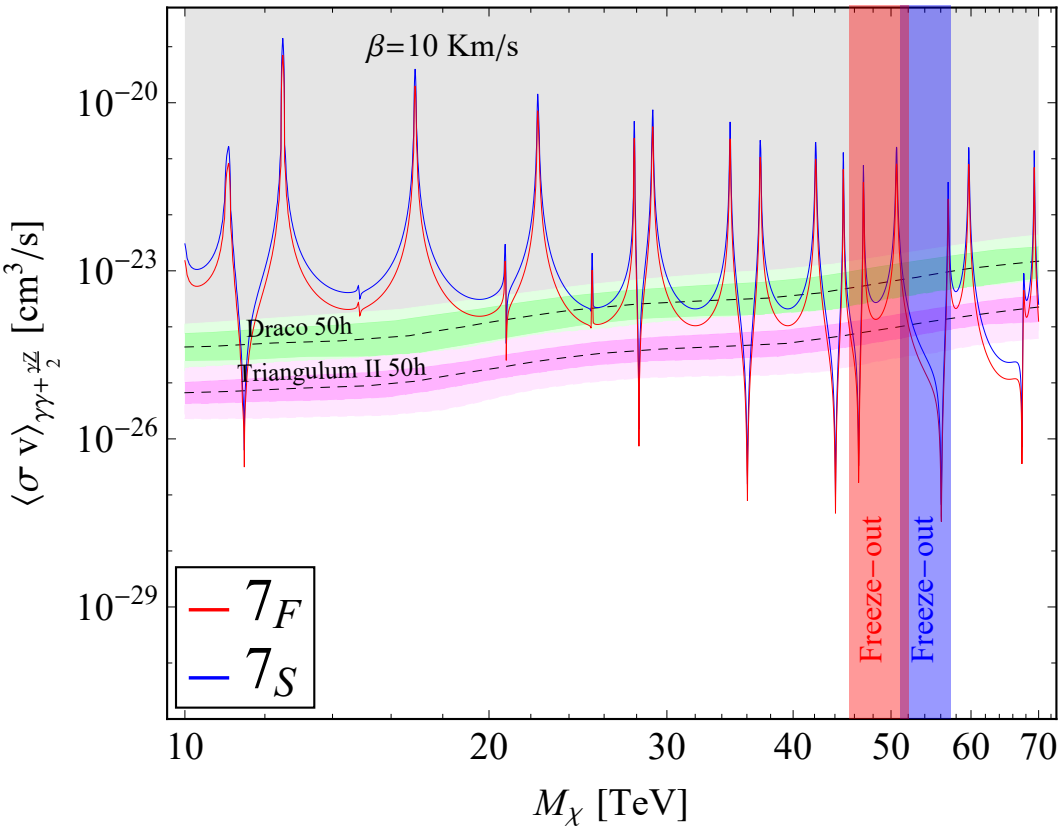

This would mean that it is unlikely both for the pion and to the electron/positron created after its decay to leave any trace in the detector. Furthermore, from Bethe-Bloch formula we know that at small energies the energy-loss of a charged particle is proportional to $1/v^2$ and therefore the energy loss is really rapid. Atlas and CMS algorithms of path reconstruction often ask the transverse momentum to be $p_T > 400\,\text{MeV}$. Obviously the Neutral Dark Matter particle also goes undetected and we therefore have some disappearing tracks in our detector! Notice that this feature is not only a feature of minimal Dark Matter but of every electroweak multiplet added to the SM.

- **Minimal Invariant Mass**: the idea is simply to look (for DM multiplets with $n < 5$) for which direct production is viable to processes such as

$$l^+l^- \to \chi_i\chi_j + X$$

Where X is some set of particle of the SM. If to fix ideas we look at the so called Mono-V processes, the X contains only a SM vector boson. The SM model background for the process

$$l^+l^- \to \chi_i\chi_{-i}\gamma$$

is constituted from processes like

$$l^+l^- \to \nu_l\bar{\nu}_l\gamma.$$

Clearly, being neutrinos almost massless we have on average in the first process a larger fraction of Missing Invariant Mass that goes unseen by the detectors.

$$MIM = (s + m_V^2 - 2\sqrt{s}E_V)^{\frac{1}{2}}$$

Selecting only events with $MIM \gtrsim 2\,\text{GeV}$ allows to maximize the significance of the new physics processes. We can repeat the same analysis also for other sets of particles X, for example double vector bosons emission, called Di-V. For more details on the analysis and a complete classification of all Mono-V and Di-V processes for fermions and scalars see [55].

Chapter 3

Sommerfeld Enhancement

The Sommerfeld Enhancement is a non-perturbative effect due to long range interaction that enhance the cross-section of short-range or contact interactions.

The Sommerfeld Enhancement was studied for the first time from the physicist Arthur Sommerfeld in the context of beta decays in 1931 [3].

One of the simplest processes in which the effect enters is electron capture

$$e^- + p^+ \to n + \nu_e$$

The process is mediated by weak forces which (at low energies) can be thought as contact interactions in the context of Fermi EFT. For the capture to happen the electron and the proton should thus be in the same point, the probability of finding them in the same point is enhanced from the fact they attract as they have opposite electrical charge!!

To put in some numbers let us look at an even simpler classical model [30]: the capture of an object of mass m from a star of mass M and radius R. If we switch off gravity the cross section is simply the geometrical cross section

$$\sigma_0 = \pi R^2$$

If we now insert gravity in the picture the cross section is enhanced to

$$\sigma = \pi b^2$$

where b is the impact parameter at infinity for which the least approach distance from the star is R. Using energy and angular momentum conservation

$$\frac{1}{2}mv^2 = -\frac{GMm}{R} + \frac{1}{2}mv^2\frac{b^2}{R^2}$$

$$b^2 = R^2\left(1 + \frac{2GM}{Rv^2}\right)$$

$$\sigma = \sigma_0\left(1 + \frac{2GM}{Rv^2}\right) \tag{3.1}$$

As expected in the limit $G_N \to 0$ the cross section is the geometric one, but for how weak the interaction can be, there will always be a velocity

$$v \sim \sqrt{\frac{GM}{R}}$$

under which the effect is important. As we would expect intuitively the effect is dominant in the low velocity regime and is negligible when the kinetic energy is high enough to disregard potential interactions. This simple toy model shows the main features of the Sommerfeld enhancement which is the quantum counterpart of this effect.

The same effect is relevant for Dark Matter pair annihilation. This was first, relatively recently, pointed out by Hisano [24] discussing supersymmetric Dark Matter, but then became a widely discussed feature of several Dark Matter models. Being the annihilation cross section a crucial quantity for thermal candidates of Dark Matter.

3.1 Sommerfeld with Scalars

We will consider for simplicity a theory of 3 scalars: one heavy and complex χ (Dark Matter), one light and real ϕ (the long-range mediator) and one complex field ψ (which we do not care much about and will exemplify a Standard Model particle) and we will take massless just not to clutter the page with one more mass term.

The process we are willing to study is how the long range mediator affects the annihilation cross section

$$\chi\bar{\chi} \to \psi\bar{\psi}$$

The Lagrangian we are going to discuss is

$$\mathcal{L} = \partial_\mu\chi\partial^\mu\chi^\dagger + \partial_\mu\psi\partial^\mu\psi^\dagger + \frac{1}{2}\partial_\mu\phi\partial^\mu\phi - M^2\chi\chi^\dagger - \frac{1}{2}m^2\phi^2 - \lambda(\chi\chi^\dagger)(\psi\psi^\dagger) - \mu\chi\chi^\dagger\phi$$

Where we inserted a trilinear coupling between χ and ϕ and a contact 4-particle number changing interaction between χ and ψ describing annihilation.

As seen above the effect we intend to study is dominant in the low energy regime, therefore we will do the non-relativistic approximation of the above equation.

If we integrate out the light scalars, which appear at most quadratically in the above Lagrangian, we end up with:

$$S = \int d^4x \left(\partial_\mu\chi\partial^\mu\chi^\dagger - M^2\chi\chi^\dagger - \lambda(\chi\chi^\dagger)(\psi\psi^\dagger)\right) - \frac{1}{2}\int d^4x \int d^4y\, \mu^2\chi(x)\chi^\dagger(x)\Delta_F(x-y)\chi(y)\chi^\dagger(y) \quad (3.2)$$

The coordinate space expression of the Feynman propagator is well-known, but for a massive propagator it involves the Bessel functions. To keep everything as simple and transparent as possible we then take the massless limit: $m = 0$. The Feynman propagator then arises without subtleties by contour integration with the correct $i\epsilon$ prescription and from the Fourier transform of the Heaviside step-function.

$$\Delta_F(x-y) = -\frac{1}{4\pi}\delta((x-y)^2) + \frac{i}{4\pi^2}\mathcal{P}\left(\frac{1}{(x-y)^2}\right)$$

The non-relativistic limit follows inserting all the factors of c we have neglected above and rotating the filed χ

$$\chi \to \chi e^{-iMc^2t}$$

At order-0 in $\frac{1}{c}$ the Lagrangian density is

$$\mathcal{L} = 2iM\chi^\dagger(x)\frac{\partial}{\partial t}\chi(x) + \chi^\dagger(x)\nabla^2\chi(x) - \chi(x)\chi(x)^\dagger \int d^3\mathbf{y}\, \left(\lambda\psi(t_x,\mathbf{y})\psi^\dagger(t_x,\mathbf{y})\delta^3(\mathbf{x}-\mathbf{y}) - \frac{\mu^2\chi(t_x,\mathbf{y})\chi^\dagger(t_x,\mathbf{y})}{8\pi|\mathbf{x}-\mathbf{y}|}\right)$$

where we have used the non-relativistic approximation of Δ_F:

$$\mathcal{P}\left(\frac{1}{(x-y)^2}\right) \sim O\left(\frac{1}{c^2}\right) \qquad \delta((x-y)^2) \sim \frac{\delta(t_x - t_y)}{4\pi c|\mathbf{x}-\mathbf{y}|}$$

and the integration over dy^0 provides an additional factor of c which allows the δ-term to be order 0 an reproduce the Coulomb potential (and we have an additional factor of $\frac{1}{2}$ to avoid double counting). We have also rewritten the λ term in a somewhat arbitrary form to emphasize that it does indeed correspond to a point-like interaction.

3.2 From Schrödinger Equation

The previous Lagrangian is the Lagrangian of Schrödinger equation.
If we rescale the fields and project to the fixed number of particles states of Quantum Mechanics (formally we should look at an observable such as $2 \to 2$ scattering and use LSZ formula), we obtain that the equation describing scattering is indeed the Schrödinger equation. integrating out the coordinate of the centre of mass and looking only to the dynamics of the relative coordinate is

$$i\frac{\partial}{\partial t}\chi = -\frac{\nabla^2}{2M}\chi + \frac{\mu^2}{32\pi M^2 r}\chi \tag{3.3}$$

The number-changing contact interaction cannot be described in this formalism (being number changing), but its probability is clearly proportional to the probability of finding the two particles χ and $\bar{\chi}$ in the same place!

The Sommerfeld enhancement is thus defined as

$$S = \left|\frac{\chi(0)}{\chi_0(0)}\right|^2 \tag{3.4}$$

where χ is the solution to the above equation, while χ_0 is the solution to the equation when we switch off the light mediator (and thus put $\mu = 0$) and the two wave-functions have the same normalization at infinity.

The problem is therefore now reduced to look at a scattering process in non-relativistic quantum mechanics from a Coulomb potential!
This is a well-studied problem that we know how to solve. If we take the incident wave to be

$$\chi_{inc} = e^{ikz}$$

Equation (3.3) can be solved as we solve it for the hydrogen atom. We look at the eigenvalue equation and express the Laplacian in terms of the angular momentum (a great derivation that avoids lots of calculations is [49])

$$-\frac{1}{2M}\left(\frac{\partial^2}{\partial r^2} - \frac{L^2}{r^2} + \frac{2}{r}\frac{\partial}{\partial r}\right)\chi + \frac{\mu^2}{32\pi M^2 r}\chi = \frac{k^2}{2M}\chi$$

as usual we expand the wave-function in terms of the spherical harmonics

$$\chi = \sum_{l,m}\frac{u_l}{r}Y_m^l$$

and obtain the radial equation

$$-\frac{1}{2M}\left(u_l''(r) - \frac{l(l+1)}{r^2}u_l\right) + \frac{\mu^2}{32\pi M^2 r}u_l = \frac{k^2}{2M}u_l$$

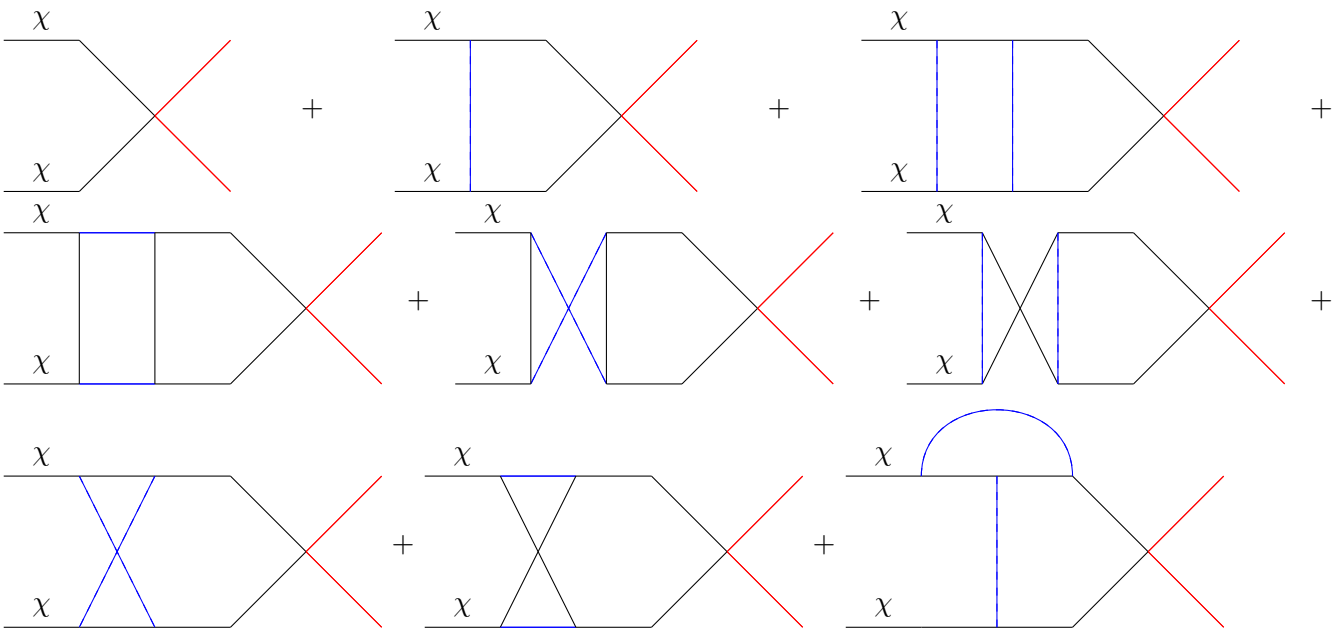

Figure 3.1: Set of diagrams contributing to the scattering $\chi\chi \to \psi\psi$ at 2-loop. The χ particles are represented by black line, ψ from red and ϕ from blue ones

As usual at $r \ll \frac{1}{M}$ the equation takes the approximate form

$$u_l'' \simeq \frac{l(l+1)}{r^2} u_l$$

$$u_l \propto r^{l+1}$$

We can immediately see therefore that only u_0 contributes to the Sommerfeld enhancement as it is the only function for which $\lim_{r\to 0} \frac{u_l(r)}{r} \neq 0$. The equation we have to solve is thus

$$u_0'' + k^2 u_0 = \frac{\mu^2}{16\pi M} \frac{u_0}{r}$$

3.3 From Feynman Diagrams

The Schrödinger equation for the scattering amplitude can be obtained in full generality resumming an infinite series of Feynman diagrams.

These diagrams correspond to possibly infinite light scalar exchange before the point annihilation.

But why does perturbation theory fail in this problem?

We could argue that as long as μ is small all the massless scalar exchange should be suppressed by powers of μ and thus we can just keep the first few terms of the series.

3.3.1 How perturbation theory fails

We already have a hint that perturbation theory should fail. Looking at equation (3.1) the expansion constant enters with a v^{-1} and therefore for a low enough v perturbation theory stops working.

The diagrams contributing to $\chi\chi \to \psi\psi$ scattering to 1 and 2-loops are reported in 3.1.

Let us study the 1-loop diagram! We will show that the imaginary part picks up the characteristic $\frac{1}{v}$ behaviour.

Computing the imaginary part of the amplitude is simple if we use the cutting rules. Once we put on-shell also the external legs we recognize immediately that there is only one kinematically allowed cut: the one putting on-shell the 2 χ particles in the loop 3.1, otherwise we would have a triple vertex of on-shell particles 2 of which have the same mass.

$$2\,Im\,\mathcal{M}_{\text{1-loop}} = (i\lambda)(-i\mu)^2 \int \frac{d^4k}{(2\pi)^4}(2\pi)^2\delta((p_1-k)^2-M^2)\delta((p_2+k)^2-M^2)\frac{i}{k^2-m^2}$$

The momenta are chosen according to 3.2. Going to the CM frame we have

$$p_1 = (E_p, \vec{p}) \quad p_2 = (E_p, -\vec{p})$$

$$\begin{aligned} 2\,Im\,\mathcal{M}_{\text{1-loop}} &= -\frac{\mu^2\lambda}{4\pi^2}\int d^4k\,\delta(4E_pk^0)\delta(\vec{k}^2-2\vec{p}\cdot\vec{k})\frac{1}{\vec{k}^2+m^2} = \\ &= -\frac{\lambda\mu^2}{32\pi E_p|\vec{p}|}\int_{\left|\vec{k}\right|=0}^{\left|\vec{k}\right|=2|\vec{p}|} d\left|\vec{k}\right|\frac{\left|\vec{k}\right|}{\left|\vec{k}\right|^2+m^2} = \\ &= -\frac{\lambda\mu^2}{64\pi E_p|\vec{p}|}\ln\left(1+\frac{4|\vec{p}^2|}{m^2}\right) \end{aligned}$$

If we now take the non-relativistic approximation of this equation for $|\vec{p}| \ll M$, meaning

$$E_p \simeq M \quad |\vec{p}| \simeq Mv$$

we end up with

$$Im\,\mathcal{M}_{\text{1-loop}} = -\frac{\lambda\mu^2}{128\pi M^2 v}\ln\left(1+4v^2\frac{M^2}{m^2}\right) \tag{3.5}$$

This equation is beautifully regularized: the imaginary part of the amplitude goes to zero both if the velocity is $v \ll \frac{m}{M}$ and if $v \gg \frac{m}{M}$. In particular we have that the maximum value of the amplitude is reached for

$$v = 0.99015\frac{m}{M} \simeq \frac{m}{M}$$

$$(Im\,\mathcal{M}_{\text{1-loop}})_{max} \simeq -\frac{\lambda\mu^2}{128\pi Mm}\ln(5) \simeq -\frac{\lambda\mu^2}{80\pi Mm}$$

The Sommerfeld enhancement is relevant for velocities around this maximum value. In particular if we take the tree level amplitude

$$\mathcal{M}_{tree} = -\lambda$$

the Sommerfeld enhancement is relevant, meaning

$$1 \lesssim \frac{(Im\,\mathcal{M}_{\text{1-loop}})_{max}}{\mathcal{M}_{tree}} \simeq \frac{\mu^2}{80\pi Mm}$$

And therefore

$$\mu \gtrsim 4\sqrt{5\pi}(Mm)^{\frac{1}{2}}$$

In general, if we define the dimensionless parameter α characterising the interaction strength of our theory.

$$\alpha = \frac{\mu^2}{16\pi M^2}$$

the above relation takes the much nicer (and a little bit more general result)

$$\alpha M \gtrsim m$$

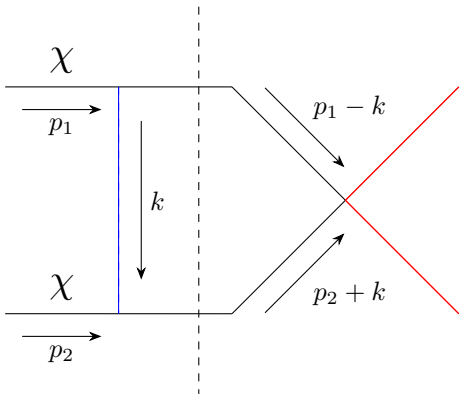

Figure 3.2: Diagram of the one-loop diagram of Sommerfeld enhancement with momentum flows and cuts

We want to stress that M is the mass of the interacting particle and m is the mass (of the, possibly much lighter, mediator) We can therefore notice that the Sommerfeld enhancement is always relevant when we have massless mediators! And in this case the Sommerfeld enhancement appears not to be bounded. The crucial fact is that in our theory we always have infrared regulators, such as thermal masses in primordial plasma or experimental resolution in collider experiments.

3.3.2 Resumming Diagrams

As we have understood doing the previous loop computation, ladder diagrams contribute with powers of $\frac{\alpha}{v}$ and we must therefore resum all contributions to those diagrams when the velocity of the particles gets of order $v \sim \alpha^{\frac{1}{2}}$.

What we wish to show now is that the Schrödinger equation can be obtained also resumming all the loop diagrams.

Is it surprising that resumming an infinite series of diagrams could give us a differential equation?

Essentially no, we have always learned it since we started studying quantum field theory: if we take the Lagrangian of a free real scalar field

$$\mathcal{L} = \frac{1}{2}\partial_\mu\phi\partial_\mu\phi - \frac{1}{2}m^2\phi^2$$

we can obtain the free propagator for the theory solving the differential equation

$$(\partial^2 + m^2)\Delta_F(x) = \delta(x)$$

Or if we consider the mass term as an interaction term and not as part of the free field equation

$$\mathcal{L}_{free} = \frac{1}{2}\partial_\mu\phi\partial_\mu\phi \qquad \mathcal{L}_{int} = -\frac{1}{2}m^2\phi^2$$

$G(p) =$ 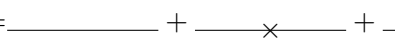 $+ \dots\dots$

$$= \frac{i}{p^2} + \frac{i}{p^2}(-im^2)\frac{i}{p^2} + \frac{i}{p^2}(-im^2)\frac{i}{p^2}(-im^2)\frac{i}{p^2} + \frac{i}{p^2}(-im^2)\frac{i}{p^2}(-im^2)\frac{i}{p^2}(-im^2)\frac{i}{p^2} + \dots..$$

$$= \frac{i}{p^2}\left(1 + (-im^2)\frac{i}{p^2} + \left((-im^2)\frac{i}{p^2}\right)^2 + \left((-im^2)\frac{i}{p^2}\right)^3 + ...\right)$$

$$= \frac{i}{p^2}\frac{1}{1-(-im^2)\frac{i}{p^2}} = \frac{i}{p^2 - m^2}$$

Where "$\times$" represents a mass insertion. And we can easily go to position space with

$$\Delta_F(x) = \int \frac{d^4p}{(2\pi^4)} G(p) e^{ipx}$$

Clearly if the mass is a small interaction (we should always state with respect to what and the answer is with respect to the typical energy scale of our particles, for example in the chiral Lagrangian of QCD we treat mass like a perturbation because $m_u, m_d \ll \Lambda_{\text{QCD}}$) we can just take the first terms of the series and forget about the ones with more mass insertions, but if the mass is not small (at low energy the mass is a relevant operator) we have to consider the whole series and some over an arbitrary number of insertions. We are just trying to do this operation for the 4-point function instead of the 2-point function!!

In the case of the 2-point function we have resummed a geometric series, so it was pretty easy. It turns out that the way to obtain the integral equation to resum the 4-point function is conceptually identical to the way resum the geometric series. If we represent the dressed propagator $G(p)$ with

$G(p) =$ 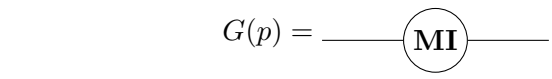

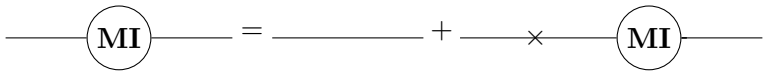

(3.6)

$$G(p) = \frac{i}{p^2} + \frac{i}{p^2}(-im^2)G(p) \tag{3.7}$$

And from this equation we obviously obtain the same propagator as before. This equation is the exact analogue of the equation we use to resum the geometric series (which in fact appears inside the propagator):

$$\begin{aligned} S(a) =& 1 + a + a^2 + a^3 + ... \\ =& 1 + a(1 + a + a^2 + ...) \\ =& 1 + aS(a) \end{aligned}$$

$$S(a) = \frac{1}{1-a}$$

It is important to keep in mind that this formula only works if $|a| < 1$ i.e. if the series converges. If the series diverges the above equation still gives the finite result $S(a) < 0$ which makes no sense.

3.3.3 Bethe-Salpeter equation

Proceeding as hinted above we must now try to resum the diagrams contributing to the 4-point function. Following [32][33], we begin by considering 2 quantities:

- Γ which is the non-perturbative 4-point function we want to compute.
- $\tilde{\Gamma}$ which is the 4-point function obtained summing every 2-particle irreducible digram. We should be a little bit cautious saying 2-particle irreducible, because what we really mean in our toy model is 2-χ particle irreducible, meaning that the diagram should remain connected when we cut 2 χ lines. Of course this definition is a little bit arbitrary and depends on the integral equation we want to obtain, but this definition permits to obtain the simplest integral equation, not having to sum on loops of different-particle exchange in the below diagram.

As you can see 3.3 is of the exact same form of (3.6) and corresponds to the integral equation

$$\Gamma(p_1, p_2; p_3, p_4) = \tilde{\Gamma}(p_1, p_2; p_3, p_4) - i \int \frac{d^4q}{(2\pi)^4} \tilde{\Gamma}(p_1, p_2; q, p_1+p_2-q) G(q) G(p_1+p_2-q) \Gamma(q, p_1+p_2-q; p_3, p_4) \tag{3.8}$$

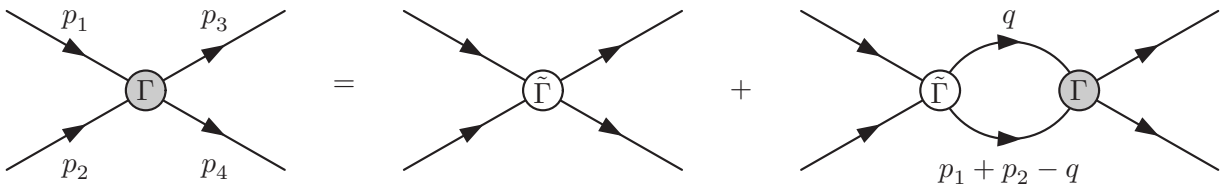

Figure 3.3: Diagrammatic Form of Bethe-Salpeter equation, taken from [33]

This is the Bethe-Salpeter equation in its full glory where $G(p)$ are the dressed χ propagators in our case entailing the physical mass. This equation is very difficult to solve exactly, especially because it would require to know the exact form of $\tilde{\Gamma}$, which excluding trivial theories requires summing an infinite amount of Feynman diagrams. In our toy model for example we have at

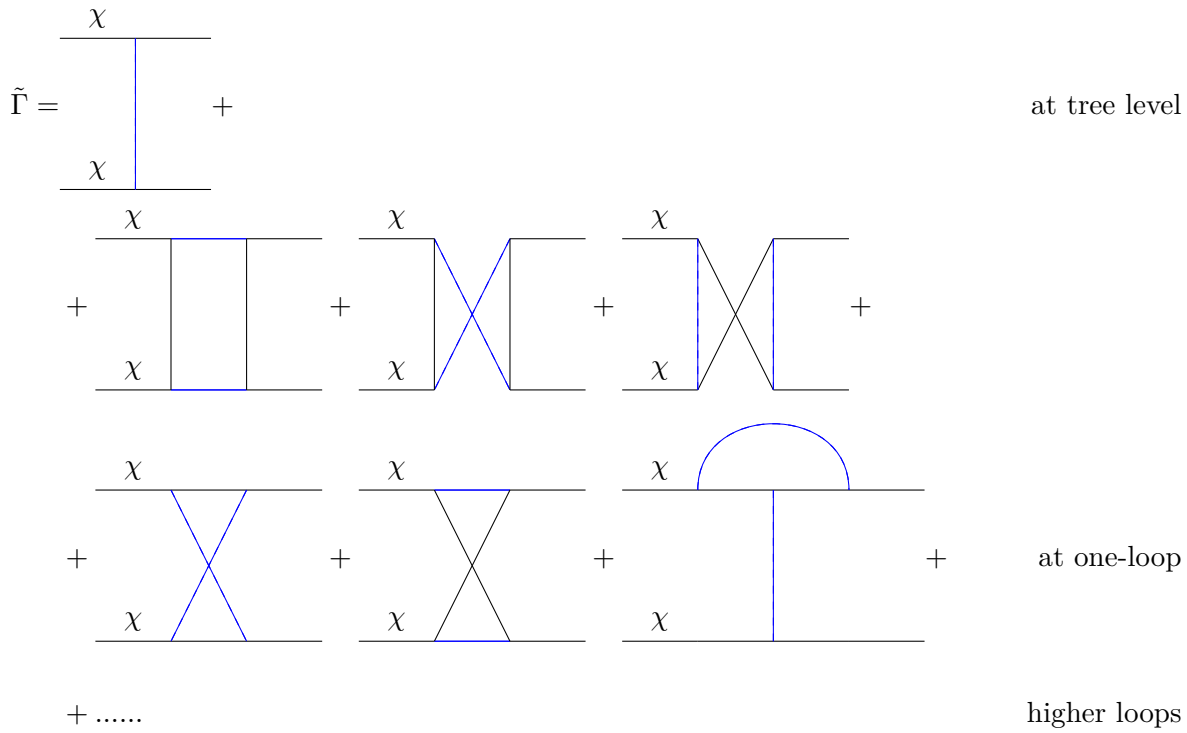

We are considering only the trilinear vertex as we are not really interested in the total non-perturbative 4-point function of the full theory, which for example would contain also the diagrams in which 2 ψ particles are exchanged at loop level, instead we want to compute the non-perturbative corrections to the λ vertex. If we really wish then to obtain the non perturbative interaction of the full theory it is then easy to resum all the corrected λ vertices with a geometric series. We therefore define the corrected vertex $\mathcal{M}$.

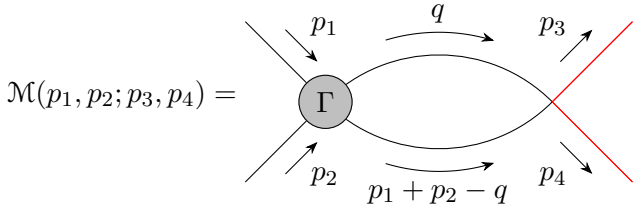

(3.9)

The integral equation for $\mathcal{M}$ is easily given in the same way as above

$$\mathcal{M}(p_1,p_2;p_3,p_4) = \lambda - i\int \frac{d^4q}{(2\pi)^4} G(q)G(p_1+p_2-q)\tilde{\Gamma}(p_1,p_2;q,p_1+p_2-q)\mathcal{M}(q,p_1+p_2-q;p_3,p_4)$$

If we only take the first order in μ^2 (the tree-level diagram), we are just resumming the ladder diagrams, while cross ladder exchange and other loop effects are at a higher μ^2 order.
Therefore at tree level for the compact 4-point vertex $\tilde{\Gamma}$ we have

$$i\tilde{\Gamma}(p_1,p_2;p_3,p_4) = \frac{-i\mu^2}{(p_1-p_3)^2-m^2}$$

and therefore always at tree-level

$$\mathcal{M}(p_1,p_2;p_3,p_4) = \lambda + i\int \frac{d^4q}{(2\pi)^4}\frac{1}{q^2-M^2}\frac{1}{(p_1+p_2-q)^2-M^2}\frac{\mu^2}{(p_1-q)^2-m^2}\mathcal{M}(q,p_1+p_2-q;p_3,p_4) \tag{3.10}$$

So far we haven't made any non-relativistic approximation. We can finally change a little bit notation in the momentum integrals and introduce

$$P = \frac{p_1+p_2}{2} = \frac{p_3+p_4}{2} \qquad p = \frac{p_1-p_2}{2} \qquad p' = \frac{p_3-p_4}{2} \qquad q \to P+q$$

in this coordinates equation (3.10) becomes

$$\mathcal{M}(p,p',P) = \mathcal{M}(p_1,p_2;p_3,p_4) = \lambda + i\int \frac{d^4q}{(2\pi)^4}\frac{1}{(P+q)^2-M^2}\frac{1}{(P-q)^2-M^2}\frac{\mu^2}{(p-q)^2-m^2}\mathcal{M}(q,p',P) \tag{3.11}$$

3.3.4 Non-relativistic approximation

What we want to do now is a non-relativistic approximation of (3.10). We start by approximating the full potential given by the exchange of mediators with the instantaneous potential and a correction we can then include through perturbation theory

$$\frac{1}{k^2-m^2} = -\frac{1}{\vec{k}^2+m^2} + \left(\frac{1}{k_0^2-\vec{k}^2-m^2}+\frac{1}{\vec{k}^2+m^2}\right) = -\frac{1}{\vec{k}^2+m^2} + \frac{k_0^2}{(k^2-m^2)(\vec{k}^2+m^2)}$$

$$\mathcal{M}(\tilde{p},p',P) \simeq \lambda - i\int \frac{d^4q}{(2\pi)^4}\frac{1}{(P+q)^2-M^2}\frac{1}{(P-q)^2-M^2}\frac{\mu^2}{(\vec{\tilde{p}}-\vec{q})^2+m^2}\mathcal{M}(q,p',P)$$

Where once we solved this equation we should put $\tilde{p}=p$. This is necessary because to solve this integral equation we will rescale the amplitude by a factor that would be 0 if evaluated at $\tilde{p}=p$. If we now suppose that $\mathcal{M}(q,p',P)$ has no poles in q^0 [1]. We can proceed with contour integration. We now work in the CM reference frame where $\vec{P}=0$ as a consequence we immediately have

$$P^0 = \sqrt{\vec{p}^2+M^2}$$

we then define to avoid clutter

$$\omega = \sqrt{\vec{q}^2+M^2}$$

Accounting for the $i\epsilon$ prescription there are 2 poles above the real axis.

[1] Consider the iteration of the integral equation (3.10) the first iteration will contain λ, which has no poles in q^0. In the following steps this remains true as the integral equation leaves $\tilde{p}^0$ untouched and at every iteration I have to substitute it with q. Notice that this is only possible because of the structure of instantaneous vector boson propagators.

1. The first propagator gives the pole

$$q^0_{*1} = \sqrt{(\vec{P} - \vec{q})^2 + M^2} + P^0 = \omega + P^0$$

and the residue of the integrand which has q^0 dependence (so just the first 2 propagators and the amplitude) is

$$Res(q^0_{*1}) = -\frac{\mathcal{M}((q^0_{*1}, \vec{q}), p', P^0)}{8\omega P^0 (P^0 + \omega)}$$

The denominator of the residue can be rewritten as

$$\frac{1}{\omega(P^0 + \omega)} = \frac{1}{P^0}\left[\frac{1}{\omega} - \frac{1}{P^0 + \omega}\right]$$

2. The second propagator analogously has a pole at

$$q^0_{*2} = \sqrt{(\vec{P} + \vec{q})^2 + M^2} - P^0 = \omega - P^0$$

and with the same conventions used above

$$Res(q^0_{*2}) = \frac{\mathcal{M}((q^0_{*2}, \vec{q}), p', P^0)}{8\omega P^0 (P^0 - \omega)}$$

$$\frac{1}{\omega(P^0 - \omega)} = \frac{1}{P^0}\left[\frac{1}{\omega} + \frac{1}{P^0 - \omega}\right]$$

In the non-relativistic approximation $\omega, P^0 \simeq M$ this means that the only enhanced term is the one having denominator

$$\propto \frac{1}{P^0 - \omega}$$

$$\mathcal{M}(\tilde{p}, p', P) \simeq \lambda + \int \frac{d^3\vec{q}}{(2\pi)^3} \frac{\mu^2}{(\vec{\tilde{p}} - \vec{q})^2 + m^2} \frac{1}{8P_0^2} \frac{1}{P^0 - \omega} \mathcal{M}((q^0_{*2}, \vec{q}), p', P)$$

Now we substitute the non-relativistic approximation for $P^0 - \omega$ for which the two rest energies cancel

$$P^0 - \omega \simeq \frac{\vec{p}^2}{2M} - \frac{\vec{q}^2}{2M}$$

The relative momentum $\vec{p}$ is a parameter fixed by initial conditions, we can therefore define

$$\mathcal{E}_p = \frac{\vec{p}^2}{2M}$$

as the non-relativistic energy of each incoming particle in the CM frame.

$$\mathcal{M}(\tilde{p}, p', P) \simeq \lambda - \frac{\mu^2 M}{(2\pi)^3} \int \frac{d^3\vec{q}}{4P_0^2} \frac{1}{(\vec{\tilde{p}} - \vec{q})^2 + m^2} \frac{1}{\vec{q}^2 - 2M\mathcal{E}_p} \mathcal{M}((q^0_{*2}, \vec{q}), p', P)$$

To get rid of the factor $(\vec{k}^2 - 2m\mathcal{E}_p)^{-1}$ we rescale our amplitude defining

$$\mathcal{M}(\tilde{p}, p', P) = \left(\frac{\vec{\tilde{p}}^2}{2M} - \mathcal{E}_p\right) \psi_p(\tilde{p}, p', P)$$

This is the rescaling we were talking about previously. With this redefinition the integral equation we are trying to solve becomes

$$\left(\frac{\vec{\tilde{p}}^2}{2M} - \mathcal{E}_p\right)\psi_p(\tilde{p}, p', P) \simeq \lambda - \frac{\mu^2}{(2\pi)^3}\int \frac{d^3\vec{q}}{8P_0^2}\frac{1}{(\vec{\tilde{p}} - \vec{q})^2 + m^2}\psi_p(\vec{q}, p', P)$$

We are now ready to Fourier transform to position space to obtain the Schrödinger equation!! Defining

$$\hat{\psi}_p(\vec{x}) = \int \frac{d^3\vec{\tilde{p}}}{(2\pi)^3}e^{i\vec{\tilde{p}}\cdot\vec{x}}\psi(\tilde{p}, p', P)$$

the integral equation in position space becomes a differential equation

$$\left(-\frac{\nabla^2}{2M} - \mathcal{E}_p\right)\hat{\psi}_p(\vec{x}) = \lambda\delta^{(3)}(\vec{x}) - \frac{\mu^2}{32\pi P_0^2}\frac{e^{-m|\vec{x}|}}{|\vec{x}|}$$

Finally approximating $P^0 \simeq M$ we find

$$\left(-\frac{\nabla^2}{2M} + \frac{\mu^2}{32\pi M^2}\frac{e^{-m|\vec{x}|}}{|\vec{x}|} - \mathcal{E}_p\right)\hat{\psi}_p(\vec{x}) = \lambda\delta^{(3)}(\vec{x}) \tag{3.12}$$

The function $\hat{\psi}_p$ is then simply given by the Green function associated to this equation scaled by the tree-level amplitude

$$\hat{\psi}_p(\vec{x}) = \lambda G_p(\vec{x})$$

The Green function of an operator can be found from the eigenvalue equation [2], then

$$G_p(\vec{x}) = \int \frac{d^3\vec{k}}{(2\pi)^3}\frac{\phi_{\vec{k}}(\vec{x})\phi^*_{\vec{k}}(0)}{\frac{k^2}{2M} - \mathcal{E}_p}$$

And the $\phi_{\vec{k}}$ are given by the eigenvalue equation

$$\left(-\frac{\nabla^2}{2M} + \frac{\mu^2}{32\pi M^2|\vec{x}|} - \frac{k^2}{2M}\right)\phi_{\vec{k}} = 0$$

and normalized in such a way that the completeness equation holds

$$\int \frac{d^3\vec{k}}{(2\pi)^3}\phi_{\vec{k}}(\vec{x})\phi^*_{\vec{k}}(\vec{x}') = \delta^{(3)}(\vec{x} - \vec{x}')$$

[2] To fix ideas let us consider a finite dimensional operator A_{ij}, we want to find an operator ϕ_{jk} satisfying

$$A_{ij}\phi_{jk} = \delta_{ik}$$

if $e_i^{(b)}$ are eigenvectors of A_{ij} with eigenvalues $a^{(b)}$:

$$A_{ij}e_j = a^{(b)}e_i^{(b)}$$

and no sum on index between brackets is intended. If A is symmetric, it admits a basis of orthonormal eigenvectors which hence satisfy the completeness relation

$$\sum_b e_i^{(b)}e_j^{(b)} = \delta_{ij}$$

and then we have the really simple formula for ϕ:

$$\phi_{ij} = \sum_b \frac{e_i^{(b)}e_j^{(b)}}{a^{(b)}}$$

The Sommerfeld Enhancement is given by

$$\begin{aligned}
S &= \lim_{\tilde{p}\to p}\left|\frac{\mathcal{M}(\tilde{p},p',P)}{\lambda}\right|^2 = \\
&= \lim_{\tilde{p}\to p}\left|\frac{\left(\frac{\vec{\tilde{p}}^2}{2M}-\mathcal{E}_p\right)\psi_p(\tilde{p},p',P)}{\lambda}\right|^2 = \\
&= \lim_{\tilde{p}\to p}\left|\left(\frac{\vec{\tilde{p}}^2}{2M}-\mathcal{E}_p\right)\int d^3\vec{x}\, e^{-i\vec{\tilde{p}}\cdot\vec{x}}G_p(\vec{x})\right|^2 = \\
&= \lim_{\tilde{p}\to p}\left|\left(\frac{\vec{\tilde{p}}^2}{2M}-\mathcal{E}_p\right)\int d^3\vec{x}\, e^{-i\vec{\tilde{p}}\cdot\vec{x}}\int\frac{d^3\vec{k}}{(2\pi)^3}\frac{\phi_{\vec{k}}(\vec{x})\phi^*_{\vec{k}}(0)}{\frac{k^2}{2M}-\mathcal{E}_p}\right|^2 = \\
&= \left|\int d^3\vec{k}\,\phi_{\vec{k}}(0)\delta^{(3)}(\vec{k}-\vec{p})\right|^2 = \left|\phi_{\vec{p}}(0)\right|^2
\end{aligned}$$

Where we have used the identity

$$\lim_{\tilde{p}\to p}(\vec{\tilde{p}}^2-\vec{p}^2)\int\frac{d^3\vec{x}}{(2\pi)^3}\frac{\phi_{\vec{k}}(\vec{x})}{\vec{k}^{\,2}-\vec{p}^2-i\epsilon} = \delta^3(\vec{k}-\vec{p})$$

The proof of this identity is based on scattering in NR Quantum Mechanics and can be found in [**Appendix B**, 32].

Notice that choosing a pure contact interaction (the annihilation potential to SM particles really is confined to the origin) makes sure that only s-wave annihilation is important. If instead our annihilation potential were mediated by a massive particle (with mass $\tilde{M}$) for example, in the previous equations instead of $\lambda\delta^{(3)}(\vec{x})$ we would have obtained in (3.12)

$$\left(-\frac{\nabla^2}{2M}+\frac{\mu^2}{32\pi M^2}\frac{e^{-m|\vec{x}|}}{|\vec{x}|}-\mathcal{E}_p\right)\hat{\psi}_p(\vec{x}) = \hat{\mathcal{M}}_0(\vec{x}) = U_0 \tag{3.13}$$

Where U_0 is a Yukawa potential up to some normalization constants. Then ψ_p would no more be proportional to $G(\vec{x})$ but would be given by its convolution with the tree-level annihilation potential U_0

$$\psi_p(\vec{x}) = \int d^3\vec{x}\,' G(\vec{x}-\vec{x}\,')U_0(\vec{x}\,')$$

and therefore the formula for the Amplitude changes to further include also higher order l-waves

$$\mathcal{M}(p,p',P) = \int d^3\vec{x}\,\phi_{\vec{p}}(\vec{x})U_0(\vec{x})$$

which has the dominant contribution still given by the s-wave for every U_0 peaked at the origin, but as long as U_0 is non-zero outside the origin also higher order l-waves will give a smaller contribution.

3.3.5 Sommerfeld for Coulomb Potential

We have solved the Schrödinger eigenvalue equation for scattering

$$-\frac{1}{r}\frac{\partial^2}{\partial r^2}(r\chi)-\frac{L^2}{r^2}\chi+\frac{\alpha M}{r}\chi = k^2\chi$$

where we used the previous convention

$$\alpha = \frac{\mu^2}{16\pi M^2}$$

The solution to this equation can always be expanded in partial waves, which for azimuthally symmetric scattering potentials is

$$\chi = \sum_l A_l P_l(\cos\theta) R_{kl}(r)$$

The $R_{kl}(r)$ are solutions to the equation

$$-\frac{1}{r}\frac{\partial^2}{\partial r^2}(rR_{kl}) - \frac{l(l+1)^2}{r^2}R_{kl} + \frac{\alpha M}{r}R_{kl} = k^2 R_{kl}$$

and have well-known asymptotic behaviours: if the potential goes like less than $\frac{1}{r^2}$ for $r \to 0$ and go to zero sufficiently fast at long distance, $R_{k,l}$ approaches asymptotically the solution of equation

$$-\frac{1}{r}\frac{\partial^2}{\partial r^2}(rR_{kl}) - \frac{l(l+1)^2}{r^2}R_{kl} = 0 \qquad r \to 0$$

and we have

$$R_{kl} \propto r^l \qquad r \to 0$$

and thus we are only interested to the solutions with $l = 0$. The asymptotic behaviour at infinity for $l = 0$ is given by

$$-\frac{1}{r}\frac{\partial^2}{\partial r^2}(rR_{k0}) = k^2 R_{k0} \qquad r \to \infty$$

and the solution is given by

$$R_{k0} = \frac{2}{r}\sin(kr + \delta_0)$$

The fact that the Coulomb potential dies off really slowly can give a mild dependence of δ_0 on r, in particular a logarithmic dependence. We can expand this result in partial spherical ingoing and outgoing waves. Imposing that the ingoing waves should have the same form of the $l = 0$ components of the partial wave expansion of

$$e^{ikz} \supset \frac{1}{2ikr}P_0(\cos\theta)(e^{-ikr} + e^{ikr})$$

we find

$$A_0 = \frac{1}{2k}e^{i\delta_0}$$

If we now define

$$u_0 = \frac{R_{k0}}{r}$$

then u_0 is given by the radial equation, with the boundary conditions seen above.

$$u_0'' + k^2 u_0 = \frac{\alpha M}{r}u_0 \tag{3.14}$$

The solution for u_0 is given in terms of the confluent hypergeometric functions

$$u_0(r) = e^{ikx}x\left[c_1 F\left(1 - \frac{i\alpha M}{2k}, 2, 2ixk\right) + c_2 U\left(1 - \frac{i\alpha M}{2k}, 2, 2ixk\right)\right]$$

we should now impose the boundary conditions

$$u_0 \to r \qquad r \to 0$$

$$u_0 \to 2\sin(kr + \delta) \qquad r \to \infty$$

The first condition gives $c_2 = 0$ because

$$F(a,b,z) = \sum_n \frac{a^{(n)}}{b^{(n)}} z^n$$

and $a^{(n)}$ is the rising factorial defined as $a^{(0)} = 1$ and $a^{(n+1)} = (a+n)a^{(n)}$. Instead the function U is given by

$$U(a,b,z)\frac{\Gamma(1-b)}{\Gamma(a+1-b)}F(a,b,z) + \frac{\Gamma(b-1)}{\Gamma(a)}z^{1-b}F(a+1-b,2-b,z)$$

and therefore for $z \to 1$ we have $F \to 1$ and $U \propto \frac{1}{z}$. Taking the asymptotic expansion for $x \to \infty$ we obtain

$$u_0 \to = -\frac{i}{2k} i^{-ia} c_1 \left(\frac{e^{ikx}(2kx)^{-ia}}{\Gamma(1-ia)} - \frac{e^{-ikx}(2kx)^{+ia}}{\Gamma(1+ia)} \right)$$

where we have taken

$$a = \frac{\alpha M}{2k}$$

Using that explicitly we have

$$(\Gamma(1-ia))^* = \Gamma(1+ia)$$

and that we can reabsorb an arbitrary phase in c_1 we have

$$c_1 = 2k\Gamma(1-ia)e^{-\frac{\pi}{2}a}$$

Combining this with the normalization constant A_0 we find

$$\chi(0) = \Gamma(1-ia)e^{i\delta_0}e^{-\frac{\pi}{2}a}$$

and so finally

$$S = |\chi(0)|^2 = e^{-\pi a}|\Gamma(1-ia)|^2 = \left| \frac{2\pi a}{e^{2\pi a} - 1} \right|^2$$

We have used the identity

$$|\Gamma(1-ia)|^2 = \Gamma(1-ia)\Gamma(1+ia) = \Gamma(1-ia)\Gamma(ia)(ia) = {}^3\frac{\pi}{\sin(i\pi a)}(ia) = \frac{\pi a}{\sinh(\pi a)}$$

$$S = \left| \frac{2\pi \frac{\alpha}{v}}{1 - e^{\frac{2\pi\alpha}{v}}} \right| \tag{3.15}$$

which is the Sommerfeld Enhancement for a repulsive Coulomb potential! The velocity v is the relative velocity between the particles (so the double of their velocity in the centre of mass frame).

[3] We used the identity

$$\Gamma(z)\Gamma(1-z) = \frac{\pi}{\sin(\pi z)}$$

This identity is not that easy to prove, but taking the integral definition of the Γ function

$$\Gamma(z)\Gamma(1-z) = \int_0^\infty du \int_0^\infty dt e^{-(t+u)} \left(\frac{t}{u}\right)^{z-1} \frac{1}{u} = \int_0^\infty dx \frac{x^{z-1}}{1+x}$$

where we have made the changes of variables $y = t + u$ and $x = \frac{t}{u}$. The last integral is still nasty, but can be evaluated through contour integration (it has one pole in 0 and one pole in -1 for $0 < Re z < 1$).

3.3.6 Generic l-waves

If the cross section is not s-wave dominated, but is instead l-wave dominated, meaning

$$\mathcal{M}_0 = \lambda p^l$$

Taking the partial wave expansion, using the completeness relation for the angular part (which contains the Legendre Polynomials) [32] and using the asymptotic value R_{pl} for small r of we find

$$\mathcal{M}(p,p') = \sqrt{\frac{\pi}{2}\frac{(2l+1)!!}{l!}}\frac{1}{p}\left(\frac{\partial}{\partial r}\right)^l R_{pl}|_{r=0}\,\lambda$$

With R_{pl} always given by the eigenvalue equation. For the Coulomb potential we are blessed with an analytic expression for these eigenfunctions which we obtain imposing suitable boundary conditions as we did for the $l = 0$ case:

$$R_{pl}(r) = p\sqrt{\frac{2}{\pi}\prod_{s=1}^{l}(s^2+a^2)e^{-\frac{\pi}{2}a}\Gamma(1-ia)}\frac{(2pr)^l e^{-ipr}}{(2l+1)!F(l+1-ia,2l+2,2ipr)}$$

The derivative with respect to r is now easy to obtain and

$$S = \left(\prod_{s=1}^{l}(s^2+a^2)\right)\frac{e^{-\pi a}}{l!^2}\frac{\pi a}{\sinh(\pi a)} \tag{3.16}$$

Which reproduces the result we had obtained above for $l = 0$.

3.4 Minimal Dark Matter

The general framework we have derived in the previous sections can be applied to the case of Minimal Dark Matter to the extent of computing its annihilation cross section and then, solving the Boltzmann equation its relic abundance as a hot Dark Matter candidate. In the following we will follow [28][27]. Computing the Sommerfeld effect for MDM implies a major complication as MDM particles can oscillate, by exchange of charged bosons from a component of the multiplet to other.

To fix ideas we will initially focus on a real scalar MDM triplet. We have thus added to the SM the states χ_-, χ_0, χ_+, which can form couples of incoming states, these states are free to oscillate between those with the same quantum numbers.

3.4.1 Input from Particle Physics

States can be classified by all the following quantum numbers:

- $S = 0$ as we are focusing on scalar DM. This is the reason why in the first place I chose to analyse in detail a scalar triplet.
- $Y = 0$ as we have seen, states with $Y \neq 0$ are forbidden by direct detection, unless we give up minimality and consider the further renormalizable operator proportional to λ_H.
- $L = 0$ as we will be considering only s-wave annihilation. It is not complicated to consider also p-wave or further waves, but they constitute a minor correction to the annihilation cross section.
- The charge Q, which, as we have taken $Y = 0$. coincides with the weak-isospin quantum number. This quantum number clearly cannot be fixed, so we will use it to classify our possibly oscillating states:

– $Q = 0$:

$$\chi_0\chi_0 \longleftrightarrow \chi_+\chi_-$$

– $Q = \pm 1$:

$$\chi_0\chi_\pm$$

– Q=± 2:

$$\chi_\pm\chi_\pm$$

In this problem we thus have only one state which is able to oscillate and whose dynamics we will have to study as a 2-states system described by a 2×2 matrix.

To encode the dynamics of every one of these states we use two matrices with indices i and j varying on all the possible oscillating states. One matrix $V_{i,j}$ containing the imaginary part of the $2 \to 2$ body propagator. On the diagonal we have the potential interaction due to the internal interaction of the single state (so for example electrostatic interactions for the $\chi_+\chi_-$ state) and off diagonal the charged vector Yukawa potential mediating transitions between state i and state j.

The other matrix we are interested in is the one representing the imaginary part of the same propagator, $\Gamma_{i,j}$ this matrix contains on the diagonal the tree-level annihilation rates and on the diagonal something which can be interpreted by cutting rules as a sort of product between these rates. Notice looking at the expression below that we have already factored out a $\delta^{(3)}(\vec{r})$ in the definition of Γ.

The system is then described by the effective Lagrangian

$$\mathcal{L} = \int d^3\vec{r} \sum_{S_z} \psi^*_{S_z} \left(i\frac{\partial}{\partial t} - \frac{\nabla_x^2}{2M} - \frac{\nabla_r^2}{2M} - V(r) + 2i\Gamma\delta^3(\vec{r}) \right) \psi_{S_z}$$

We have split the formula as a sum over S_z eigenfunction, but in the proceeding I will omit the subscript. Then the Schrödinger equation is given by

$$-\frac{1}{M}\frac{\partial}{\partial r^2}\psi_i^{(j)} + \sum_{i'} V_{i,i'}\psi_{i'}^{(j)} = K\psi_i^{(j)}$$

The boundary conditions are given by

$$\psi_i^{(j)}(0) = \delta_{ij}$$

$$\frac{\partial}{\partial r}\psi_i^{(j)}(\infty) = i\sqrt{M(K - V(\infty)_{i,i})}\psi_i^{(j)}(\infty)$$

the index (j) is needed to fix the incoming states to which we are interested. The Sommerfeld enhancement is then given from the optical theorem[4]

$$\sigma_i v = c_i \frac{1}{2M_{i_1}M_{i_2}} (A_{ij}\Gamma_{j,j'}A^*_{ij'})$$

[4]This definition might appear counter intuitive as it is the counterpart of stating that in a one-dimensional system

$$S = \left| \frac{\psi(\infty)}{\psi(0)} \right|$$

but can be proven to be equivalent to our previous definition using the fact that the Wronskian of the radial Schrödinger equation is constant [30]

$$W(r) = u_1'(r)u_2(r) - u_2'(r)u_1(r) = const$$

in the last section we required $u(r)$ to be a solution to the radial equation, to go to zero in the origin and to $\frac{1}{k}\sin(kr + \delta)$. We consider also the solution u_2 going like $\frac{1}{k}\cos(kr + \delta)$ at infinity and to some constant A in the origin. The Wronskian is then

$$W(r) = W(\infty) = 1$$

and the matrix A_{ij} is given by

$$A_{ij} = \lim_{r\to\infty} \frac{\psi_i^{(j)}}{e^{iRe\sqrt{M(K-V(\text{inf}))_{i,i}}r}}$$

Notice that the oscillating phase would in any case go away in the computation of σ_i, but the matrix A could be ill-defined if we do not factor it out.

The matrix potential are given by the spatial Fourier transform of the non-relativistic approximation of the amputated propagator. Approximating $M_i \simeq M_j = M$ except when we have proportionality on the mass splitting (we are working in the fairly accurate approximation $\Delta M \ll M$) and redefining

$$\tilde{\Gamma}_{i,j} = \frac{1}{2M^2}\Gamma_{i,j}$$

$$\sigma_i \simeq= c_i(A_{ij}\tilde{\Gamma}_{j,j'}A^*_{ij'})$$

In [27] they report, for scalar $S = 0$ and $Y = 0$ the expressions

$$\tilde{\Gamma}_{ii',jj'} = \frac{N_{ii'}N_{jj'}}{16\pi M^2}\sum_{A,B}\{T^A, T^B\}_{ii'}\{T^A, T^B\}_{jj'}$$

$$V_{ii',jj'} = (M_i + M_j - 2M)\delta_{ij}\delta_{i'j'} + N_{ii'}N_{jj'}\sum_{AB} K_{AB}(T^A_{ij}T^B_{i'j'} + T^A_{ij'}T^B_{i'j})\frac{e^{-m_A r}}{4\pi r}$$

Where the coupling constants of the vector bosons are reabsorbed inside the generators, and indices A, B vary on all the generators associated to vector bosons:

$$T^A \in \{T^\gamma, T^Z, T^+, T^-\}$$

The matrix K_{AB} takes into account the propagator structure, meaning that I must contract A wit A and Z with Z (being real fields) but W^+ with W^- being complex fields. This formula has to be taken with a pinch of salt:

- The mass term $(M_i + M_j - 2M)$ comes from the non relativistic approximation of Schrödinger equation, taken with respect to the reference energy of the lightest state $2M$.
- The potential term arises either from the non-relativistic approximation or from tree-level vector boson exchange, so it is a classical object. The Annihilation matrix Γ (or equivalently $\tilde{\Gamma}$) instead arises at loop level (as you can see from the fact that it contains 4 power of the couplings inside the generators). At tree level in fact the matrix is proportional to $\delta(\vec{p}^2 + m_A^2)$ in the CM frame which is kinematically forbidden to go on shell. The leading order contribution then arises from loop level box diagrams, crossed box diagrams and triangular diagrams.
- We should be careful on what we intend when applying the above formula to interactions involving diagonal generators as there are some subtleties regarding the mass term for real fields.

computing it in the origin gives

$$1 = W(0) = u'(0)A$$

and so $u = \frac{r}{A} + O(r^2)$ near the origin and therefore $S = \frac{1}{|A|^2}$ .The boundary conditions we are requiring for our ψ instead are $\psi' \to ik\psi$ at infinity and $\psi(0) = 1$ therefore it is easy to see $\psi = \frac{1}{A}(u_1 + iu_2)$ and the Sommerfeld Enhancement is

$$S = \frac{1}{|A|^2} = \left|\frac{\psi(\infty)}{\psi(0)}\right|^2$$

The result is analogously proven for the multi-dimensional case.

As a shorthand to do the explicit computations we have

$$\alpha_W = \frac{g^2}{4\pi} \qquad A = \alpha_{em}\frac{e^{-m_\gamma r}}{r} + \alpha_W c_W^2 \frac{e^{-m_Z r}}{r} \qquad B = \alpha_W \frac{e^{-m_W r}}{r}$$

and ΔM defined as in (2.4) Applying now our result to the specific case of a Dark Matter triplet we find

- $S = 0$ and $Q = 0$:

$$\tilde{\Gamma}^{S=0}_{Q=0} = \frac{2\pi\alpha_W^2}{M^2}\begin{pmatrix} 3 & \sqrt{2} \\ \sqrt{2} & 2 \end{pmatrix}$$

$$V^{S=0}_{Q=0} = \begin{pmatrix} 2\Delta M - A & -\sqrt{2}B \\ -\sqrt{2}B & 0 \end{pmatrix}$$

- $S = 0$ and $Q = \pm 1$, the physics is exactly the same if we exchange χ^+ and χ^- up to a total $SU(2)$ rotation that must not change the physics.

$$\tilde{\Gamma}^{S=0}_{Q=1} = \frac{2\pi\alpha_W^2}{M^2} \qquad V = \Delta M + B$$

- $S = 0$ and $Q = \pm 2$:

$$\tilde{\Gamma}^{S=0}_{Q=1} = \frac{2\pi\alpha_W^2}{M^2} \qquad V = 2\Delta M + A$$

3.4.2 Masses of the vector bosons

We will then want to solve the Boltzmann equation from a time where the DM species were in equilibrium with the thermal bath to the present day.

In this span of time the masses of the vector bosons in the Standard Model change because of two effects: induced Thermal Masses and Electroweak Phase Transition this was first systematically done in [46]. As we shall see freeze out for MDM species actually happens to be in the ballpark of $100\,\text{GeV} - 10\,\text{TeV}$ therefore it happens at the same energies at which electroweak phase transition takes place. The $W^\pm, Z, \gamma$ is a legitimate basis to carry out calculations even when the $SU(2)_L \times U(1)_Y$ symmetry is unbroken, but when this happens all the vector bosons are massless (at zero temperature). We will assume [18] that the Vacuum Expectation Value of the Higgs goes as

$$v(T) = vRe\left(\sqrt{1 - \frac{T^2}{T_c^2}}\right)$$

with $T_c = 200\,\text{GeV}$. The induced thermal mass (in general in medium interactions change a bit the structure of propagators from the vacuum form, but the main induced effect is a thermal mass) is given from [21][15]:

$$(m_Y^2)_{Th} = \frac{11}{6}b^2T^2 \qquad (m_W^2)_{Th} = \frac{11}{6}g^2T^2$$

This means that the masses of charged bosons in the unbroken phase of the Standard Model are

$$m_W^2 = \frac{g^2v^2}{4} + \frac{11}{6}g^2T^2$$

while for neutral vector bosons we have the following mixing mass matrix

$$M_{BW} = \begin{pmatrix} \frac{v^2b^2}{4} + \frac{11}{6}b^2T^2 & \frac{v^2bg}{4} \\ \frac{v^2bg}{4} & \frac{v^2g^2}{4} + \frac{11}{6}g^2T^2 \end{pmatrix}$$

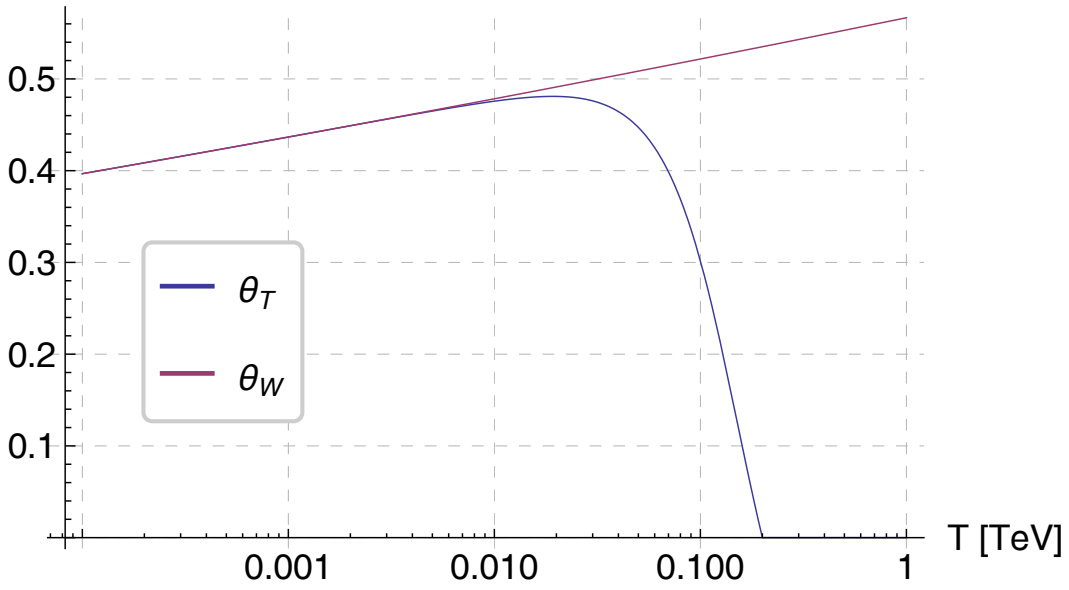

Figure 3.4: Evolution of θ_T needed to diagonalize the mass matrix in comparison to θ_W. Obviously when $T > T_c$ the matrix is already diagonal, when T drops below T_c the angle rapidly tends to reach θ_W.

which can be diagonalized in terms of an angle θ_T

$$\theta_T = \frac{1}{2}\arctan\left(\frac{2bg}{g^2-b^2}\frac{1}{1+\frac{22}{3}\frac{T^2}{v^2}}\right)$$

and so $\theta_T \to \theta_W$ for $T \to 0$. Strictly speaking also $\theta_W = \arctan\frac{b}{g}$ is a function of temperature because of the running of couplings. Because of the adiabatic theorem [57], this variation does not cause transition from γ to Z under conditions which are very easily satisfied. We still call the mass basis eigenstates γ and Z:

$$A_\mu = c_T B_\mu + s_T W^3_\mu$$
$$Z_\mu = c_T W^3_\mu - s_T B_\mu$$

And their masses are

$$m^2_\gamma = (m^v_Z)^2\left(1+\frac{22}{3}\frac{T^2}{v(T)^2}\right)\frac{\sin(\theta_T+\theta_W)\sin(\theta_W-\theta_T)}{\cos(2\theta_T)}$$
$$m^2_Z = (m^v_Z)^2\left(1+\frac{22}{3}\frac{T^2}{v(T)^2}\right)\frac{\cos(\theta_T+\theta_W)\cos(\theta_W-\theta_T)}{\cos(2\theta_T)}$$

With m^v_Z defined as

$$m^v_Z = \frac{\sqrt{g^2+b^2}v(T)}{2}$$

In this way it is obvious that these masses go to the known masses for $T \to 0$.

3.4.3 Boltzmann Equation

To find the relic density we should now do an accurate description of freeze out through the Boltzmann equation.

MDM is described by a co-annihilation equation:

$$\frac{dn}{dt} + 3Hn = -\langle\sigma v\rangle_{eff}(n^2 - n^2_{eq})$$

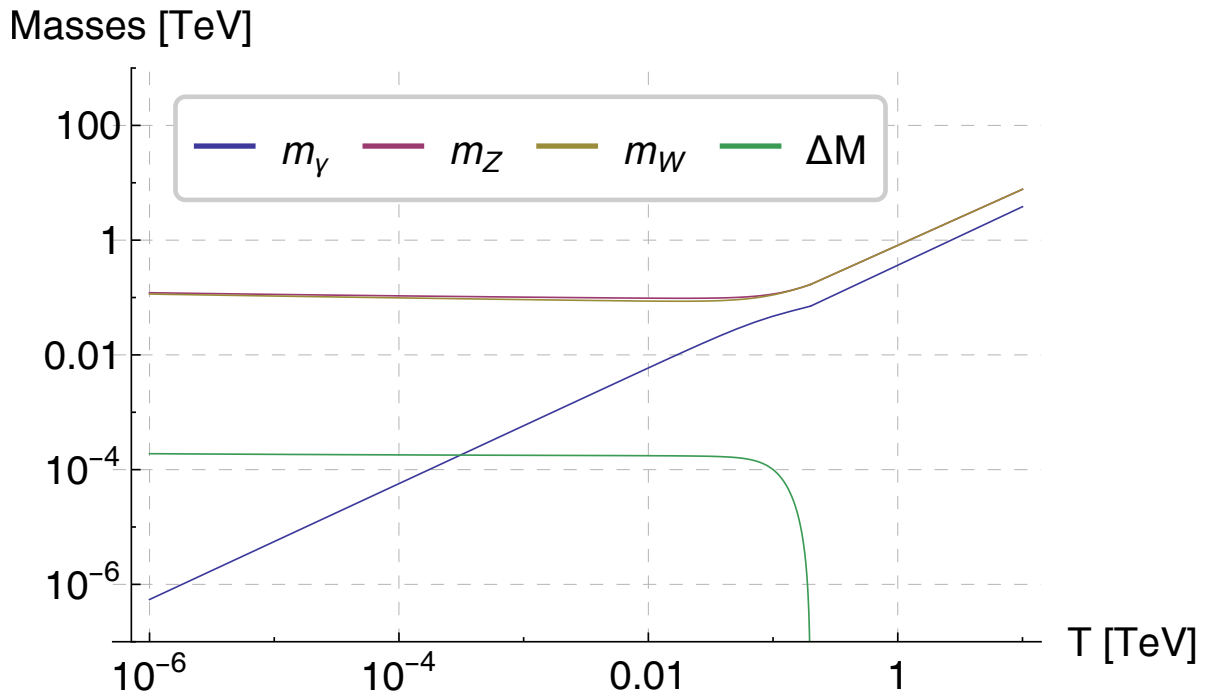

Figure 3.5: Running of the eigenstates of the mass matrix of electroweak vector bosons. In the plot we show also the running of the mass splitting Δ_M between Dark matter particles.

$$\langle \sigma v \rangle_{eff} = \sum_{i,j} \langle \sigma_{ij} v \rangle r_i r_j$$

$$r_i = \frac{n_i}{n} = \frac{g_i M_i^{\frac{3}{2}} e^{-\Delta M_i/T}}{\sum_i g_i M_i^{\frac{3}{2}} e^{-\Delta M_i/T}}$$

We proceed as well known defining the comoving number density as

$$Y = \frac{n}{s}$$

If no DOF disappear from my thermal bath both quantities scale like $1/a^3$ and hence Y is approximately a constant after freeze-out.

Then changing our parameter from t to $x = M/T$ which is still strictly increasing in time, we have

$$\frac{dY}{dx} = -\frac{\langle \sigma v \rangle_{eff}}{Hx} \left(1 - \frac{x}{3g_{*s}} \frac{d\, g_{*s}}{dx}\right) s(Y^2 - Y_{eq}^2)$$

where we exploited

$$s = \frac{2\pi^2}{45} g_{*s} T^3 \propto a^{-3}$$

and hence

$$\frac{dT}{dt} \left(3T^2 g_{*s} + T^3 \frac{d}{dT} g_{*s}\right) = -3 g_{*s} T^3 H$$

The term containing the variation of $g_* s$ is normally neglected, but we keep it because our freeze out is near the Electroweak Phase Transition where the DOF of the thermal bath change quite abruptly.

We should now do the thermal average of our cross section. This implies we should solve our Schrödinger equation for a thermal ensemble of kinetic initial energies and then average out the cross section obtained

this way. We cannot do any better since the Sommerfeld-enhanced cross section is quadratically dependent on the wavefunction and the conservation of probability equation we can derive from it is non-linear.

This is a lengthy procedure and we will show the explicit numerically computed plot just for the case of the scalar triplet.

3.4.4 Computational details and Results

To solve Boltzmann equation we use the values of $g_{*s}(T)$, $g_*(T)$ and $i(T)$ as defined in [40] and tabulated in http://laine.itp.unibe.ch/eos15/ adding the contributions due to the MDM degrees of freedom. In particular

$$i(T) = \frac{\frac{d\rho}{dT}}{\frac{2\pi^2}{15}T^3}$$

Hence $i(T)$ represents sort of an effective degree of freedom for the thermal capability of the primordial bath. We use the Friedman equation to relate them to $H(T)$ and the fluid equation to compute dT/dt from $c(T)$.

Other known constants (α_W, α_{EM}, s_0, ρ_{crit}, M_z...) have been taken from [65] and their running has been accounted for.

We assume that MDM is far from degeneracy. Hence its equilibrium distribution is given by

$$n_{eq} = g \int \frac{d^3\vec{p}}{(2\pi)^3} e^{-\frac{\sqrt{(\vec{p})^2+M^2}-\mu}{T}} = \frac{g}{2\pi^2} e^{\frac{\mu}{T}} M^2 T K_2\left(\frac{M}{T}\right)$$

Furthermore the fundamental constants are evaluated a the typical size of the exchanged energy. Therefore we have two qualitatively different energy scales.

$$\alpha(\mu) = \begin{cases} \alpha(\mu \simeq M) & \text{for the annihilation process} \\ \alpha(\mu \simeq T) & \text{for vector bosons exchanges} \end{cases}$$

We can notice from figure 3.7 that just before the DM mass $M \simeq 2.9\,\text{TeV}$ correctly reproducing the DM relic abundance there is a structure that is signal of the presence of a sharp resonance in the Dark Matter annihilation.

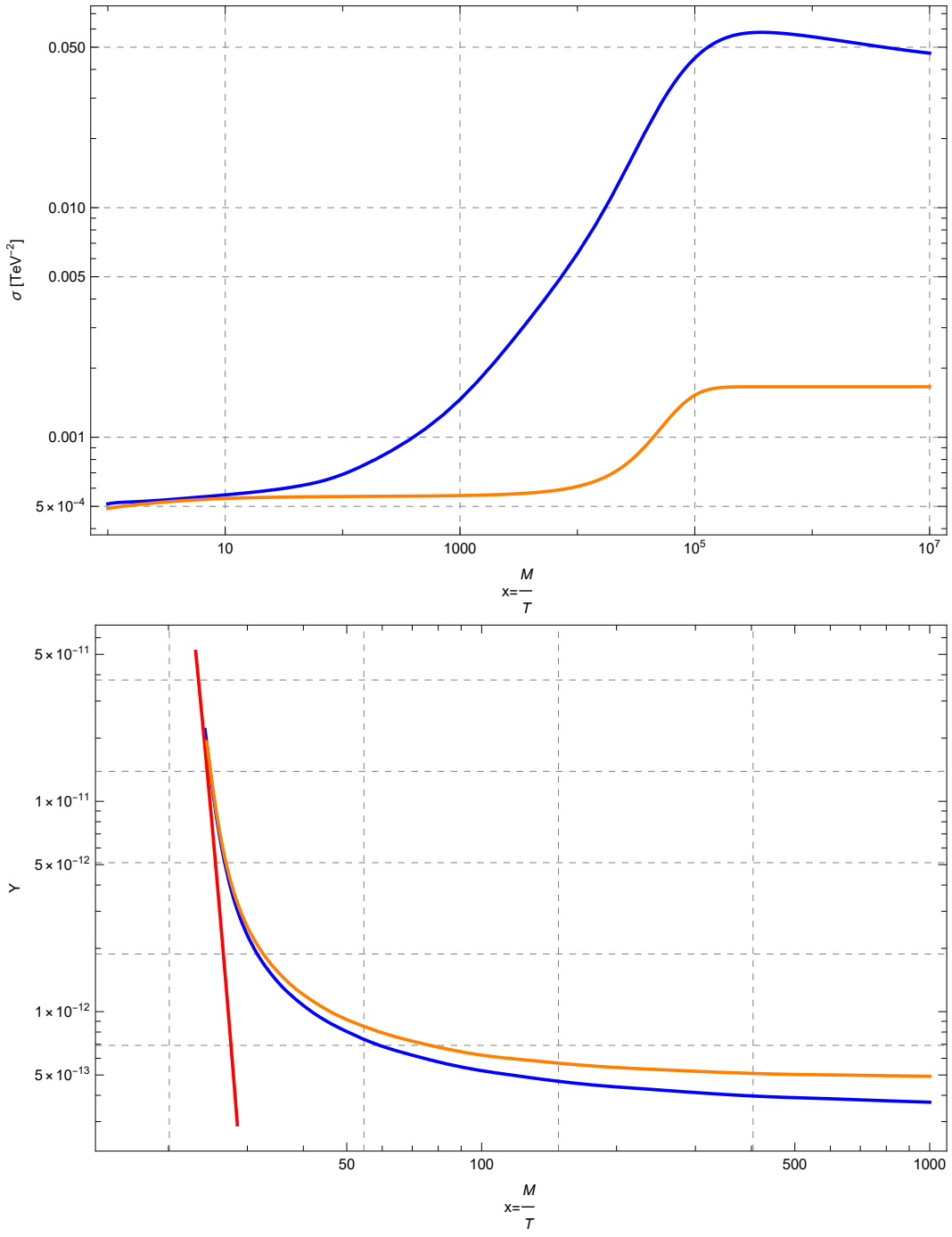

Figure 3.6: The plots represent the thermally averaged cross section and the corresponding solution to the Boltzmann equation for a Dark Matter mass of $M = 2.9\,\text{TeV}$. In Blue we have the results including non-perturbative Sommerfeld corrections, while in orange we show the tree-level approximation without including these, as naively done in **??**.

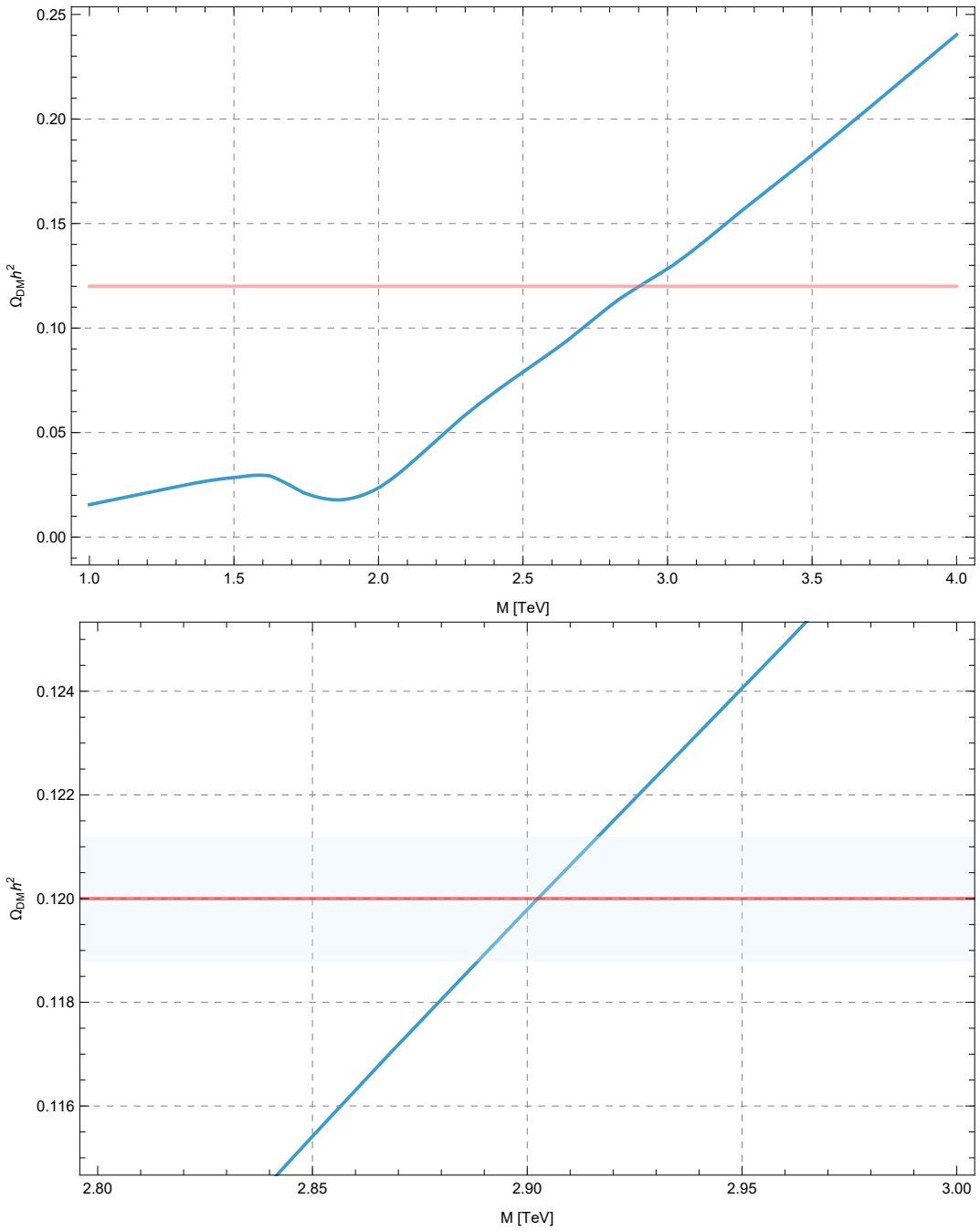

Figure 3.7: The plots show the Dark Matter relic density obtained as a function of the Dark Matter mass. In the figure Below we provide a zoom around the relevant window at which the scalar triplet mass reproduced the observed density as measured by Planck [50].

Quantum numbers			DM mass
$SU(2)_L$	$U(1)_Y$	Spin	in TeV
2	1/2	0	
2	1/2	1/2	
3	0	0	2.90 ± 0.09
3	0	1/2	3.1 ± 0.1
3	1	0	
3	1	1/2	
4	3/2	0	
4	3/2	1/2	
5	0	0	10.2 ± 0.3
5	0	1/2	9.0 ± 0.3
7	0	0	26 ± 1

Table 3.1: Update of table **??** with non-perturbative, non-relativistic Sommerfeld contributions included. A relative error of $\sim 3\%$ because of the finite size of our Thermal Ensemble on which we averaged the cross section. We have computed only corrections to candidates with $Y = 0$ because they are the only viable because of direct detection if we want to stick to minimality.

Chapter 4

Further Developments

In this section we will analyse different aspects of the Sommerfeld effect. First we will review all the limitations of the non-relativistic approximations we have done in the previous section when resumming ladder diagrams and explain why this method is really difficult to generalize to include relativistic corrections. Then we will briefly mention some Sommerfeld-like effect we neglected in this work. Finally we will apply the Sommerfeld corrections seen before to a new range of DM models coannihilating with some colored partner to show how Sommerfeld corrections are a robust feature of all thermal DM models allowing some sort of long-range potential interaction.

4.1 Debating relativistic corrections

Relativistic corrections may be sizeable as freezeout happens when

$$x = \frac{M}{T} \sim 25$$

and (at least in the instantaneous freezeout approximation) this is the most meaningful point where the whole Dark Matter relic density is determined. At this value of x the Dark Matter isn't strictly non-relativistic...in the sense that

$$v \sim \sqrt{\frac{T}{M}} \sim \frac{1}{5}$$

and we could have lost some corrections in the above procedure.

We could try to do this via perturbation theory from the Schrödinger equation, but this is computationally really hard to do because it would mean having to know with good precision the wavefunction at every point in order to the integrate it again on the whole space...and this only to compute the first order correction.

4.1.1 An exact differential equation

Let us summarize briefly all the approximations we made deriving the non-relativistic formula to resum all ladder diagrams of the exact integral equation in QFT.

We started from the equation

$$\mathcal{M}(\tilde{p}, p', P) = \mathcal{M}_0(\tilde{p}, p', P) - i \int \frac{d^4q}{(2\pi)^4} G(P+q) G(P-q) \tilde{\Gamma}(\tilde{p}, q, P) \mathcal{M}(q, p', P)$$

1. We took the tree level approximation of the 2PI $\chi\chi \to \chi\chi$ propagator entering (3.8). This is not truly a non-relativistic approximation and is easily circumventable by adding higher loop contributions to our expression for $\tilde{\Gamma}$.

2. We took the instantaneous approximation of the interaction propagator, corresponding to the $\tilde{\Gamma}$. This is fine in the non-relativistic approximation where

$$k^0 \sim Mv^2$$

$$\vec{k} \sim Mv$$

and hence the term we are neglecting (containing both the retardation and the "magnetic" interaction) is

$$\frac{k_0^2}{(k^2-m^2)(\vec{k}^{\,2}+m^2)} \sim \frac{1}{\vec{k}^{\,2}+m^2} \cdot \min\left\{\frac{M^2}{m^2}v^4,\, v^2\right\}$$

Therefore in adapting to a relativistic approximation we could have a 4% error already at this point. Not to make this approximation we could think of keeping the entire form of the propagator. Adding perturbations would exactly mean ending up with a perturbed Schrödinger equation and perturbation theory for this problem seems quite heavy computationally.

3. We made the (justified) assumption that in the non-relativistic approximation the matrix element $\mathcal{M}(q,p,t)$ was pole-free in q_0. This is exactly true for the pure s-wave tree level function we were considering in the preceding section. Now instead our tree-level annihilation graph is given by a pair annihilation of the heavy scalar field. Therefore

$$\mathcal{M}_0(\tilde{p},p',P) = i4\mu^2\left(\frac{1}{(\tilde{p}-p')^2-m^2}+\frac{1}{(\tilde{p}+p')^2-m^2}\right)$$

the two different contributions are given by u and t channel contributions. The point is that now the tree-level amplitude as a pole in $\tilde{p}^{\,0}$. But you can see from an explicit computation that these poles do not contain the small denominators

$$\sim \frac{1}{P^0-\omega}$$

and thus in the non-relativistic approximation it is still a valid assumption to consider $\mathcal{M}_0$ pole-free in its first argument. Now we would like to argue that therefore also $\mathcal{M}$ is to some extent pole-free. Unfortunately this cannot be done unless we give up on the attempt we would have liked to do to keep the full interaction propagator and not just its instantaneous approximation. You could now say that if we solve the same integral equation for hydrogen it has to give us poles (corresponding to the bound states) but these are poles in $P=\sqrt{s}/2$ not in $\tilde{p}$ and thus the argument we gave above is safe.

4. The fourth approximation, as anticipated, is to neglect the non-relativistic enhanced terms in our expansion

$$\frac{1}{P^0+\omega} \sim \frac{1}{2M} \ll \frac{1}{Mv^2} \sim \frac{1}{P^0-\omega}$$

again this is a very good non-relativistic approximation, but cannot be done if we are trying to compute relativistic corrections.

5. We took the non-relativistic approximation of

$$P^0-\omega \simeq \frac{\vec{p}^{\,2}}{2M}-\frac{\vec{p}^{\,2}}{2M}$$

this is not really something we need as we could have just defined ψ_p using the full expression of $P^0-\omega$ but helps in recovering later exactly the form of the Schrödinger equation.

The points highlighted above in this derivation give little to no hope of being able to extend with little effort the non-relativistic approximation and include relativistic corrections. It is clearly unfeasible to contour integrate on q^0 now, not knowing the poles of my amplitude $\mathcal{M}(q, p', P)$. Also if we wish to do something relativistically we should try to treat both energy and momentum on equal footing.

A naive attempt we could make at the problem is to say we would like to find a solution that contains the Fourier transform of the interacting potential. For now I therefore want to redefine $\mathcal{M}$ in order to reabsorb the denominators of which I do not care about (contained in $G(P+q)$ and $G(P-q)$. Exactly in the same fashion that we defined

$$\mathcal{M}(\tilde{p}, p', P) = \left(\frac{\vec{\tilde{p}}^2}{2M} - \mathcal{E}\right)\psi_p(\tilde{p}, p', P)$$

We now define

$$\mathcal{M}(\tilde{p}, p', P) = ((P+\tilde{p})^2 - M^2)((P-\tilde{p})^2 - M^2)\phi_p(\tilde{p}, p', P)$$

in the CM frame $\vec{P} = 0$, $p^0 = 0$ and $P_0^2 = \vec{p}^2 - M^2$. It is therefore still necessary to keep p and $\tilde{p}$ distinct and send $\tilde{p}$ to its on-shell value later on.

$$((P+\tilde{p})^2 - M^2)((P-\tilde{p})^2 - M^2)\phi_p(\tilde{p}, p', P) = \mathcal{M}_0(\tilde{p}, p', P) - i\int \frac{d^4q}{(2\pi)^4}\frac{\mu^2}{(\tilde{p}-q)^2 - m^2}\mathcal{M}(q, p', P)$$

Fourier transform to position space gives

$$[(P^2 - \partial^2 - M^2) + 4(P\cdot\partial)^2]\hat{\phi}_p = \hat{\mathcal{M}}_0 - \frac{m\mu^2}{4\pi^2}\frac{K_1(m\sqrt{-x^2+i\epsilon})}{\sqrt{-x^2+i\epsilon}}\hat{\phi}_p$$

This equation is in principle exact but of limited utility. In fact it is not separable (neither doing a change of coordinates) so we would need to solve the equation on the entire space. Furthermore the limit for epsilon going to 0 and branch cuts in the RHS are not so simple to handle, for example we have already seen that in the massless case they yield a δ-function.

4.1.2 Higher loop corrections

A more successful strategy could be to include higher loop corrections in our result. We have argued that the Sommerfeld enhancement constitutes a resummation of all the loop contribution that are v-enhanced as $\left(\frac{\alpha}{v}\right)^n$ and that loop corrections other than ladder diagrams are suppressed by an additional power of α

$$\sim \alpha\left(\frac{\alpha}{v}\right)^n$$

as they are loop corrections to the effective vertex $\tilde{\Gamma}$. This means that including 1-loop effects would make the first neglected piece in the result of order

$$\sim \frac{\alpha^2}{v}$$

This may or may not be sufficient according to the value of α and the required precision. It is eventually possible to incorporate higher loop effects, but the matrix element computation become really difficult to compute at 2-loops especially for non-trivial models with lots of possible diagrams.

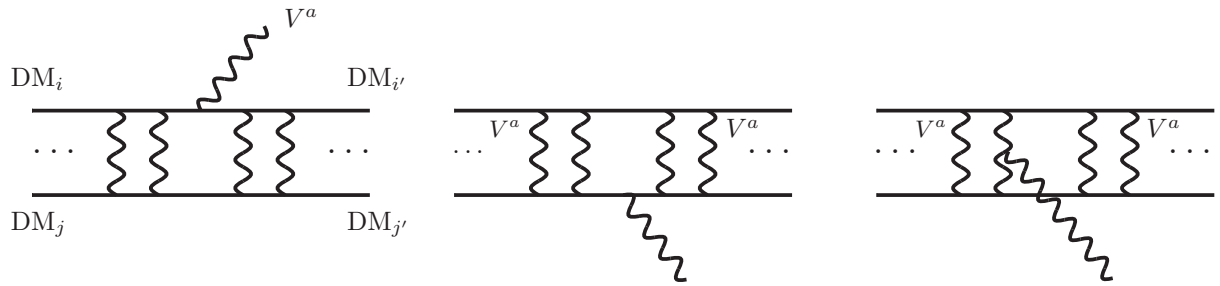

Figure 4.1: Relevant Diagrams for bound states formation. Taken from [46].

4.2 Bound States Corrections

Besides the Sommerfeld correction there are other very similar correction that we have ignored in this work and we want at least to mention.

The Sommerfeld effect arises resumming a virtually infinite number of potential photon exchanges between two particles, which never radiate an on-shell vector boson. The counterpart of this is that when solving Schrödinger equation for scattering the total energy is conserved and always positive and thus no bound states are accessible.

We have thus neglected the diagrams depicted in 4.1 in which the two particles, after radiating a photon form a bound state. Bound states can be analysed with the same formalism we have developed in this work via Bethe-Salpeter equation. In fact the resonances we found earlier in the scattering cross section have an intimate connection with bound states given by Levinson theorem [4][57]. For a Coulomb potential there is an infinite number of available bound states at negative energy. Instead for Yukawa potential there is a finite number of those and only if its Bohr radius is smaller than the inverse of the mediator mass. This additional annihilation processes enhances ulteriorly the cross section of DM-DM annihilation, causing the mass needed to reproduce the DM relic density to increase even more. For a complete and detailed discussion of these effects, which even includes applications to minimal Dark Matter see [46].

4.3 Colored Partner Co-annihilation

To further elucidate the fundamental role of Sommerfeld corrections when computing Dark Matter Relic density for a vast range of thermal Dark Matter models we will investigate DM co-annihilation with a colored partner (which can eventually be a gluino or a squark in supersymmetry) [35] [45].

This treatment provides a way to further elucidate group theoretical arguments such as color decomposition.

4.3.1 Model

We take a Dark Matter particle χ co-annihilating with a colored partner χ'. We take them stabilized by a $\mathbb{Z}_2$ symmetry so they can just decay one into the other and annihilate to SM particles. We take the DM particle χ to have no or negligible interaction at tree-level with the rest of the Standard Model while we take the particles χ' colored and therefore interacting with gluons. This interaction of course introduces a loop level interaction $\chi\,\chi \to SM\,SM$, but we will assume it is negligible for co-annihilation with respect to the χ' annihilation section.

As we have seen before the interactions between χ and χ' is not important for co-annihilation as long as the number of dark particles is conserved in the interaction. We are thus assuming there is a faint coupling on the process maintaining χ and χ' in kinetic equilibrium and providing an annihilation channel

for $\chi\chi'$ (which may be for example Yukawa-like). We can thus remain agnostic regarding the exact form of the interaction between χ and χ' and assume it is just strong enough to keep the χ particles in kinetic equilibrium also after freeze-out.

In principle we can take χ' to be both a fermion or a scalar and in an arbitrary representation of the $SU(3)_C$ color group. To fix ideas and provide some concrete computations we will analyse in detail the case where χ' is a fermion or a scalar in the fundamental representation of $SU(3)_C$. There is absolutely no need to assume anything on the statistics of χ, but since we need its degrees of freedom for co-annihilations we will take it of the same statistics of χ'.

$$\mathcal{L}_{\chi'} = \begin{cases} \bar{\chi'}(i\not{D} - M)\chi' & \text{for a fermion} \\ (D_\mu\chi')^\dagger(D_\mu\chi') - M^2\chi'^\dagger\chi' \end{cases}$$
$$D_\mu = \partial_\mu - ig_s G_\mu^A T^A$$

and T^A are the $SU(3)_C$ generators.

The only other parameter we need to fix, besides M which will be fixed looking for the correct relic abundance, is the mass splitting between χ and χ'. We will take the limit $\Delta M \to 0$ for the mass splitting.

4.3.2 Interactions

We will first study the colored interaction potential between the χ' particles. The QCD interactions are confined below $\Lambda_{QCD} \sim 200\,\text{MeV}$ but provide a Coulomb-like potential above this scale. The potential can be computed to one loop as [6]

$$V(r) = -\frac{\alpha_S(\mu)C(R)}{r}\left[1 + (c_1 + 2c_2(\gamma_E + \log(\mu r)))\,\frac{\alpha_S(\mu)C(R)}{4\pi}\right] \simeq -\frac{\alpha_S\left(\mu \simeq \frac{1}{r}\right)C(R)}{r}$$
$$c_1 = \frac{31}{3} - \frac{10}{9}n_f \qquad c_2 = 11 - \frac{2}{3}n_f$$

where $C(R)$ is the Casimir of the irreducible representation in which the 2 particles are taken and n_f is the number of active quark flavours at the scale μ. The QCD potential between two different representations $R \otimes R'$ can easily be written, at least at tree level as

$$V(r) = \frac{\alpha_S}{r}\sum_A T_R^A \otimes T_{R'}^A = \frac{\alpha_S}{2r}\left(\sum_Q C(Q)\mathbb{I}_Q - (C(R) + C(R'))\mathbb{I}\right)$$

Where Q are the irreducible representation in which the tensor representation can be decomposed

$$R \otimes R' = \sum_Q Q$$

Every irreducible representation in which the initial state can be decomposed thus interacts with its own coupling constant. To elucidate how the minus we initially put in the potential (as it has the same structure as the QED potential) goes away we can analyse $q\bar{q}$ scattering which is a well-understood SM interaction. The Feynman rules give us a potential like

$$-\frac{\alpha_S}{r}\sum_a T_{\mathbf{3}}^a|_k^i T_{\mathbf{3}}^a|_j^h$$

where our process is $(i,j) \to (k,h)$ on a colour basis and the different orderings of the indices are due to the different orientations of the fermion lines and both generators are in the fundamental representation.

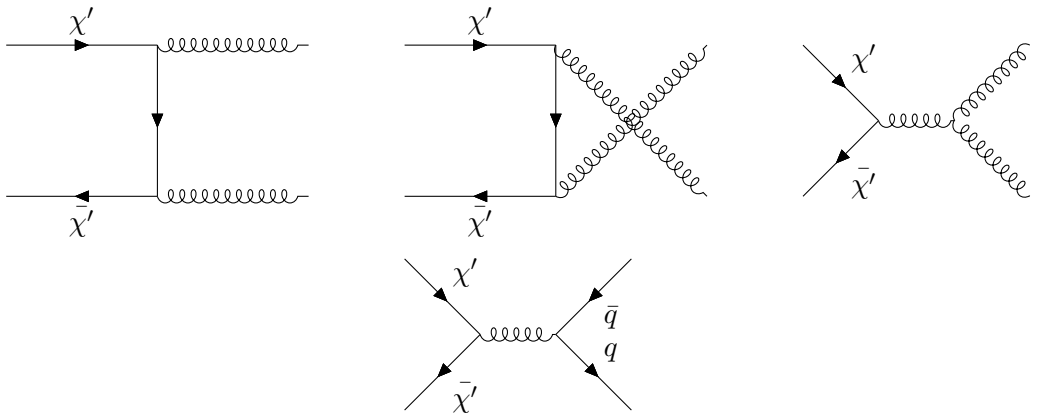

Figure 4.2: The 4 diagrams contributing to annihilation $\chi'\,\chi' \to g\,g$

To put the indices in the right order, to obtain a tensor going from initial to final color configurations, we should transpose the second generators. Using that

$$(T^a_{\mathbf{3}})^\dagger = T^a_{\mathbf{3}} \qquad \text{thus} \qquad (T^a_{\mathbf{3}})^T = (T^a_{\mathbf{3}})^* = -T^a_{\bar{\mathbf{3}}}$$

we obtain the minus sign we were searching for. Notice that for example looking to qq scattering wouldn't give this factor as the fermion lines would be in the same order, so there is no need for transposition. This subtlety only arises as we are trying to combine two representations with opposite charges into a complex representation. If we apply this to our fermion $\mathbf{3} \otimes \bar{\mathbf{3}} = \mathbf{8} \oplus \mathbf{1}$ annihilation we have

$$C(3) = \frac{4}{3} \qquad C(1) = 0 \qquad C(8) = 3$$

$$V(r) = \frac{\alpha_S}{r} \begin{cases} -\frac{4}{3} & (\mathbf{1}) \\ \frac{1}{6} & (\mathbf{8}) \end{cases}$$

The feature that the QCD potential is attractive for color singlet states and repulsive for color octet states is often presented as an intuitive explanation of confinement We now want to understand whether such a decomposition in which different irreducible representation of the initial states have different interaction strength takes place also for the annihilation cross section. What we now want to compute is the annihilation rate of χ' to SM particles. When χ' is a fermion we have 4 different diagrams contributing 4.2 when χ is a fermion and an additional seagull diagram when χ' is a scalar. When they annihilate into quarks the amplitude is

$$\mathcal{M}|^i_j \propto T^A_{\chi'}|^i_j \otimes T^A_F$$

Where we specified that the quarks transform in the fundamental representation of $SU(3)_C$. The generators transform in the adjoint representation ($\mathbf{8}$ for $SU(3)_C$), this means that the initial states also have to be in the $\mathbf{8}$ representation to have as an open channel the $q\bar{q}$ annihilation. For the decay into gluons the procedure is a little bit more involved the matrix element can in general be written as

$$\mathcal{M}^{AB} = aT^A_{\chi'}T^B_{\chi'} + bT^B_{\chi'}T^A_{\chi'}$$

which can be separated into symmetric and anti-symmetric parts

$$\mathcal{M}^{AB} = a'\{T^A_{\chi'}, T^B_{\chi'}\} + b'[T^A_{\chi'}, T^B_{\chi'}]$$

If we disregard the anomalous term $G\tilde{G}$ in the QCD Lagrangian, strong interactions conserve CP. Thus we can conclude that if the initial state is described by the quantum numbers (l, s), the matrix element

M^{AB} is

$$M^{AB} \propto \begin{cases} \{T^A_{\chi'}, T^B_{\chi'}\} & \text{if } l+s \text{ is even} \\ [T^A_{\chi'}, T^B_{\chi'}] & \text{if } l+s \text{ is odd} \end{cases}$$

In the antisymmetric case we reach the same conclusions as for $q\bar{q}$ annihilation. In fact

$$[T^A, T^B] = if^{ABC}T^C$$

and thus the only difference is that gluons are in the adjoint representation of $SU(3)_C$ while quarks are in the fundamental. The s-channel for example presents this exact structure. The symmetric part instead has to be decomposed in its irreducible representations:

$$\mathcal{M}^{AB}|^i_j = [\mathbf{1}]^i_j + [\mathbf{8}]^i_j$$

$$[\mathbf{1}]^i_j = \frac{1}{3}\delta^i_j \mathcal{M}^{AB}|^m_m$$

$$[\mathbf{8}]^i_j = \mathcal{M}^{AB}|^i_j - \frac{1}{3}\delta^i_j \mathcal{M}^{AB}|^m_m$$

You can easily see that when the amplitude gets squared the interference term between the [**8**] and [**1**] vanishes. We thus obtain

$$\mathcal{M}^{AB}|^i_j \mathcal{M}^{AB}|^j_i \propto 2\,\mathrm{tr}\big(T^A T^A T^B T^B\big) + 2\,\mathrm{tr}\big(T^A T^B T^A T^B\big) = 2C(R)d(R)\left(2C(R) - \frac{1}{2}C(adj)\right)$$

$$[\mathbf{1}]^i_j [\mathbf{1}]^j_i = \frac{1}{3}\mathcal{M}^{AB}|^m_m \mathcal{M}^{AB}|^n_n \propto \frac{4}{3}\,\mathrm{tr}\big(T^A T^B\big)\,\mathrm{tr}\big(T^A T^B\big) = \frac{4}{3}I(R)^2(N^2-1)$$

If again we apply all of this to the $\mathbf{3}\otimes\bar{\mathbf{3}}$ case we obtain that

$$\big|\mathcal{M}^{AB}\big|^2 = \frac{7}{2}|\mathbf{1}|^2$$

$$\big|\mathcal{M}^{AB}\big|^2 = \frac{7}{5}|\mathbf{8}|^2$$

$$\sigma_{\mathbf{3}\otimes\bar{\mathbf{3}}\to gg} = \begin{cases} \frac{5}{7}\sigma^{sym}_{\mathbf{3}\otimes\bar{\mathbf{3}}\to gg}(\mathbf{8}) + \frac{2}{7}\sigma^{sym}_{\mathbf{3}\otimes\bar{\mathbf{3}}\to gg}(\mathbf{1}) & \text{if } l+s \text{ is even} \\ \sigma^{asym}_{\mathbf{3}\otimes\bar{\mathbf{3}}\to gg}(\mathbf{8}) & \text{if } l+s \text{ is odd} \end{cases}$$

$$\sigma_{\mathbf{3}\otimes\bar{\mathbf{3}}\to q\bar{q}} = \sigma_{\mathbf{3}\otimes\bar{\mathbf{3}}\to q\bar{q}}(\mathbf{8})$$

This treatment can be done for every tensor representation and takes the name of color decomposition. Clearly more involved is the tensor product more involved will be the decomposition. The cross section on the RHS are function of the representation as they may well incorporate Sommerfeld effects according to whether or not we want to account for them analytically or numerically. Sommerfeld corrections will be different for each representation as the interaction strength, as seen above, is a function of the representation.

Now we can proceed in exactly the same way as we did for MDM. In fact particles in different representations of spin, or color cannot mix. And in a first approximation we can study only s-wave annihilation ($l = 0$). Further corrections to can be computed also analytically [45] and Sommerfeld can be included through (3.16).

Spinors

Computing the invariant cross section we can compute the invariant matrix element from which we can extract the quantities on the RHS, at tree-level these quantities are independent from the representation:

$$\sigma^{sym}_{\mathbf{3}\otimes\bar{\mathbf{3}}\to gg} v_{rel} = \frac{\pi\alpha_S^2}{M^2}\left(1+\frac{1}{2}v_{rel}^2+\frac{9}{40}v_{rel}^4+O(v_{rel}^6)\right)\mathrm{tr}\big(\{T^A_{\chi'},T^B_{\chi'}\}\{T^A_{\chi'},T^B_{\chi'}\}\big)$$

$$\sigma^{asym}_{\mathbf{3}\otimes\bar{\mathbf{3}}\to gg} v_{rel} = \frac{\pi\alpha_S^2}{4M^2}\left(1+\frac{1}{4}v_{rel}^2+\frac{7}{24}v_{rel}^4+O(v_{rel}^6)\right)\mathrm{tr}\big([T^A_{\chi'},T^B_{\chi'}][T^A_{\chi'},T^B_{\chi'}]\big)$$

$$\sigma_{\mathbf{3}\otimes\bar{\mathbf{3}}\to q\bar{q}} = \frac{7\pi\alpha_S^2}{16M^2}\left(1-\frac{4}{21}v_{rel}^2-\frac{29}{336}v_{rel}^4+O(v_{rel}^6)\right)\mathrm{tr}\big(T^A_{\chi'}T^B_{\chi'}\big)\,\mathrm{tr}\big(T^A_F T^B_F\big)$$

These cross sections aren't averaged over initial states, which would contribute a factor of $\frac{1}{36}$ since for co-annihilation then we would need to sum over all possible initial states once again.

Scalars

For scalars the interactions are even simpler in the low energy limit.

As given above by CP conservation the s-channel antisymmetric contribution to the matrix element is p-wave suppressed.

This has an easy physical interpretation: as the total angular momentum is conserved, the two spin-0 initial particle cannot convert to a spin-1 mediator unless they carry angular momentum!

Therefore both quark decay and the antisymmetric part of the matrix element are p-wave suppressed.

$$\sigma^{sym}_{\mathbf{3}\otimes\bar{\mathbf{3}}\to gg} v_{rel} = \frac{2\pi\alpha_S^2}{M^2}\left(1-\frac{61}{84}v_{rel}^2-\frac{27}{280}v_{rel}^4+O(v_{rel}^6)\right)\mathrm{tr}\big(\{T^A_{\chi'},T^B_{\chi'}\}\{T^A_{\chi'},T^B_{\chi'}\}\big)$$

$$\sigma_{\mathbf{3}\otimes\bar{\mathbf{3}}\to q\bar{q}} = \frac{\pi\alpha_S^2 v_{rel}^2}{54M^2}\,\mathrm{tr}\big(T^A_{\chi'}T^B_{\chi'}\big)\,\mathrm{tr}\big(T^A_F T^B_F\big)$$

The p-wave suppression for scalar fields changes quite dramatically the effect of Sommerfeld corrections. As we have seen above Sommerfeld corrections enhance the Singlet cross section and suppress the octet cross section. The presence of 6 quark flavours in the SM is such that if $q\bar{q}$ annihilation is not p-wave suppressed it would dominate over gg annihilation and therefore we expect the repulsion to dominate over the attraction between Singlets configurations.

Furthermore there is another interesting effect: the coupling of the Octet to QCD is particularly small. In fact the Casimir of a $SU(3)$ representation indexed by (p,q) [43] is known to be [37]

$$C((p,q)) = \frac{p^2+q^2+3p+3q+pq}{3}$$

This means that any bigger representation of $SU(3)$ will have a stronger (repulsive) coupling constant and a more relevant Sommerfeld effect.

We could ask what the relative ratio of Octet and Singlet channel has to be in order for the leading Sommerfeld correction to be attractive.

It is easy to carry out this computation using the Coulomb analytical approximation of the Sommerfeld potential and we obtain. We obtain that the Sommerfeld effect transition from slightly repulsive to slightly attractive when the ratio between the singlet channel and the octet channel is about 4.

All these features can be clearly observed in the plots plots of the thermally averaged cross section for the two models 4.3 4.4.

4.3.3 Relic Density

The above considerations on the thermally averaged sections have consequences on the Relic densities of the two models.

For scalars the Sommerfeld corrections yield a significant increase to the cross section and thus a significant increase 4.5 in the mass necessary to reproduce observed DM abundance from $M \simeq 2.1\,\text{TeV}$ to $M \simeq 2.6\,\text{TeV}$.

For fermion instead the corrections are almost negligible because of the small coupling of the Octet added to the fact that the enhancement from the singlet partially compensate the small reduction of the octet cross section. The resulting correction to the mass is of the same size of our uncertainty 4.6.

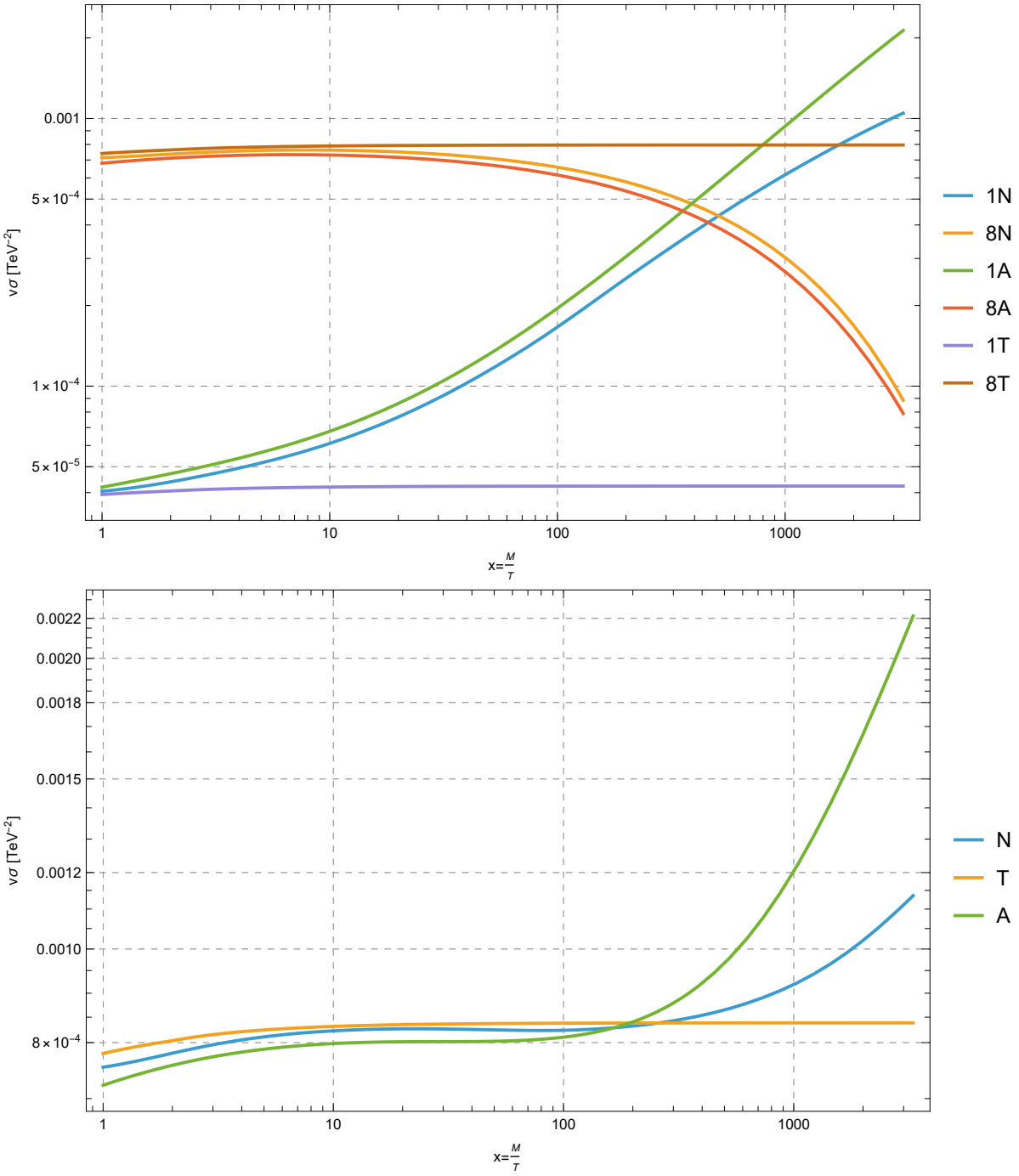

Figure 4.3: Plots of the thermally averaged cross sections for a fermion color triplet with $M = 3.3\,\text{TeV}$. Labels "T" indicate the tree level computation, "A" the analytic Sommerfeld effect considering the QCD potential as a perfect Coulomb potential and "N" the Sommerfeld effect obtained by numerically solving the Schrödinger equation and accounting for gluon thermal masses. In the first plot the cross section is divided in the Octet and Singlet channels in order to show both repulsive and attractive Sommerfeld effect.

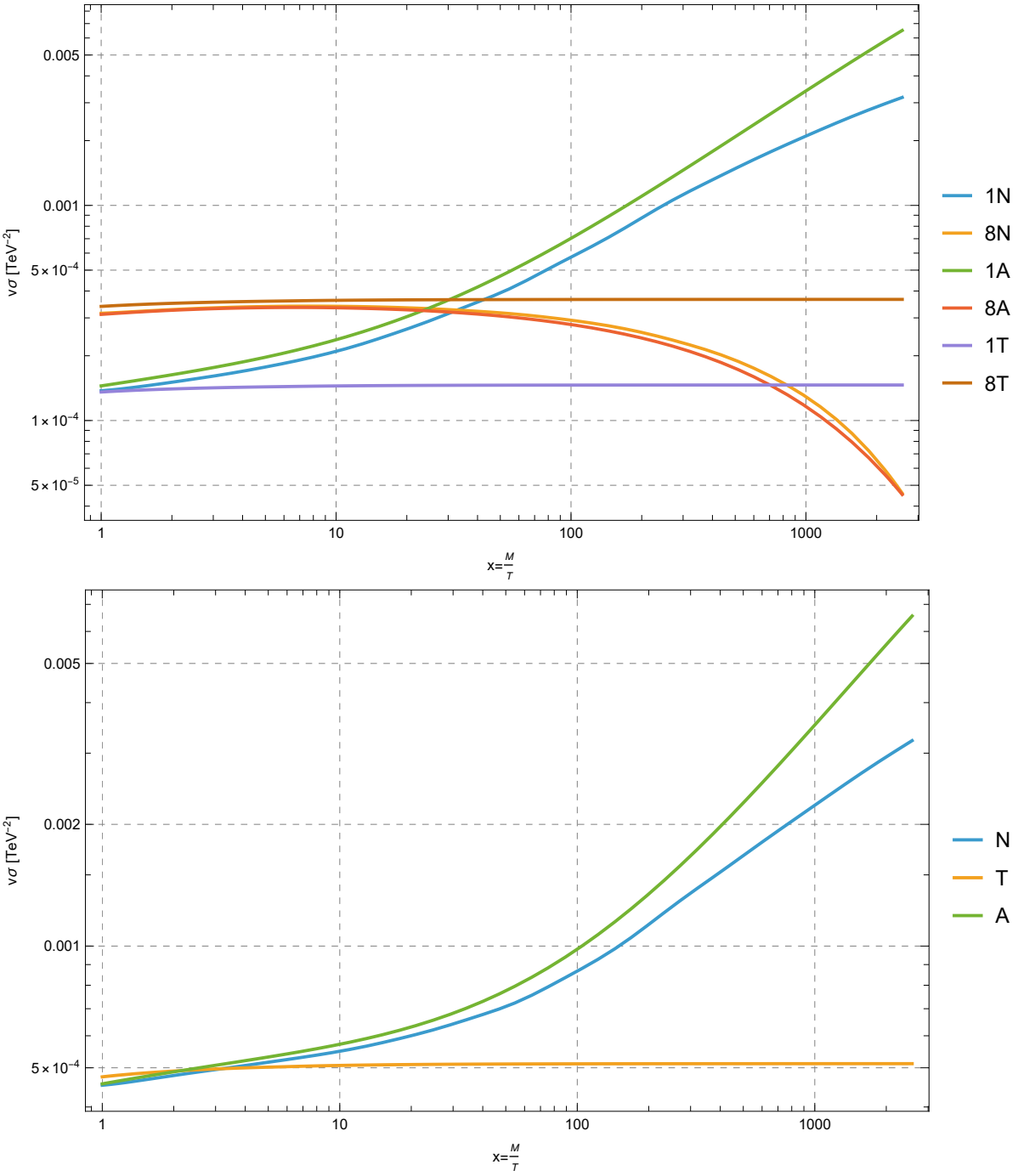

Figure 4.4: Plots of the thermally averaged cross sections for a scalar color triplet with $M = 2.6\,\text{TeV}$. Labels "T" indicate the tree level computation, "A" the analytic Sommerfeld effect considering the QCD potential as a perfect Coulomb potential and "N" the Sommerfeld effect obtained by numerically solving the Schrödinger equation and accounting for gluon thermal masses. In the first plot the cross section is divided in the Octet and Singlet channels in order to show both repulsive and attractive Sommerfeld effect.

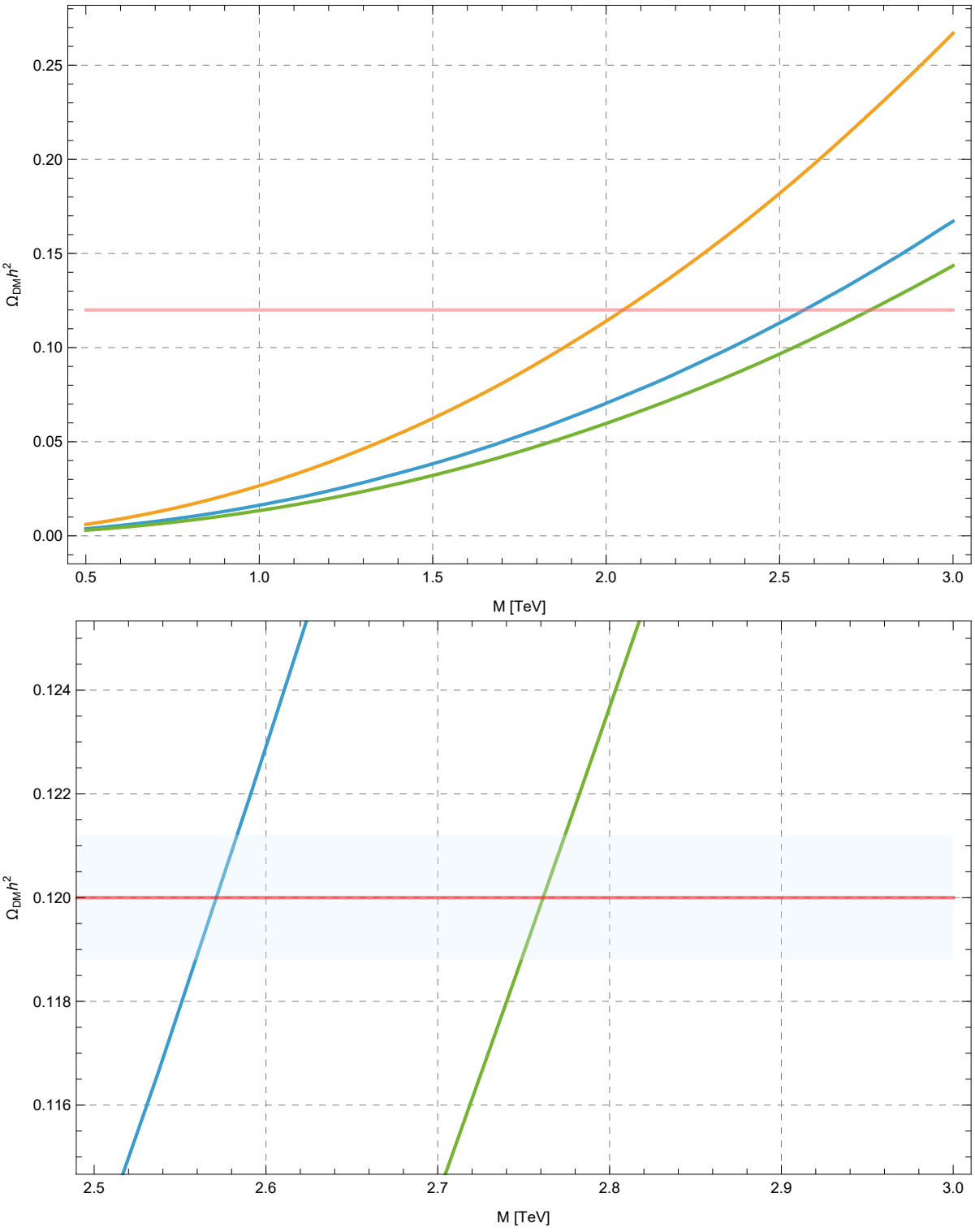

Figure 4.5: Plots of the relic density for a scalar color triplet in the limit $\Delta M = 0$. Labels "T" indicate the tree level computation, "A" the analytic Sommerfeld effect considering the QCD potential as a perfect Coulomb potential and "N" the Sommerfeld effect obtained by numerically solving the Schrödinger equation and accounting for gluon thermal masses.

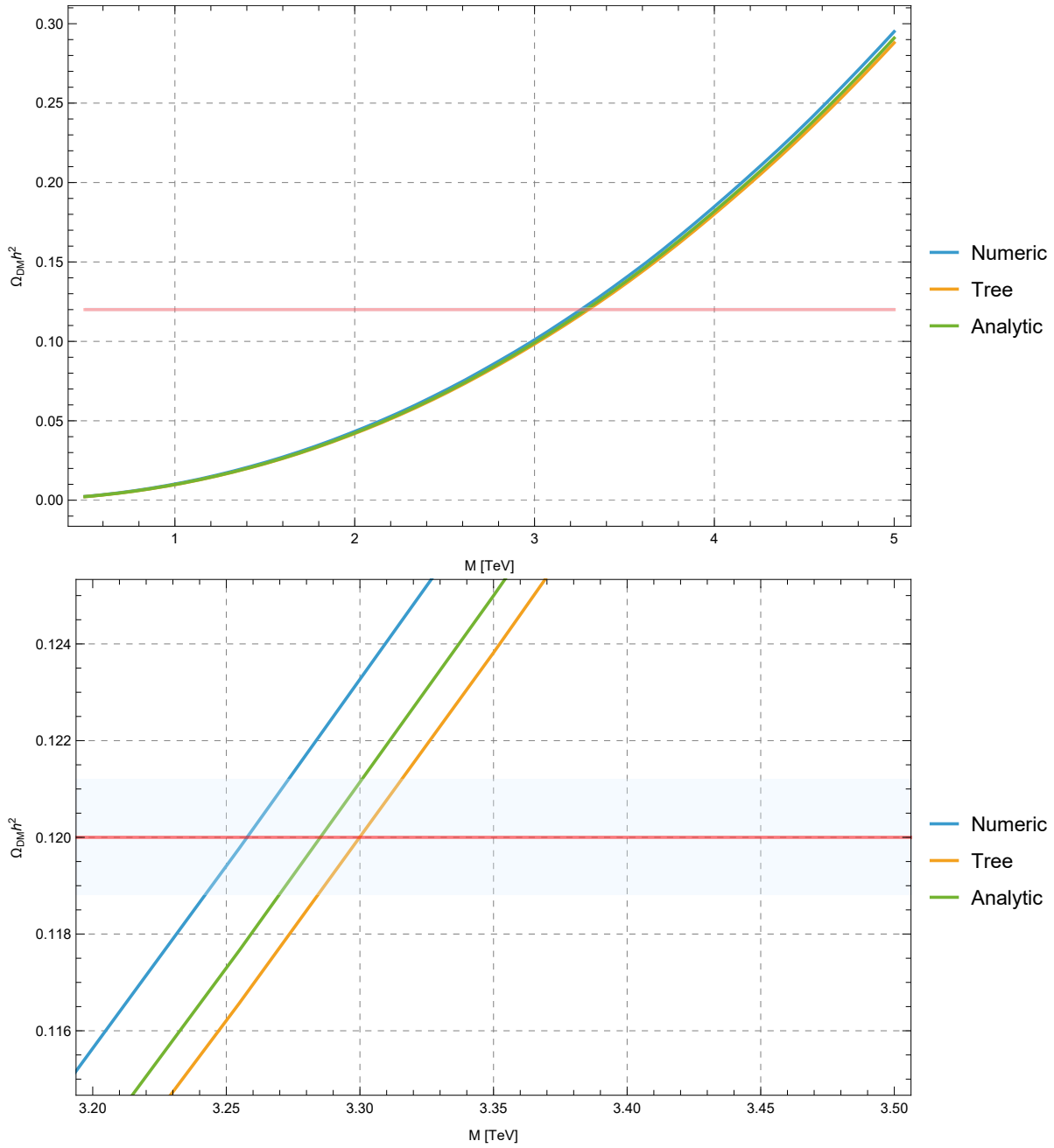

Figure 4.6: Plots of the relic density for a fermion color triplet in the limit $\Delta M = 0$. Labels "T" indicate the tree level computation, "A" the analytic Sommerfeld effect considering the QCD potential as a perfect Coulomb potential and "N" the Sommerfeld effect obtained by numerically solving the Schrödinger equation and accounting for gluon thermal masses.

Conclusions

This thesis has explored the impact of the Sommerfeld effect on the thermal relic abundance of dark matter from a quantum field theory perspective. The primary goal was to derive the Sommerfeld enhancement from first principles, identifying its origin in the resummation of ladder diagrams that dominate the annihilation amplitude at low relative velocities. This allowed us to understand the relevant approximations made as the relative importance of ladder diagrams and of the low-velocity enhanced terms. We discussed how including relativistic corrections, whether through loop computations or non-relativistic perturbation theory, is primarily a computational effort rather than a conceptual one.

The Minimal Dark Matter (MDM) framework served as the initial testing ground for this formalism. We reproduced the known enhancement of annihilation cross sections in electroweak multiplets due to long-range gauge interactions. These corrections significantly affect the predicted mass ranges required to obtain the observed relic density, causing them to change by factors of their same order. Such shifts underscore the inadequacy of relying solely on perturbative estimates for precision cosmology, particularly in the multi-TeV regime.

Building on the MDM benchmark, the thesis extended the analysis to less-explored dark matter scenarios. These include models with nontrivial gauge quantum numbers, interactions mediated by colored partners, and variations in the thermal history such as co-annihilation. We developed a formalism that can be adapted to general QCD-like theories of the Dark Sector.

The conclusions of this study carry important implications for DM phenomenology. First, they demonstrate that even well-motivated and "minimal" models may require revisiting in light of nonperturbative effects. Second, they provide a practical framework for incorporating Sommerfeld corrections into relic density calculations, enabling more accurate confrontations between theory and data. Finally, they highlight new opportunities and constraints for experimental searches: models previously thought to be excluded may be viable once corrections are included, and vice versa.

As precision cosmology and experimental DM searches continue to advance, theoretical predictions must keep pace. The Sommerfeld effect proves to be a cornerstone in this effort. This thesis offers both a conceptual framework and new results that contribute to a more accurate and complete picture of thermal dark matter.

Appendix A

Standard Model and Conventions

The Standard Model (SM) of particle physics is a quantum field theory developed during the second half of the 20th century unifying our present understanding of 3 (strong, weak and electromagnetic interactions) out of the 4 known fundamental forces (the previous 3 interactions and gravity).
The SM strongly relies on the principle of gauge symmetry. Its Lagrangian is given writing the most general $SU(3)_C \otimes SU(2)_L \otimes U(1)_Y$ gauge invariant (renormalizable) Lagrangian. Therefore we have a total amount of 12 gauge bosons: 8 fields G^A_μ of the $SU(3)$ group describing strong interactions, and $3+1$ gauge bosons (W^A_μ and B_μ) relative to the electroweak sector.
All these bosons have vector-like representations under the Lorentz group. Fermions in the standard model instead are more subtle: the Lorentz group $SO(1,3)$ can be factorized as $SU(2)_L \otimes SU(2)_R$ and thus all the Lorentz group representations can be indexed by the spin relative to these two fields: (j_L, j_R), in this context vector-like representations are equivalent to $\left(\frac{1}{2}, \frac{1}{2}\right)$. The Standard Model matter content is constituted only by spin-$\frac{1}{2}$ fermions, therefore we have only left-handed spinors $\lambda \sim \left(\frac{1}{2}, 0\right)$ and right-handed spinors $\rho \sim \left(0, \frac{1}{2}\right)$. Analogously with what we just did for the Lorentz group we can classify all the matter content of the Standard Model by the representations under which they transform under the three gauge groups

$$(d_c, d_L, Q_y)$$

where d_c is the dimension of the field representation under $SU(3)_c$, d_w is the dimension of the field representation under $SU(2)_L$ and Q_y is the charge under $U(1)_Y$. Using this criteria, we can divide fermions in:

- **Quarks**: left-handed quarks are fermions charged under all factors of the SM gauge group (while right-handed ones do not interact through the weak charged currents). Quarks are the only particles to be charged under the $SU(3)$ strong interactions (they are said to carry color charge). There are 6 quark flavours (and 6 corresponding anti-quark flavours) divided into 3 generations of doublets of the $SU(2)$ weak factor. We have the following quark fields:
  - Left-handed doublets:
  $$Q^{(f)}_{i,a} \sim \left(3, 2, \frac{1}{6}\right)$$
  - Right-handed up quarks:
  $$u^{(f)}_a \sim \left(3, 1, \frac{1}{3}\right)$$
  - Left-handed down quarks:
  $$d^{(f)}_a \sim \left(3, 1, -\frac{2}{3}\right)$$

Where α is a color index, i is a $SU(2)$ index and (f) ranges over all the possible 3 flavours. Fixed all the possible indexes all fields are Weyl spinors.

- **Leptons**: leptons are also fermions, but they do not interact through strong interactions (so they do not present color charge). As for quarks, there are 6 different flavours of leptons again divided into 3 generations of doublets. We have the following lepton fields:

  – Left-handed doublets:

  $$L_i^{(f)} \sim \left(1, 2, -\frac{1}{2}\right)$$

  – Right-handed singlets:

  $$e^{(f)} \sim (1, 1, -1)$$

  With the same conventions as before. Notice that in the Standard model we do not have right-handed neutrinos (and the left-handed neutrino fields, which are the upper components of $L_i^{(f)}$ are massless).

- **Higgs**: the Higgs field is a scalar which is not charged under the strong interactions. This boson has the role to give mass to both weak bosons (by means of spontaneous symmetry breaking, in the unitarity gauge) and fermions. Its goldstone bosons are "eaten" from the gauge fields acquiring mass and leaving just one real scalar field h known as the Higgs boson.

  $$H_i \sim \left(1, 2, \frac{1}{2}\right)$$

  Where this time, as said before, these fields are scalars and the index i is again an $SU(2)_L$ index.

The Standard Model has an outstanding accord with experimental testing, with tensions only where really complex measurements or calculations have to be carried out. Between its major successes, we have:

- The prediction of the existence of the gluon and its properties in 1973 (by Fritzsch, Leutwyler and Gell-Mann), six years before its experimental detection at PETRA (1979).
- The prediction of the existence and properties of weak $W^{\pm}$ and Z bosons by the Glashow-Salam-Weinberg electroweak model (around 1968) and then discovered at CERN in 1983.
- The prediction of a third generation of quarks by Kobayashi and Maskawa in 1973, to explain CP violation in the weak interactions. The bottom quark was detected at Fermilab in 1977 for the first time but the top quark had to wait until 1995.
- The last piece of the Standard Model to be detected was the Higgs boson (incorporated in the standard model in 1967) which was found at CERN in 2012.

A.1 SM Lagrangian

The full Lagrangian of the Standard Model, considering all fermion fields as Weyl spinors, is:

$$\begin{aligned}\mathcal{L}_{\rm SM} = &-\frac{1}{4}G^A_{\mu\nu}G^{A\mu\nu} - \frac{1}{4}W^I_{\mu\nu}W^{I\mu\nu} - \frac{1}{4}B_{\mu\nu}B^{\mu\nu} + \\ &+\sum_{f=1}^{3}\Big[i(Q^{\dagger(f)i,a})_{\dot\alpha}\bar\sigma^{\mu\dot\alpha\beta}D_\mu(Q^{(f)}_{i,a})_\beta + i(u^{\dagger(f)a})^\alpha\sigma^\mu_{\alpha\dot\beta}D_\mu(u^{(f)}_a)^{\dot\beta} + i(d^{\dagger(f)a})^\alpha\sigma^\mu_{\alpha\dot\beta}D_\mu(d^{(f)}_a)^{\dot\beta} + \\ &+i(L^{\dagger(f)i})_{\dot\alpha}\sigma^{\mu\dot\alpha\beta}D_\mu(L^{(f)}_i)_\beta + i(e^{\dagger(f)})^\alpha\sigma^\mu_{\alpha\dot\beta}D_\mu(e^{(f)})^{\dot\beta}\Big] + \\ &+ (D^\mu H)^\dagger(D_\mu H) - V(H) + \\ &-\left[\sum_{f,g=1}^{3}\left(y_u^{(f,g)}\epsilon^{ij}(Q^{(f)}_{i,a})_\alpha H_j(u^{\dagger(g)a})^\alpha + y_d^{(f,g)}(Q^{(f)}_{i,a})_\alpha H^{\dagger i}(d^{\dagger(g)a})^\alpha + y_e^{(f,g)}(L^{(f)}_i)_\alpha H^{\dagger i}(e^{\dagger(g)})^\alpha\right)\right] + \text{h.c.}\end{aligned}$$

where:

- $G^A_{\mu\nu} = \partial_\mu G^A_\nu - \partial_\nu G^A_\mu + g_s f^{ABC}G^B_\mu G^C_\nu$ is the field strength tensor for $SU(3)_C$.
- $W^I_{\mu\nu} = \partial_\mu W^I_\nu - \partial_\nu W^I_\mu + g\epsilon^{IJK}W^J_\mu W^K_\nu$ is the field strength tensor for $SU(2)_L$.
- $B_{\mu\nu} = \partial_\mu B_\nu - \partial_\nu B_\mu$ is the field strength tensor for $U(1)_Y$.
- D_μ represents the covariant derivative for the gauge interactions, of the form:

$$D_\mu = \partial_\mu - ig_W W^I_\mu T^I - ig_S G^A_\mu \mathcal{T}^A - ibB_\mu$$

- $V(H) = \mu^2 H^\dagger H + \lambda(H^\dagger H)^2$ is the Higgs potential, with obvious contraction of $SU(2)$ indices.
- H_i is the Higgs doublet, and ϵ^{ij} is the Levi-Civita symbol used to form $SU(2)$ invariant terms.
- The matrices $\sigma^\mu_{\gamma\dot\delta}$ and $\bar\sigma^{\mu\dot\alpha\beta}$ are related by

$$\bar\sigma^{\mu\dot\alpha\beta} = \epsilon^{\dot\alpha\dot\delta}\epsilon^{\beta\gamma}\sigma^\mu_{\gamma\dot\delta}$$

  and in matrix representation we have

$$\sigma^\mu_{\dot\alpha\beta} = (\mathbb{I}, \vec\sigma) \qquad \bar\sigma^{\mu\dot\alpha\beta} = (\mathbb{I}, -\vec\sigma)$$

  Where now I am indicating with $\vec\sigma$ the three Pauli matrices.

For every Gauge Group and also for the Lorentz Group we used the convention that lower indices are transforming in the fundamental representation of the group and higher indices are transforming in the conjugate representation. If we have a representation a_i of the $SU(2)_L$ Gauge Group both $a^{\dagger i}$ and $\epsilon^{ij}a_i$ transform in the conjugate representation. The first term because all gauge groups of the Standard Model are compact and thus admit a finite-dimensional unitary representation. The second term because the group is Special and thus $U^a_i U^b_j \epsilon^{ij} = \det(U)\epsilon^{ab} = \epsilon^{ab}$.
The Lorentz Group instead (although it is factorizable as $SU(2)_L \otimes SU(2)_R$) is non-compact, thus when dealing with spinor indices we must remember that the † exchanges left and right representation. The conventions we used are that undotted indices α, β transform under $SU(2)_L$ and dotted indices $\dot\alpha$, $\dot\beta$ transform under $SU(2)_R$. Therefore to go in the conjugate representation and have Lorentz invariance we are obliged to use the Levi-Civita tensor $\epsilon^{\alpha\beta}$ or $\epsilon^{\dot\alpha\dot\beta}$ to rise lower indices and when we have written an upper index in the Lagrangian we assumed this convention.

The Standard model Lagrangian can be written in a more elegant way if we give for granted all this structure and suppress color and spinor indices not to clutter the page.

$$\begin{aligned}\mathcal{L}_{\text{SM}} =& -\frac{1}{4}G^A_{\mu\nu}G^{A\mu\nu} - \frac{1}{4}W^I_{\mu\nu}W^{I\mu\nu} - \frac{1}{4}B_{\mu\nu}B^{\mu\nu} + \\ &+ \sum_{f=1}^{3}\Big[iQ^{\dagger(f)i}\bar{\sigma}^\mu D_\mu Q_i^{(f)} + iu^{\dagger(f)}\sigma^\mu D_\mu u^{(f)} + id^{\dagger(f)}\sigma^\mu D_\mu d^{(f)} + \\ &+ iL^{\dagger(f)i}\sigma^\mu D_\mu L_i^{(f)} + ie^{\dagger(f)}\sigma^\mu D_\mu e^{(f)}\Big] + \\ &+ (D^\mu H)^\dagger (D_\mu H) - V(H) + \\ &- \left[\sum_{f,g=1}^{3}\left(y_u^{(f,g)}\epsilon^{ij}Q_i^{(f)}H_j u^{\dagger(g)} + y_d^{(f,g)}Q_i^{(f)}H^{\dagger i}d^{\dagger(g)} + y_e^{(f,g)}L_i^{(f)}H^{\dagger i}e^{\dagger(g)}\right)\right] + \text{h.c.}\end{aligned}$$

A.1.1 Dirac Formalism

Everything can be made even more compact using Dirac spinors. A Dirac spinor is defined starting from 2 Weyl spinors η_α and $\chi_{\dot\alpha}$ which are mixed by the Yukawa terms of the Lagrangian.

$$\psi = \begin{pmatrix}\eta_\alpha \\ \chi^{\dot\alpha}\end{pmatrix}$$

Mind the upper index as been raised with the Levi-Civita tensor. For convenience instead of denoting the two Weyl Fermions that make up a Dirac fermion with the letters χ and η we will often use the notation

$$\psi = \begin{pmatrix}(\Psi_L)_a \\ (\Psi_R)^{\dot a}\end{pmatrix}$$

to stress their relation with the field ψ.
We can define 4 new matrices that are the analogous of σ_μ matrices:

$$\gamma^\mu = \begin{pmatrix}0 & \sigma^\mu_{\dot\alpha\beta} \\ \bar\sigma^{\mu\dot\alpha\beta} & 0\end{pmatrix}$$

And therefore the famous

$$\bar\psi = \psi^\dagger\gamma^0 = \begin{pmatrix}\chi^\alpha & \eta_{\dot\alpha}\end{pmatrix}$$

The Standard model Lagrangian in the formalism of Dirac Spinors takes the form

$$\begin{aligned}\mathcal{L}_{\text{SM}} =& -\frac{1}{4}G^A_{\mu\nu}G^{A\mu\nu} - \frac{1}{4}W^I_{\mu\nu}W^{I\mu\nu} - \frac{1}{4}B_{\mu\nu}B^{\mu\nu} + \\ &+ \sum_{f=1}^{3}\Big[i\bar{Q}^{(f)i}\gamma^\mu D_\mu Q_i^{(f)} + i\bar{L}^{(f)i}\gamma^\mu D_\mu L_i^{(f)}\Big] + \\ &+ (D^\mu H)^\dagger (D_\mu H) - V(H) + \\ &- \left[\sum_{f,g=1}^{3}\left(y_u^{(f,g)}\bar{Q}^{(f)i}\tilde{H}_i u_R^{(g)} + y_d^{(f,g)}\bar{Q}^{(f)i}H_i d_R^{(g)} + y_e^{(f,g)}\bar{L}^{(f)i}H_i e_R^{(g)}\right)\right] + \text{h.c.}\end{aligned}$$

Where $\tilde{H} = \epsilon H^*$ and can be easily verified that it transforms in the fundamental representation of $SU(2)_L$. In the last line the subscript R denotes the projection on the Weyl Spinor components through the spinor

$$\mathbb{P}_R = \frac{1}{2}\left(\mathbb{I} + \gamma^5\right) = \begin{pmatrix}0 & 0 \\ 0 & \mathbb{I}\end{pmatrix}$$

In the way we have written the Lagrangian the subscript L does not appear, but we will make use of it, so we define in the same way

$$\mathbb{P}_L = \frac{1}{2}\left(\mathbb{I} - \gamma^5\right) = \begin{pmatrix} \mathbb{I} & 0 \\ 0 & 0 \end{pmatrix}$$

And γ^5 is the well-known matrix

$$\gamma^5 = i\gamma^0\gamma^1\gamma^2\gamma^3 = \begin{pmatrix} -\mathbb{I} & 0 \\ 0 & \mathbb{I} \end{pmatrix}$$

The Dirac formalism is more compact, but a little bit more obscure. Its major advantage is that the gamma matrices satisfy the really simple algebra

$$\{\gamma^\mu, \gamma^\nu\} = 2g^{\mu\nu}$$

and this renders all matrix elements involving fermions more easy to compute. Furthermore the anti-commutation relation makes apparent how the metric enters inside the algebra. This allows the algebra to be extended easily to fractional dimension (when using dimensional regularization). One of the most important relations is for example

$$\gamma_\mu\gamma^\mu = g^{\mu\nu}g_{\mu\nu} = 4 \quad \text{continued to} \quad \gamma_\mu\gamma^\mu = d$$

Also Weyl formalism can be used in fractional dimension, through identities such as

$$\bar{\sigma}^{\mu\dot{a}b}\sigma^\nu_{b\dot{a}} = 2g_{\mu\nu}$$

but other useful identities (such as the Fierz identity) are far less trivial to generalize to fractional dimension.

A.1.2 Majorana Formalism

Majorana Formalism is the analogous of the Dirac Formalism when we have only one Weyl Spinor and we cannot build a Dirac Mass term that mixes the two spinors. If we have a Weyl Spinor X in a real representation of all of our gauge groups (so it has to be neutral under all $U(1)$ symmetries) we can give it a mass including in the Lagrangian the quite simple

$$\mathcal{L} = X^\dagger_{\dot{a}}\bar{\sigma}^{\mu\dot{a}b}\partial_\mu X_b + \frac{m}{2}X_a X^a + \frac{m}{2}X_{\dot{a}}X^{\dot{a}}$$

In analogy with what we did for the 4-components Dirac spinor we define the Majorana spinor

$$\chi = \begin{pmatrix} X_a \\ (X^\dagger)^{\dot{a}} \end{pmatrix}$$

In this formalism the above Lagrangian becomes

$$\mathcal{L} = \frac{1}{2}\bar{\chi}(i\partial\!\!\!/ - m)\chi$$

The Majorana field is the analogous for the Dirac Field of what a real field is for a complex field. By this we mean that a Majorana fermion is its own anti-particle exactly as a boson described by a scalar field. A scalar field satisfies

$$\phi^\dagger = \phi$$

which can be rewritten, introducing the charge conjugation operator C, as

$$C\phi C^{-1} = \phi^\dagger = \phi$$

Once we extend to Weyl fields the charge conjugation operator, in such a way that it exchanges the two Weyl fields that are part of a Dirac Spinor, we obtain

$$C\psi C^{-1} = \mathcal{C}\bar{\psi}^T$$

$$\mathcal{C} = \begin{pmatrix} \epsilon_{ab} & 0 \\ 0 & \epsilon^{\dot{a}\dot{b}} \end{pmatrix}$$

The Majorana field at this point satisfies

$$\chi = C\chi C^{-1} = \mathcal{C}\bar{\chi}^T$$

There are two nice applications of this relation: the first helps us to rewrite the Lagrangian in such a way that it is explicit that Majorana fields have to be in real representations of the gauge fields

$$\mathcal{L} = \frac{1}{2}\chi^T\mathcal{C}(i\partial\!\!\!/ - m)\chi$$

The second is the fact that the current bilinear

$$\bar{\chi}\gamma^\mu\chi = 0$$

Majorana singlet fields for this reason cannot be charged under any group of the standard model and multiplets couple only to fields for whose generators they are not in a diagonal representation (when they are in the mass eigenbasis). Otherwise, as we show in chapter 2, they would mix and form a set of Dirac fields.

A.2 Under the Weak Scale

At the Electroweak scale $\sim 250\,\text{GeV}$ the Higgs field acquires a vacuum expectation value (VEV) due to a phase transition of its potential. To compute observables (according to the LSZ formula) we have to expand our fields around this VEV.

The vacuum state of the Higgs potential is obviously chosen randomly between the equivalent states up to gauge transformations. We can exploit this gauge freedom (using the Unitarity Gauge) to ensure that the Higgs field has the form

$$H = \begin{pmatrix} 0 \\ \frac{v+h}{\sqrt{2}} \end{pmatrix} \tag{A.1}$$

with $\frac{v}{\sqrt{2}}$ is the VEV of the field and the Higgs Boson h describes excitations around this VEV (the factors $\sqrt{2}$ are chosen in order for the kinetic terms to be canonically normalized).

After Spontaneous Symmetry Breaking of the form (A.1) there is a residual symmetry namely the one generated by

$$Q = \begin{pmatrix} 1 & 0 \\ 0 & 0 \end{pmatrix} = T_3 + Y$$

the matrix is fixed up to a constant from hermiticity and the condition $Q\,|\Omega\rangle = 0$. The transformations generated by Q are a subset of $SU(2)_L \otimes U(1)_Y$ and form the gauge group of Quantum Electrodynamics. In this gauge, the charged W_μ^I (where we define the charge through the eigenvalues of the matrix Q) fields are given a mass, while the neutral bosons of weak isospin and hypercharge mix and give rise to a massive boson Z_μ and the electromagnetic field A_μ.

The mass of the gauge fields comes from the kinetic term of the Higgs Boson

$$(D_\mu H)^\dagger (D^\mu H) \supset \frac{1}{8}\begin{pmatrix}0 & v\end{pmatrix}\begin{pmatrix} gW_\mu^3 + bB_\mu & W_\mu^1 - iW_\mu^2 \\ W_\mu^1 + iW_\mu^2 & -gW_\mu^3 + bB_\mu\end{pmatrix}\begin{pmatrix} gW_\mu^3 + bB_\mu & W_\mu^1 - iW_\mu^2 \\ W_\mu^1 + iW_\mu^2 & -gW_\mu^3 + bB_\mu\end{pmatrix}\begin{pmatrix}0\\ v\end{pmatrix}$$

We can then define a basis of fields that is both a mass and charge eigenstate

$$W_\mu^\pm = \frac{W^1\mu \mp iW_\mu^2}{\sqrt{2}} \qquad Z_\mu = c_W W_\mu^3 - s_W B_\mu \qquad A_\mu = c_W B_\mu + s_W W_\mu^3$$

Where c_W and s_W are cosine and sine of the weak mixing angle defined by $t_W = \frac{b}{g}$. It is simple to see that A_μ is massless (as protected by the residual gauge invariance we talked about before), while

$$m_W = \frac{vg}{2} \qquad Z_\mu = \frac{v\sqrt{g^2+b^2}}{2} = \frac{m_W}{c_W}$$

In this new field basis the covariant derivative takes the form

$$\begin{aligned} D_\mu &= \partial_\mu - igW_\mu^A T^A - ibB_\mu Y + \text{strong interaction terms} = \\ &= \partial_\mu - i\frac{g}{\sqrt{2}}W_\mu^+ T^+ - i\frac{g}{\sqrt{2}}W_\mu^- T^- - i\frac{g}{c_W}Z_\mu(T_3 - s_W^2 Q) + \\ &\quad - igs_W A_\mu Q + \text{strong interaction terms} \end{aligned}$$

where the $T^\pm$ are the rising and lowering operators defined as

$$T^\pm = T^1 \pm iT^2$$

In the text we reabsorbed the coupling constants inside the generators and defined

$$gs_W Q \to T^\gamma \qquad \frac{g}{c_W}(T_3 - s_W^2) \to T^Z \qquad \frac{g}{\sqrt{2}}T^+ \to T^+ \qquad \frac{g}{\sqrt{2}}T^- \to T^-$$

Notice that in the standard representation in which T^3 is diagonal all these matrices are real and hence closed under transposition (meaning they go one into the other).

Another explicit change is in the Yukawa sector, the SSB gives a mass term to the fermions. In particular we have 3 mass matrices:

$$M_u^{(fg)} = \frac{vy_u^{(fg)}}{\sqrt{2}} \qquad M_d^{(fg)} = \frac{vy_d^{(fg)}}{\sqrt{2}} \qquad M_e^{(fg)} = \frac{vy_e^{(fg)}}{\sqrt{2}}$$

We can change our fermion field basis in order to go to the mass basis. For leptons (if we do not introduce right-handed neutrinos) this can be done quite easily. For quarks instead when we try doing so we obtain flavour violating terms in the weak interaction charged currents (namely the interactions mediated by $W^\pm$).

Let us see it in detail for M_u. The matrix $M_u M_u^\dagger$ is hermitian, thus it can be diagonalized by means of a Unitary transformation

$$D^2 = U_u^L M_u M_u^\dagger (U_u^L))^\dagger$$

where D and D^2 are diagonal matrices, as it is easy to show that the eigenvalues of $AA^\dagger$ are non-negative for every matrix A). If M_u is invertible we can define

$$U_u^R = (M_u^\dagger)^{-1}(U_u^L)^\dagger D$$

you can easily see that this matrix is unitary and that thanks to this definition

$$U_u^L M_u (U_u^R)^\dagger = D$$

The same procedure can be done for M_d. We can then redefine our fields in order to absorb these unitary matrices, but we end up with

$$i\bar{u}^{(f)i}\gamma^{\mu}V_{CKM}^{(fg)}D_{\mu}d_i^{(g)}$$
$$V_{CKM} = (U_u^L)^{\dagger}U_d^L$$

in the terms which are not diagonal in flavour, meaning in charged currents. If the neutrinos are massless instead we can reabsorb this whole structure into the neutrino mass term. We now know that at most one neutrino can be massless because of the oscillations measured in solar and atmospheric neutrino, but the right theory hasn't been discovered and incorporated in the Standard Model yet.

Appendix B

Mass Splitting in detail

B.1 Splitting for a Dirac Fermion

In the Minimal Dark Matter model we take Dirac Fermions in a non-chiral representation of the $SU(2)$ gauge group. Meaning that we take both its right-handed and left-handed components to be charged under the group and they transform in the same way. This allows the canonical mass term

$$\mathcal{L}_{mass} = M\bar{\chi}^i\chi_i = M((X_L^\dagger)^i(X_R)_i + (X_R^\dagger)^i(X_L)_i)$$

to be $SU(2)$ invariant. In this way both the left-handed and right-handed components of our Dark Matter couple to weak interactions and the coupling is thus vectorial.

We work in the Feynman gauge for both the Electromagnetic field and the weak interactions this allows the gauge boson propagators to be

$$G_{\mu\nu}(p) = \frac{-ig_{\mu\nu}}{p^2 - m_V^2}$$

with m_V the mass of the vector gauge boson. This gauge choice allows us to have no momentum dependence in the numerator of the propagator at the expense of having coupling of the weak gauge bosons with Goldstone bosons and ghosts. All these couplings do not contribute to the 1-loop correction to the mass as the only relevant correction is the so called *sunset diagram* B.1, therefore computations are far simpler in this gauge.

The mass correction follows from simple Feynman rules

$$i\Sigma(p) = -g_V^2\mu^{4-D}\int \frac{d^Dk}{(2\pi)^D}\gamma^\mu \frac{\not{p} - \not{k} + M}{(p-k)^2 - M^2}\gamma_\mu \frac{1}{k^2 - m_V^2}$$

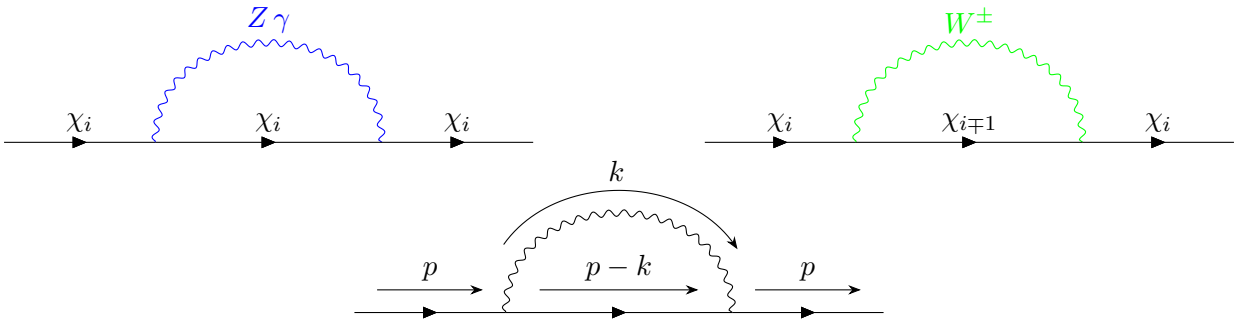

Figure B.1: Set of relevant sunset diagrams for a Dirac fermion and their momentum flow.

Where we used the conventions that for:

- **EM currents**:
$$g_V = g s_W Q \qquad m_V = 0$$
- **neutral currents**:
$$g_V = \frac{g}{c_W}(T_3 - s_W^2 Q) \qquad m_V = m_Z$$
- **charged currents**:
$$g_V^2 = \frac{g^2}{2}(T^+T^- + T^-T^+) \qquad m_V = m_W$$
some simple algebra gives $g_V^2 = g^2(T_1^2 + T_2^2)$.

In dimensional regularization the DM self-energy become becomes

$$i\Sigma(p) = -i\frac{g_V^2}{16\pi^2}\int_0^1 dx \left[\left(-\frac{4}{\epsilon} + 2 - 2\ln\left(\frac{\tilde{\mu}^2}{\Delta^2(m_V, M, x)}\right)\right)(1-x)\not{p} + \left(\frac{8}{\epsilon} - 2 + 4\ln\left(\frac{\tilde{\mu}^2}{\Delta(m_V, M, x)}\right)\right)M\right] + O(\epsilon)$$

where we used the conventions that

$$\tilde{\mu} = (4\pi e^{-\gamma_E})^{\frac{1}{2}}\mu$$
$$\Delta^2(m_V, M, x) = p^2 x(x-1) + M^2 x + m_V^2(1-x)$$

and γ_E is the Euler-Mascheroni constant.

All terms independent from the gauge mediator mass in the above expression do not contribute to the mass splitting: in fact if one term has the same coefficient for all three interactions the sum over the different g_V^2 gives just

$$\frac{1}{c_W^2}(T_3 - s_W^2 Q)^2 + s_W^2 Q^2 + (T_1^2 + T_2^2) = (T_1^2 + T_2^2 + T_3^2) + t_W^2 Y^2$$

but the right-hand-side is equal for all the components of the multiplet and therefore just contributes to the renormalization of the tree-level mass. Observing now that if the self-energy of the fermion is

$$\Sigma(p) = A\not{p} + BM$$

then the 1-loop resummed fermion propagator is

$$\frac{i}{\not{p} - M + \Sigma(p)}$$

and the physical mass is then shifted (in the approximation of small A and B which is valid in perturbation theory) to

$$M_{phys} = M(1 - A - B)$$

The shift of each component from the common renormalized mass term is then easily computed to be

$$\Delta M = \frac{g^2 M}{16\pi^2}\left(s_W^2 Q^2 f(m_Z, M) + (Q^2 - 2QY)[f(m_W, M) - f(m_Z, M)]\right)$$

we have defined

$$f(m_z, M) = 4\int_0^1 dx \ln\left(\frac{\Delta^2(m, M, x)}{\Delta^2(0, M, x)}\right) - 2\int_0^1 dx(1-x)\ln\left(\frac{\Delta^2(m, M, x)}{\Delta^2(0, M, x)}\right)$$

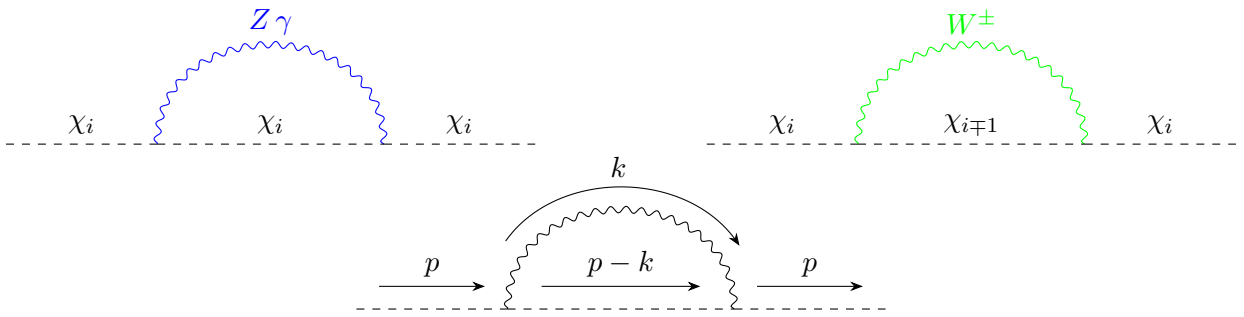

Figure B.2: Set of relevant sunset diagrams for a complex scalar field and their momentum flow.

Figure B.3: Set of relevant seagull diagrams for a complex scalar field and their momentum flow.

and the function Δ is now calculated on shell at $p^2 = M^2$, therefore

$$\Delta^2(m, M, x) = M^2x^2 + m^2(1 - x)$$

The above expression for $f(m, M)$ highlights a very interesting point: if the masses m_Z, $m_W \to 0$ which means $v \to 0$ the $SU(2)$ symmetry is unbroken and we would therefore expect all the components of the multiplet to have the same mass! This is exactly what we obtain as $f(m, M, x) \to 0$ as $m \to 0$.

The function $f(m, M)$ can be computed explicitly to find $f(m, M) = \tilde{f}\left(\frac{m}{M}\right)$

$$\tilde{f}(r) = \frac{r}{2}\left[-2r + 2r^3\ln(r) + \sqrt{r^2-4}(r^2+2)\ln\left(\frac{r^2 - 2 - r\sqrt{r^2-4}}{2}\right)\right]$$

B.2 Splitting for a Scalar Field

There are no subtleties to construct an $SU(2)$ invariant mass term for a Complex Scalar. The Feynman rules are exactly the scalar QED ones and we have two sets of relevant 1-loop corrections, namely the *sunset diagrams* B.2 and the *seagull diagrams* B.3.

The amplitudes for these two sets of diagrams are

$$i\Sigma(p)_{\text{sunset}} = g_V^2 \int \frac{d^Dk}{(2\pi)^D} i(2p_\mu - k_m u)\frac{i}{(p-k)^2 - M^2} i(2p_\nu - k_\nu)G^{\mu\nu}$$

$$i\Sigma(p)_{\text{seagull}} = g_V^2 \int \frac{d^Dk}{(2\pi)^D} g_{\mu\nu}G^{\mu\nu}$$

Where we used for g_V the same conventions on the previous section and the m_V dependence is inside $G_{\mu\nu}$. We must again chose a convenient gauge to work with, as we have showed the terms independent from the gauge bosons masses do not contribute to the mass splitting once we sum over g_V^2. The *seagull*

diagram for the photon is scaleless and thus goes to 0 if we work in dimensional regularization. Therefore there is no gauge choice that allows us to have divergences cancel explicitly in the seagull diagrams. We could try to make such a choice for the set of sunset diagrams, the convenient gauge turns out to be the Landau gauge. In this gauge the numerator of the vector boson propagator is the projector on transverse polarizations and we are then allowed to neglect the momentum dependences from k_μ in the vertices of amplitude.

$$G_{\mu\nu} = -i\frac{g_{\mu\nu} - \frac{k_\mu k_\nu}{k^2}}{k^2 - m_V^2}$$

Substituting the above propagator and proceeding with the standard one-loop computations we obtain

$$i\Sigma(p)_{\text{sunset}} = -i\frac{g_V^2 p^2}{4\pi^2}\int dx_1\, dx_2\, dx_3\, \delta(1-x_1-x_2-x_3)\left(\frac{3}{\epsilon} - 1 + \frac{3}{2}\ln\left(\frac{\tilde{\mu}^2}{\Delta^2(m_V, M, x_1, x_2, x_3)}\right)\right)$$

$$\Delta^2(m_V, M, x_1, x_2, x_3) = p^2 x_3(x_3 - 1) + M^2 x_3 + m_V^2 x_2$$

$$i\Sigma(p)_{\text{seagull}} = i\frac{g_V^2 m_V^2}{16\pi^2}\left(\frac{6}{\epsilon} + 1 + 3\ln\left(\frac{\tilde{\mu}^2}{m_V^2}\right)\right)$$

With the same steps as before we can now obtain the mass splitting, with the only difference that now the self-energy σ is a correction to the mass square, we will therefore have an additional factor of $\frac{1}{2}$ in the mass splitting. The displacement from the common renormalized tree-level mass would therefore be

$$\Delta M = \frac{g^2 M}{16\pi^2}\left(s_W^2 Q^2 f(m_Z, M) + (Q^2 - 2QY)[f(m_W, M) - f(m_Z, M)]\right)$$

Where we defined the function $f(m, M) = \tilde{f}\left(\frac{m}{M}\right)$ as

$$\tilde{f}(r) = \frac{1}{2}\left[Kr^2 - 6r^2\ln(r) + 6\int_0^1 dx_3 \int_0^{1-x_3} dx_2 \ln\left(1 + \frac{r^2 x_2}{x_3^2}\right)\right]$$

where k is a UV divergent constant accounting for the fact that the UV divergences of seagull diagrams do not vanish. The function can be explicitly computed and up to reabsorb a term proportional to r^2 and some factors of 2 inside the constant K we have

$$\tilde{f}(r) = -\frac{r}{4}\left[2r^3\ln(r) - Kr + (r^2-4)^{\frac{3}{2}}\ln\left(\frac{r^2 - 2 - r\sqrt{r^2-4}}{2}\right)\right]$$

Appendix C

Co-annihilation

In the Minimal Dark Matter Model co-annihilations are of capital importance. We have added to the Standard Model an electro-weak multiplet with one Lightest Neutral Particle (LNP) and the other having mass splittings around $\sim 100\,\mathrm{MeV}$ with respect to it.
The presence of the heavier states significantly changes the prediction of the LNP relic density. If we suppose a standard WIMP-like instantaneous freeze-out, to fix ideas, we find that it happens when the temperature of the Universe drops below the temperature

$$T_{FO} \simeq \frac{M}{25}$$

if we assume $M \sim$ TeV (we shall later see the reason for this assumption), then

$$T_{FO} \sim 10\,\mathrm{GeV}$$

and the heavier states are then accessible from the LNP and with more or less the same number density. Taking the Maxwell-Boltzmann distribution for all the particle of the multiplet we immediately see that in thermal equilibrium

$$\frac{n_{eq}^{(n)}}{n_{eq}^{(0)}} = \frac{g_n}{g_0}\left(\frac{M+\Delta M_n}{M}\right)^{\frac{3}{2}} e^{-\frac{\Delta M_n}{T}}$$

And this ratio is approximately one at freeze-out. Since eventually every non-stable species decays on the LNP, we are interested to the number density that is the sum of all the number densities of the particle in the electroweak multiplet. In the Boltzmann equation for the equilibrium density of all species we have

$$\chi_i \to \chi_{i-1} e^+ \nu_e$$

this decay is not number changing for the total density of χ particles. in fact:

$$\frac{dn_i}{dt} \supset -\Gamma_{i\to i-1} n_i$$

$$\frac{dn_{i-1}}{dt} \supset \Gamma_{i\to i-1} n_i$$

And thus once we sum over all the particles in the multiplet such decays play no-role in the resulting Boltzmann equation.

$$\frac{dn}{dt} = \sum_i \frac{dn_i}{dt} = -3Hn - \sum_{i,j} \langle \sigma_{ij} v \rangle (n_i n_j - n_{eq}^{(i)} n_{eq}^{(j)}) \tag{C.1}$$

where we defined the total number density of χ particles

$$n = \sum_i n_i$$

Assuming that at freeze-out we still have thermal equilibrium between the different partners in the multiplet. Meaning that the decays above and processes of the type

$$\chi_i X \to \chi_j X'$$

with X and X' different SM particles, are still efficient (note that this reaction also implies that we have kinetic equilibrium with the whole SM at freeze-out). This is a very easy requirement to fulfil as annihilation processes are proportional to the square of the number density of DM particles, which is suppressed at freeze-out, while these processes are proportional to the number density of DM particles times the number density of a still relativistic mediator whose number density is still relativistic. The ratio of the number densities of the different particles of the multiplet can then be well approximated by their equilibrium value and so

$$r_i = \frac{n_i}{n} = \frac{g_i M_i^{\frac{3}{2}} e^{-\Delta M_i/T}}{\sum_i g_i M_i^{\frac{3}{2}} e^{-\Delta M_i/T}}$$

in this approximation and with this conventions the Boltzmann equation can be rewritten as:

$$\frac{dn}{dt} = -3Hn - \left(\sum_{i,j} \langle \sigma_{ij} v \rangle r_i r_j \right) (n^2 - n_{eq}^2) = -3Hn - \langle \sigma v \rangle_{eff} (n^2 - n_{eq}^2)$$

$$\langle \sigma v \rangle_{eff} = \sum_{i,j} \langle \sigma_{ij} v \rangle r_i r_j$$

The thermally averaged effective cross section constructed in this way depends only on the temperature and not on the number of particles of each species or things alike. Once we have computed all the cross section of interest and the mass splitting of our model, we obtain a resulting Boltzmann equation which can be solved in the standard way.

Appendix D

Basics of Group Theory

Two excellent references for group theory in Physics and in particular in Particle Physics are [43, 22]. In this brief recap that will be useful to derive some useful identities useful for the computation of some amplitudes in non-Abelian Gauge theories.

A Lie-Group is Group G that is also a Manifold. This allows us to have both differentiation and multiplication defined on the Lie-Group. We will also immediately assume that we possess a linear representation of the group. Meaning that we have a set of $n \times n$ matrices in one-to-one mapping with the group elements $D(g)$ (where $g \in G$) such that matrix multiplication is now the operation of our group, n is called the dimension of the representation. We can now forget about the original group and just think about the new group $D(g)$. The Lie Algebra is nothing but the tangent space to the Identity in our Lie Group. And since we can go from the identity $\mathbb{I}$ of the group G to every other point $g \in G$ simply by applying g. For every path $\gamma(t)$ close to the identity we have the path $g\gamma(t)$ close to the element g. This tells us that the tangent space to the identity is isomorphic to the tangent space to every other element of the group.

$$\mathfrak{g} = T_{\mathbb{I}}G$$

Let the $\{iT^a,\, a = 1, 2, ...,\, dim\, G\}$ be a basis of our Lie Algebra, where i is the imaginary unit the T^as are commonly called generators of the Algebra. We can then write an infinitesimal transformation as

$$g(\epsilon) = \mathbb{I} + i\epsilon^a T^a + O(\epsilon^2)$$

We can see that the exponential map emerges as a way to construct finite transformations in the Lie-Group

$$g(t) = e^{it^a T^a} = \lim_{N\to\infty} \left(\mathbb{I} + \frac{it^a T^a}{N}\right)^N$$

In fact when $N \to \infty$ argument of the power belongs to the group, because of the manifold structure, and then the power also belongs to the group, because of the group structure.

We now know how to write elements of the group (at least in patch connected to the identity, but it can be shown that every Lie Group is connected by exponential arcs) in terms of elements in the algebra, therefore we can see what kinds of structure does the Lie Algebra inherit from the group. Besides the more trivial properties of groups:

1. Existence of the identity $\mathbb{I}$.
2. Existence of the inverse element.

That we have already exploited to some extent and that are obvious from the exponential map, we have two less trivial properties that impose constraints on our Lie Algebra:

3. Closure under the group operation.
4. Associativity.

If we apply these two properties to infinitesimal transformations we immediately found that, because of closure, the commutator closes in the algebra: it exist a set of constants f_{abc} called structure constants, such that

$$[T^a, T^b] = T^a T^b - T^b T^a = i\, f_{abc} T^c$$

And from the definition we see that f_{abc} is antisymmetric in the first two indices. Instead associativity imposes another constraint, called the Jacobi Identity

$$[T^a, [T^b, T^c]] + cyc(a, b, c) = 0$$

where we intend that we are summing over all the cyclic permutations of a, b and c.

Combining the two identities above gives another important result

$$f_{ade} f_{bcd} + f_{bde} f_{cad} + f_{cde} f_{abd} = 0$$

Using the antisymmetry we can rewrite this relation as

$$f_{bcd} f_{ade} - f_{acd} f_{bde} = -f_{bad} f_{dce}$$

if we define $(t_a)_{bc} = -i\, f_{abc}$ we end up with a representation of the generators, given by the structure constants, that satisfies the commutation relation

$$[t_b, t_a] = i\, f_{bad} t_d$$

this representation is known as the adjoint representation. There is another important representation of every group called the fundamental representation. It is the lowest dimensional non-trivial linear representation admitted by a group.

D.1 Unitary representations

There are two very important theorems that state the importance of Unitary transformations:

- Peter Weyl theorem: every compact Lie Group admits a faithful unitary representation.
- **Wigner theorem**: Every symmetry in Quantum Mechanics admits either a Unitary or an anti-Unitary representation.

Since we are interested in the study of Quantum Mechanics we will from now on assume that all the representations we have to deal with are unitary.

What does it tell us about the generators of the associated Lie Algebra?

If we have

$$\mathbb{I} = UU^\dagger \simeq (\mathbb{I} + i\epsilon^a T^a)(\mathbb{I} - i\epsilon^b (T^b)^\dagger) + O(\epsilon^2) \simeq \mathbb{I} + \epsilon^a (T^a - (T^a)^\dagger) + O(\epsilon^2)$$

and because this has to hold for every ϵ^a we can immediately see that the generators are hermitian

$$T^a = (T^a)^\dagger$$

This immediately tells us that the structure constants are real: taking the adjoint of the whole commutation relation we have

$$[T^a, T^b]^\dagger = -[T^a, T^b]$$
$$(i\, f_{abc} T^c)^\dagger = -i f^*_{abc} T^c$$
$$f_{abc} = f^*_{abc}$$

And therefore all the generators of the adjoint representation are complex.

D.2 Schur's Lemma

A representation is called irreducible if it has no invariant subspace. For irreducible representations the Schur Lemma applies:

If a matrix A is such that

$$AD(g) = D(g)A \qquad \forall g \in G$$

meaning that A commutes with every element of the representation, then A is a matrix proportional to the identity.

For the reasons outlined above, we take $D(g)$ to be unitary. Then (as $D(g)^\dagger = D(g^{-1})$) the statement of the theorem is equivalent to show that the theorem holds for the hermitian matrices $(A + A^\dagger)$ and $i(A - A^\dagger)$ and it thus suffices to prove the theorem for an hermitian matrix A'. With another similar step we can diagonalize the matrix A' by a unitary transformation and obtain

$$A' = WA''W^\dagger$$

with A'' diagonal. Transforming also the $D(g)$ to that basis we have that the thesis is equivalent to prove the theorem for diagonal matrices A''. We can finally write explicitly the components of the two sides

$$A''_{ij}D(g)_jk = D(g)_{ij}A''_{jk}$$

The only non-zero component are

$$A''_{ij}D(g)_{ik} = D(g)_{ik}A''_{kk}$$

This implies that either every $D(g)$ is reducible, or

$$A''_{ii} = A''_{kk} \qquad \forall i, k$$

and we have our thesis.

We have exploited a lot this lemma talking about real and complex representations, but this lemma has also other important applications, especially in physics when we talk about Casimir invariants.

D.3 Real and Pseudo-real Representations

Let us now dive a little bit into the mathematics of non-complex representations. In this section I will follow mainly the approach of [43]. From the fundamental relation (2.1)

$$D(g) = S^{-1}D^*(g)S$$

which tells us that the representation $D(g)$ is similar to its complex conjugate representation. using the same manipulations as in chapter 2, we have

$$D^T(g^{-1}) = S^T D(g)(S^T)^{-1}$$

$$D^*(g) = S^T S^{-1} D^*(g) S (S^T)^{-1}$$

$$D^*(g) = S^T S^{-1} D^*(g) (S^T S^{-1})^{-1}$$

And, because of Schur's Lemma, this implies

$$S^T S^{-1} = \eta \mathbb{I}$$

And using that $(S^T)^T = S$ we have $\eta = \pm 1$. Therefore the matrix S has to be either symmetric, in which case the representation is called real, or anti-symmetric, in which case we have a pseudo-real representation.

Another important property that we can deduce for S is that it can be chosen to be unitary. Following again the same steps as before we have that again for Schur's Lemma

$$SS^\dagger \propto \mathbb{I}$$

so far we could have freely multiplied S by a constant and all what we have written would still be true. We now fix this constant in order for S to be unitary. An important consequence is that pseudo-real representations must have even dimension (the n-linearity of the determinant tells us that anti-symmetric matrices have determinant equal to 0 in odd dimension).

You may still question why are real and pseudo-real representation really so different to deserve two different names. The difference is that, based on what we have just said, for real representations there is a basis in which the representation is truly real!! The crucial point is that if we have a unitary symmetric matrix U there is always a unitary symmetric matrix W such that $W^2 = U$ (this is easily proven by looking at the exponential form of a unitary matrix), but this is not the case for a unitary anti-symmetric matrix. If such a matrix exists we can define

$$D^*(g) = WWD(g)W^\dagger W^\dagger$$

$$(WD(g)W^\dagger)^* = WD(g)W^\dagger$$

D.4 No complex $SU(2)$ representation

The $SU(2)$ group has a very special property: the existence of the 2-index Levi-Civita tensors ϵ_{ab}, ϵ^{ab} defined to be

$$\epsilon_{21} = \epsilon^{12} = -\epsilon_{12} = -\epsilon^{21} = 1$$

and all other components equal to 0. This tensor defines a bijection between the fundamental representation and its complex conjugate. The fact that $SU(2)$ is special allows to write

$$U_a{}^b U_c{}^d \epsilon^{ca} \epsilon_{ed} = \delta^b_e$$

and we can read that

$$U^{\dagger\, a}_e = U_c{}^d \epsilon^{ca} \epsilon_{ed}$$

or in matrix notation

$$U^* = (U^\dagger)^T = \epsilon U \epsilon^T$$

And this immediately proves that the fundamental representation of $SU(2)$ is pseudo-real. Analogously we can prove that every tensor representation of the type (n, m) with $n + m$ odd is pseudo-real and every representation with $n + m$ even is real. As said before the position of the indices in the representation is not important because of the presence of the Levi-Civita tensor. The number of independent degrees of freedom of a general k-index tensor in D dimensions is

$$d = \frac{(k + D - 1)!}{k!(D - 1)!}$$

and therefore the dimension of each of our tensor representations is

$$d = \frac{(n + m + 1)!}{(n + m)!} = n + m + 1$$

And this means that all integer spin representations are real while all non-integer spin representations are pseudo-real (where we defined as always $d = 2s + 1$).

D.5 Dynkin coefficients and Casimir Invariants

We can construct a metric on our Lie Algebra, called the Killing-Cartan metric.

A metric is a bilinear non-degenerate operation from a vector space to the reals. We define it as

$$g_{ab} = \mathrm{tr}\Big(T^a T^b\Big)$$

This metric is symmetric because of the cyclicity of the trace. We can then diagonalize it by an orthogonal transformation on our vector space, meaning we can change our generators in a way that keeps invariant the commutation relations. We can then rescale our generators in order to obtain a metric proportional to the identity.

$$\mathrm{tr}\Big(\tilde{T}^a \tilde{T}^b\Big) = I(R)\delta_{ab}$$

The coefficient $I(R)$ is called Dynkin coefficient and is conventionally taken to be $\frac{1}{2}$ for the fundamental representation. We have kept the R between brackets to emphasize that these coefficients depend on the representation. We will later cover non-fundamental representations of $SU(2)$ that are of capital importance in this work and have the opportunity to work them out.

From this metric structure on the the Lie Group we can construct the so called Casimir invariant:

$$Cas = T^a T^b g^{-1}_{ab}$$

This operator technically does not belong to the Lie Algebra, but commutes with all its generators

$$[Cas, T^c] = g^{-1}_{ab} T^a [T^b, T^c] + g^{-1}_{ab} [T^a, T^c] T^b = i\, g^{-1}_{ab} f_{bcd} T^a T^d + i\, g^{-1}_{ab} f_{acd} T^d T^b = i\, g^{-1}_{ab} f_{bcd} (T^a T^d + T^d T^a) = 0$$

The last equality follows from

$$\mathrm{tr}\Big([T^a, T^b], T^c\Big) = I(R) f_{abc} g_{cd}$$

the fact that the LHS is completely anti-symmetric implies that

$$f_{abc} g_{cd} = -f_{dbc} g_{ca}$$

and applying two times the inverse metric we can show that $g^{-1}_{ab} f_{bcd}$ is antisymmetric.

Commuting with all the generators the Casimir commutes also with all the Unitary transformations generated by those and thus, by Schur's Theorem, is proportional to the identity

$$Cas = C(R)\mathbb{I}$$

There is an important relation between Dynkin and Casimir coefficients. Taking the trace of the Casimir and summing over indices a and b in the definition of the Dynkin, we find for $SU(N)$

$$C(R)\, d(R) = (N^2 - 1)\, I(R)$$

D.6 Coefficients for $SU(2)$

The group $SU(2)$ is the special unitary group of 2x2 matrices. Its fundamental representation has thus dimension 2. The generators of $SU(2)$ are hermitian traceless matrices and satisfy the commutation relation

$$[T_i, T_j] = i\, \epsilon_{ijk} T_j$$

The generators in the fundamental representation are proportional to the Pauli matrices and it is well known how to construct an n-dimensional irreducible representation of the group through ladder operators.

If we take the Standard representation of $SU(2)$ matrices (2.2) we can immediately see that

$$I(R) = \mathrm{tr}\big(T^3T^3\big) = 2\sum_{m=\{0,1/2\}}^{s} m^2 = 2\sum_{m=\{0,1/2\}}^{s}\left(2\binom{m}{2}+\binom{m}{i}\right) =$$
$$= 2\left(2\binom{s+1}{3}+\binom{s+1}{2}\right) = \frac{s(s+1)(2s+1)}{3}$$

The identities we have written are valid only for integer m but you can easily prove that the result is completely general. In terms of $n = 2s+1$ which is the dimensionality of the representation, we have

$$I(n) = \frac{n(n^2-1)}{12}$$

We can now use this results to evaluate traces of generators in arbitrary representations coming out from amplitudes computations

$$\mathrm{tr}\Big(T^aT^aT^bT^b\Big) = \mathrm{tr}(Cas\,Cas) = C(n)^2\,\mathrm{tr}\,\mathbb{I} = \left(\frac{3}{n}I(n)\right)^2 n = \frac{n(n^2-1)^2}{16}$$

Other quantities are a bit more subtle, for to compute

$$\mathrm{tr}\Big(T^aT^bT^aT^b\Big)$$

it is useful to consider

$$[T^a,[T^a,T^b]] = T^aT^aT^b + T^bT^aT^a - 2T^aT^bT^a = 2C(n)T^b - 2T^aT^bT^a$$

$$[T^a,[T^a,T^b]] = -f_{abc}f_{acd}T^d = (t_a)_{bc}(t_a)_{cd}T^d = C(adj)T^b$$

$$T^aT^bT^a = \left(C(n) - \frac{1}{2}C(adj)\right)T^b$$

substituting in the previous trace we had to compute

$$\mathrm{tr}\Big(T^aT^bT^aT^b\Big) = \left(C(n) - \frac{1}{2}C(adj)\right)C(n)n = \left(\frac{n^2-1}{4} - 10\right)\frac{n^2-1}{4}n = \frac{n(n^2-1)(n^2-5)}{16}$$

D.7 Tensor Representations

If we have two representations R and R' (which we will take to be irreducible) we can combine those in a tensor representation $R\otimes R'$ defined as the representation that acts on the tensor product of the space where R and R' are defined.

$$u_iv_j \to U^R|^a_i U^{R'}|^b_j u_a v_b$$

Taking U^R and $U^{R'}$ to be infinitesimal transformations we end up with

$$u_iv_j \to u_iv_j + i\epsilon_A T^A_R|^a_i u_a v_j + i\epsilon_A T^A_{R'}|^b_j u_i v_b + O(\epsilon^2)$$

It is then clear that the generators of the tensor representation are defined as

$$T^A_{RR'} = T^A_R\otimes\mathbb{I}_{R'} + \mathbb{I}_R T^A_{R'}$$

These generators can be easily shown to satisfy the commutation relation. Furthermore tensor representations are generally reducible meaning they can be decomposed as a direct sum of irreducible representations Q that act only on a subspace leaving the rest of the space invariant.

$$R \otimes R' = \bigoplus_Q Q$$

Doing color decomposition it was important to compute stuff like $\sum_A T_R^A \otimes T_{R'}^A$ this can be done computing

$$\sum_A T_{RR'}^A T_{RR'}^A = \sum_A \left(2T_R^A \otimes T_{R'}^A + \mathbb{I}_R \otimes (T_{R'}^A T_{R'}^A) + (T_R^A T_R^A) \otimes \mathbb{I}_{R'}\right) = 2\sum_A T_R^A \otimes T_{R'}^A + (C(R) + C(R'))\mathbb{I}$$

At the same time it can be shown that

$$\mathrm{tr}\left(T_{RR'}^A T_{RR'}^B\right) = (d(R)I(R') + d(R')I(R))\delta^{AB}$$

this relations ensures that all my irreducible representations are normalized in the same way from the structure inherited by the tensor product and so the total Casimir of the tensor representation is

$$\sum_A T_{RR'}^A T_{RR'}^A$$

acting on each irreducible representation (thanks to Schur Lemma) as

$$\sum_A T_{RR'}^A T_{RR'}^A = \sum_Q C(Q)\mathbb{I}_Q$$

and this is the relationship we used for color decomposition. From this formulas we have just derived we can immediately extract the values of Casimir and Dynkin coefficients for the adjoint representation of $SU(N)$, and in general for every representation we can obtain from a tensor product. It is well-known that $\mathbf{F} \otimes \bar{\mathbf{F}} = \mathbf{1} \oplus \mathbf{A}$. From the formula on Dynkin indices we get

$$I(\mathbf{A}) = \frac{N}{2} + \frac{N}{2} = N$$

and therefore

$$C(A) = N$$

the same value can be derived taking the trace of the relation between Casimir and recalling that the trivial representation $\mathbf{1}$ must clearly have a null Casimir.

Bibliography

[1] Henri Poincaré. *La voie lactée et la théorie des gaz*. Vol. 4. 1908.

[2] J. C. Kapteyn. "First Attempt at a Theory of the Arrangement and Motion of the Sidereal System". In: *The Astrophysical Journal* 55 (May 1922), p. 302. DOI: 10.1086/142670.

[3] A. Sommerfeld. "Über die Beugung und Bremsung der Elektronen". In: *Annalen der Physik* 403.3 (Jan. 1931), pp. 257–330. ISSN: 1521-3889. DOI: 10.1002/andp.19314030302. URL: http://dx.doi.org/10.1002/andp.19314030302.

[4] Norman Levinson. "Kgl. Danske Videnskab. Selskab, Mat". In: *Fys. Medd* 25.9 (1949), pp. 1–29.

[5] Vera C. Rubin and Jr. Ford W. Kent. "Rotation of the Andromeda Nebula from a Spectroscopic Survey of Emission Regions". In: *The Astrophysical Journal* 159 (Feb. 1970), p. 379. ISSN: 1538-4357. DOI: 10.1086/150317. URL: http://dx.doi.org/10.1086/150317.

[6] W. Fischler. "Quark-antiquark potential in QCD". In: *Nuclear Physics B* 129.1 (1977), pp. 157–174. ISSN: 0550-3213. DOI: https://doi.org/10.1016/0550-3213(77)90026-8. URL: https://www.sciencedirect.com/science/article/pii/0550321377900268.

[7] R. D. Peccei and Helen R. Quinn. "Constraints imposed by CP conservation in the presence of pseudoparticles". In: *Physical Review D* 16.6 (Sept. 1977), pp. 1791–1797. ISSN: 0556-2821. DOI: 10.1103/physrevd.16.1791. URL: http://dx.doi.org/10.1103/PhysRevD.16.1791.

[8] R. D. Peccei and Helen R. Quinn. "CP Conservation in the Presence of Pseudoparticles". In: *Physical Review Letters* 38.25 (June 1977), pp. 1440–1443. ISSN: 0031-9007. DOI: 10.1103/physrevlett.38.1440. URL: http://dx.doi.org/10.1103/PhysRevLett.38.1440.

[9] Steven Weinberg. "A New Light Boson?" In: *Physical Review Letters* 40.4 (Jan. 1978), pp. 223–226. ISSN: 0031-9007. DOI: 10.1103/physrevlett.40.223. URL: http://dx.doi.org/10.1103/PhysRevLett.40.223.

[10] F. Wilczek. "Problem of Strong P T Invariance in the Presence of Instantons". In: *Physical Review Letters* 40.5 (Jan. 1978), pp. 279–282. ISSN: 0031-9007. DOI: 10.1103/physrevlett.40.279. URL: http://dx.doi.org/10.1103/PhysRevLett.40.279.

[11] Jihn E. Kim. "Weak-Interaction Singlet and Strong CP Invariance". In: *Physical Review Letters* 43.2 (July 1979), pp. 103–107. ISSN: 0031-9007. DOI: 10.1103/physrevlett.43.103. URL: http://dx.doi.org/10.1103/PhysRevLett.43.103.

[12] M.A. Shifman, A.I. Vainshtein, and V.I. Zakharov. "Can confinement ensure natural CP invariance of strong interactions?" In: *Nuclear Physics B* 166.3 (Apr. 1980), pp. 493–506. ISSN: 0550-3213. DOI: 10.1016/0550-3213(80)90209-6. URL: http://dx.doi.org/10.1016/0550-3213(80)90209-6.

[13] A. R. Zhitnitsky. "On Possible Suppression of the Axion Hadron Interactions. (In Russian)". In: *Sov. J. Nucl. Phys.* 31 (1980), p. 260.

[14] Michael Dine, Willy Fischler, and Mark Srednicki. "A simple solution to the strong CP problem with a harmless axion". In: *Physics Letters B* 104.3 (Aug. 1981), pp. 199–202. ISSN: 0370-2693. DOI: 10.1016/0370-2693(81)90590-6. URL: http://dx.doi.org/10.1016/0370-2693(81)90590-6.

[15] David J. Gross, Robert D. Pisarski, and Laurence G. Yaffe. "QCD and instantons at finite temperature". In: *Rev. Mod. Phys.* 53 (1 Jan. 1981), pp. 43–80. DOI: 10.1103/RevModPhys.53.43. URL: https://link.aps.org/doi/10.1103/RevModPhys.53.43.

[16] Bob Holdom. "Two U(1)'s and ϵ charge shifts". In: *Physics Letters B* 166.2 (Jan. 1986), pp. 196–198. ISSN: 0370-2693. DOI: 10.1016/0370-2693(86)91377-8. URL: http://dx.doi.org/10.1016/0370-2693(86)91377-8.

[17] Glenn D. Starkman et al. "Opening the window on strongly interacting dark matter". In: *Phys. Rev. D* 41 (12 June 1990), pp. 3594–3603. DOI: 10.1103/PhysRevD.41.3594. URL: https://link.aps.org/doi/10.1103/PhysRevD.41.3594.

[18] Michael Dine et al. "Towards the theory of the electroweak phase transition". In: *Physical Review D* 46.2 (July 1992), pp. 550–571. ISSN: 0556-2821. DOI: 10.1103/physrevd.46.550. URL: http://dx.doi.org/10.1103/PhysRevD.46.550.

[19] Manuel Drees and Mihoko M. Nojiri. "Neutralino-nucleon scattering reexamined". In: *Phys. Rev. D* 48 (8 Oct. 1993), pp. 3483–3501. DOI: 10.1103/PhysRevD.48.3483. URL: https://link.aps.org/doi/10.1103/PhysRevD.48.3483.

[20] Scott Dodelson and Lawrence M. Widrow. "Sterile neutrinos as dark matter". In: *Physical Review Letters* 72.1 (Jan. 1994), pp. 17–20. ISSN: 0031-9007. DOI: 10.1103/physrevlett.72.17. URL: http://dx.doi.org/10.1103/PhysRevLett.72.17.

[21] Michel Le Bellac. *Thermal Field Theory*. Cambridge University Press, Aug. 1996. ISBN: 9780511721700. DOI: 10.1017/cbo9780511721700. URL: http://dx.doi.org/10.1017/CBO9780511721700.

[22] Howard Georgi. *Lie algebras in particle physics*. Frontiers in Physics. Philadelphia, PA: Westview Press, Oct. 1999.

[23] Wayne Hu, Rennan Barkana, and Andrei Gruzinov. "Fuzzy Cold Dark Matter: The Wave Properties of Ultralight Particles". In: *Physical Review Letters* 85.6 (Aug. 2000), pp. 1158–1161. ISSN: 1079-7114. DOI: 10.1103/physrevlett.85.1158. URL: http://dx.doi.org/10.1103/PhysRevLett.85.1158.

[24] Junji Hisano, Sh. Matsumoto, and Mihoko M. Nojiri. "Unitarity and higher-order corrections in neutralino dark matter annihilation into two photons". In: *Physical Review D* 67.7 (Apr. 2003). ISSN: 1089-4918. DOI: 10.1103/physrevd.67.075014. URL: http://dx.doi.org/10.1103/PhysRevD.67.075014.

[25] Marco Cirelli, Nicolao Fornengo, and Alessandro Strumia. "Minimal dark matter". In: *Nuclear Physics B* 753.1–2 (Oct. 2006), pp. 178–194. ISSN: 0550-3213. DOI: 10.1016/j.nuclphysb.2006.07.012. URL: http://dx.doi.org/10.1016/j.nuclphysb.2006.07.012.

[26] Douglas Clowe et al. "A Direct Empirical Proof of the Existence of Dark Matter". In: *The Astrophysical Journal* 648.2 (Aug. 2006), pp. L109–L113. ISSN: 1538-4357. DOI: 10.1086/508162. URL: http://dx.doi.org/10.1086/508162.

[27] Marco Cirelli, Alessandro Strumia, and Matteo Tamburini. "Cosmology and astrophysics of minimal dark matter". In: *Nuclear Physics B* 787.1–2 (Dec. 2007), pp. 152–175. ISSN: 0550-3213. DOI: 10.1016/j.nuclphysb.2007.07.023. URL: http://dx.doi.org/10.1016/j.nuclphysb.2007.07.023.

[28] Junji Hisano et al. "Non-perturbative effect on thermal relic abundance of dark matter". In: *Physics Letters B* 646.1 (Mar. 2007), pp. 34–38. ISSN: 0370-2693. DOI: 10.1016/j.physletb.2007.01.012. URL: http://dx.doi.org/10.1016/j.physletb.2007.01.012.

[29] Jürgen Ehlers. "Editorial note to: F. Zwicky The redshift of extragalactic nebulae". In: *General Relativity and Gravitation* 41.1 (Nov. 2008), pp. 203–206. ISSN: 1572-9532. DOI: 10.1007/s10714-008-0706-5. URL: http://dx.doi.org/10.1007/s10714-008-0706-5.

[30] Nima Arkani-Hamed et al. "A theory of dark matter". In: *Physical Review D* 79.1 (Jan. 2009). ISSN: 1550-2368. DOI: 10.1103/physrevd.79.015014. URL: http://dx.doi.org/10.1103/PhysRevD.79.015014.

[31] Alexey Boyarsky, Oleg Ruchayskiy, and Mikhail Shaposhnikov. "The Role of Sterile Neutrinos in Cosmology and Astrophysics". In: *Annual Review of Nuclear and Particle Science* 59.1 (Nov. 2009), pp. 191–214. ISSN: 1545-4134. DOI: 10.1146/annurev.nucl.010909.083654. URL: http://dx.doi.org/10.1146/annurev.nucl.010909.083654.

[32] Roberto Iengo. "Sommerfeld enhancement: general results from field theory diagrams". In: *Journal of High Energy Physics* 2009.05 (May 2009), pp. 024–024. ISSN: 1029-8479. DOI: 10.1088/1126-6708/2009/05/024. URL: http://dx.doi.org/10.1088/1126-6708/2009/05/024.

[33] S Cassel. "Sommerfeld factor for arbitrary partial wave processes". In: *Journal of Physics G: Nuclear and Particle Physics* 37.10 (Aug. 2010), p. 105009. ISSN: 1361-6471. DOI: 10.1088/0954-3899/37/10/105009. URL: http://dx.doi.org/10.1088/0954-3899/37/10/105009.

[34] Dmitry Budker et al. "Proposal for a Cosmic Axion Spin Precession Experiment (CASPEr)". In: *Phys. Rev. X* 4.2 (2014), p. 021030. DOI: 10.1103/PhysRevX.4.021030. arXiv: 1306.6089 [hep-ph].

[35] Andrea De Simone, Gian Francesco Giudice, and Alessandro Strumia. "Benchmarks for dark matter searches at the LHC". In: *Journal of High Energy Physics* 2014.6 (June 2014). ISSN: 1029-8479. DOI: 10.1007/jhep06(2014)081. URL: http://dx.doi.org/10.1007/JHEP06(2014)081.

[36] Luca Di Luzio et al. "Accidental matter at the LHC". In: *Journal of High Energy Physics* 2015.7 (July 2015). ISSN: 1029-8479. DOI: 10.1007/jhep07(2015)074. URL: http://dx.doi.org/10.1007/JHEP07(2015)074.

[37] Brian C Hall. *Lie groups, lie algebras, and representations*. en. 2nd ed. Graduate texts in mathematics. Cham, Switzerland: Springer International Publishing, May 2015.

[38] Tesla E. Jeltema and Stefano Profumo. "Discovery of a 3.5 keV line in the Galactic Centre and a critical look at the origin of the line across astronomical targets". In: *Mon. Not. Roy. Astron. Soc.* 450.2 (2015), pp. 2143–2152. DOI: 10.1093/mnras/stv768. arXiv: 1408.1699 [astro-ph.HE].

[39] J. Aleksić et al. "The major upgrade of the MAGIC telescopes, Part II: A performance study using observations of the Crab Nebula". In: *Astroparticle Physics* 72 (Jan. 2016), pp. 76–94. ISSN: 0927-6505. DOI: 10.1016/j.astropartphys.2015.02.005. URL: http://dx.doi.org/10.1016/j.astropartphys.2015.02.005.

[40] Michela D'Onofrio and Kari Rummukainen. "Standard model cross-over on the lattice". In: *Physical Review D* 93.2 (Jan. 2016). ISSN: 2470-0029. DOI: 10.1103/physrevd.93.025003. URL: http://dx.doi.org/10.1103/PhysRevD.93.025003.

[41] Valentin Lefranc et al. "Dark Matter in lines: Galactic Center vs. dwarf galaxies". In: *Journal of Cosmology and Astroparticle Physics* 2016.09 (Sept. 2016), pp. 043–043. ISSN: 1475-7516. DOI: 10.1088/1475-7516/2016/09/043. URL: http://dx.doi.org/10.1088/1475-7516/2016/09/043.

[42] Vivian Poulin, Pasquale D. Serpico, and Julien Lesgourgues. "A fresh look at linear cosmological constraints on a decaying Dark Matter component". In: *Journal of Cosmology and Astroparticle Physics* 2016.08 (Aug. 2016), pp. 036–036. ISSN: 1475-7516. DOI: 10.1088/1475-7516/2016/08/036. URL: http://dx.doi.org/10.1088/1475-7516/2016/08/036.

[43] Anthony Zee. *Group theory in a nutshell for physicists*. en. In a Nutshell. Princeton, NJ: Princeton University Press, Mar. 2016.

[44] B. P. Abbott et al. "Multi-messenger Observations of a Binary Neutron Star Merger*". In: *The Astrophysical Journal Letters* 848.2 (Oct. 2017), p. L12. ISSN: 2041-8213. DOI: 10.3847/2041-8213/aa91c9. URL: http://dx.doi.org/10.3847/2041-8213/aa91c9.

[45] Sonia El Hedri, Anna Kaminska, and Maikel de Vries. "A Sommerfeld toolbox for colored dark sectors". In: *The European Physical Journal C* 77.9 (Sept. 2017). ISSN: 1434-6052. DOI: 10.1140/epjc/s10052-017-5168-z. URL: http://dx.doi.org/10.1140/epjc/s10052-017-5168-z.

[46] Andrea Mitridate et al. "Cosmological implications of Dark Matter bound states". In: *Journal of Cosmology and Astroparticle Physics* 2017.05 (May 2017), pp. 006–006. ISSN: 1475-7516. DOI: 10.1088/1475-7516/2017/05/006. URL: http://dx.doi.org/10.1088/1475-7516/2017/05/006.

[47] R. Mukherjee. "Observing the energetic universe at very high energies with the VERITAS gamma ray observatory". In: *Advances in Space Research* 62.10 (Nov. 2018), pp. 2828–2844. ISSN: 0273-1177. DOI: 10.1016/j.asr.2018.04.002. URL: http://dx.doi.org/10.1016/j.asr.2018.04.002.

[48] Carlos Blanco and Dan Hooper. "Constraints on decaying dark matter from the isotropic gamma-ray background". In: *Journal of Cosmology and Astroparticle Physics* 2019.03 (Mar. 2019), pp. 019–019.

ISSN: 1475-7516. DOI: 10.1088/1475-7516/2019/03/019. URL: http://dx.doi.org/10.1088/1475-7516/2019/03/019.

[49] Jacob Katriel. "A physically motivated derivation of the Laplacian in terms of the total angular momentum operator". In: *European Journal of Physics* 40.4 (June 2019), p. 045401. ISSN: 1361-6404. DOI: 10.1088/1361-6404/ab16a1. URL: http://dx.doi.org/10.1088/1361-6404/ab16a1.

[50] N. Aghanim et al. "Planck 2018 results. V. CMB power spectra and likelihoods". In: *Astron. Astrophys.* 641 (2020), A5. DOI: 10.1051/0004-6361/201936386. arXiv: 1907.12875 [astro-ph.CO].

[51] N. Aghanim et al. "Planck2018 results: VI. Cosmological parameters". In: *Astronomy & Astrophysics* 641 (Sept. 2020), A6. ISSN: 1432-0746. DOI: 10.1051/0004-6361/201833910. URL: http://dx.doi.org/10.1051/0004-6361/201833910.

[52] Luca Di Luzio et al. "The landscape of QCD axion models". In: *Phys. Rept.* 870 (2020), pp. 1–117. DOI: 10.1016/j.physrep.2020.06.002. arXiv: 2003.01100 [hep-ph].

[53] Andrea Caputo et al. "Dark photon limits: A handbook". In: *Physical Review D* 104.9 (Nov. 2021). ISSN: 2470-0029. DOI: 10.1103/physrevd.104.095029. URL: http://dx.doi.org/10.1103/PhysRevD.104.095029.

[54] Daniel Baumann. *Cosmology*. Cambridge University Press, 2022.

[55] Salvatore Bottaro et al. "Closing the window on WIMP Dark Matter". In: *The European Physical Journal C* 82.1 (Jan. 2022). ISSN: 1434-6052. DOI: 10.1140/epjc/s10052-021-09917-9. URL: http://dx.doi.org/10.1140/epjc/s10052-021-09917-9.

[56] Salvatore Bottaro et al. "The last complex WIMPs standing". In: *The European Physical Journal C* 82.11 (Nov. 2022). ISSN: 1434-6052. DOI: 10.1140/epjc/s10052-022-10918-5. URL: http://dx.doi.org/10.1140/epjc/s10052-022-10918-5.

[57] Barton Zwiebach. *Mastering quantum mechanics*. en. London, England: MIT Press, Apr. 2022.

[58] J. Aalbers et al. "First Dark Matter Search Results from the LUX-ZEPLIN (LZ) Experiment". In: *Physical Review Letters* 131.4 (July 2023). ISSN: 1079-7114. DOI: 10.1103/physrevlett.131.041002. URL: http://dx.doi.org/10.1103/PhysRevLett.131.041002.

[59] Christopher Dessert et al. *Was There a 3.5 keV Line?* 2023. arXiv: 2309.03254 [astro-ph.CO]. URL: https://arxiv.org/abs/2309.03254.

[60] M. Aker et al. *Direct neutrino-mass measurement based on 259 days of KATRIN data*. 2024. arXiv: 2406.13516 [nucl-ex]. URL: https://arxiv.org/abs/2406.13516.

[61] Marco Cirelli, Alessandro Strumia, and Jure Zupan. *Dark Matter*. 2024. arXiv: 2406.01705.

[62] James M. Cline. *Status of Dark Photons*. 2024. arXiv: 2405.08534 [hep-ph]. URL: https://arxiv.org/abs/2405.08534.

[63] Albert Escrivà, Florian Kühnel, and Yuichiro Tada. "Primordial black holes". In: *Black Holes in the Era of Gravitational-Wave Astronomy*. Elsevier, 2024, pp. 261–377. ISBN: 9780323956369. DOI: 10.1016/b978-0-32-395636-9.00012-8. URL: http://dx.doi.org/10.1016/B978-0-32-395636-9.00012-8.

[64] Aleko Khukhunaishvili. *Measurement of the effective leptonic electroweak mixing angle and Drell-Yan forward-backward asymmetry using pp collisions at $\sqrt{s} = 13$ TeV*. 2024. arXiv: 2405.11484 [hep-ex]. URL: https://arxiv.org/abs/2405.11484.

[65] S. Navas et al. "Review of particle physics". In: *Phys. Rev. D* 110.3 (2024), p. 030001. DOI: 10.1103/PhysRevD.110.030001.